Earth and Space Science

REVIEW ARTICLE
10.1029/2025EA004868

Observation and Coordination Needs for Current, Near-Future, and Next Generation Earth-Observing SAR Systems

Cathleen E. Jones[1,2], Ake Rosenqvist[3,4], Björn Rommen[5], Magdalena Fitrzyk[6], Eric Rignot[1,7], Bernd Scheuchl[7], Yujie Zheng[8], Andrew Hooper[9], Mark Simons[10], Tomokazu Kobayashi[11], Paul Siqueira[12], Maurizio Santoro[13], Takeo Tadono[4], Laura Hess[14], Heather McNairn[15], Laura Frulla[16], Malin Johansson[2], Wolfgang Dierking[2], Line Rouyet[17], Annett Bartsch[18], Paco Lopez Dekker[19], and Johnny A. Johannessen[20]

[1]Jet Propulsion Laboratory, California Institute of Technology, Pasadena, CA, USA, [2]UiT the Arctic University of Norway, Tromsø, Norway, [3]solo Earth Observation, soloEO, Tokyo, Japan, [4]Japan Aerospace Exploration Agency, JAXA, Tsukuba, Japan, [5]European Space Agency (ESA), ESTEC, Noordwijk, The Netherlands, [6]Remote Sensing Applications Consultants Ltd, c/o European Space Agency, ESRIN, Frascati, Italy, [7]University of California Irvine, Irvine, CA, USA, [8]University of Texas Dallas, Dallas, TX, USA, [9]COMET, University of Leeds, Leeds, UK, [10]California Institute of Technology, Pasadena, CA, USA, [11]Geospatial Information Authority of Japan, Tsukuba, Japan, [12]University of Massachusetts, Amherst, MA, USA, [13]Gamma Remote Sensing, Gümligen, Switzerland, [14]University of California Santa Barbara, Santa Barbara, CA, USA, [15]Agriculture and Agri-Food Canada, Ottawa, ON, Canada, [16]Comisión Nacional de Actividades Espaciales, CONAE, Buenos Aires, Argentina, [17]NORCE Research AS, Tromsø, Norway, [18]b.geos GmbH, Korneuburg, Austria, [19]Technical University Delft, Delft, The Netherlands, [20]Nansen Environmental and Remote Sensing Center, Bergen, Norway

Abstract This paper summarizes an evaluation by experts of how coordination of Earth-observing Synthetic Aperture Radar (SAR) missions among the world's space agencies could advance toward game-changing scientific discoveries and fully realizing SAR's practical capability to address many issues facing society. We consider key science disciplines for which spaceborne SAR sensors are routinely used, with an emphasis on SAR imaging instruments. We outline the current state of the science and identify critical information gaps for 10 disciplines: Ice Sheets and Glaciers, Solid Earth Science, Hazards, Forests and Biomass, Wetlands, Agriculture and Crop Monitoring, Soil Moisture, Sea Ice, Permafrost, and Oceans. We provide recommendations on how these gaps can be addressed by coordination of missions currently operating or in development, then look forward to the next decade during which as-yet-unplanned coordinated SAR constellations could be game-changing. We identify synergies and conflicts between the optimal SAR configurations required for individual disciplines to achieve transformational science advancement. Finally, we provide summary recommendations for beneficial coordination that consider SAR-enabled Earth science studies both as a whole and within the context of multiple individual disciplines that have benefited from a common observational strategy. Overall, there are clear benefits that can be derived from coordinated utilization of spaceborne SAR assets based on their individual capabilities and availability, and through coordinated and shared data and observation strategies.

Plain Language Summary Various space agencies around the world operate Earth-observing synthetic aperture radar (SAR) missions to address scientific and operational priorities of their countries or collaborations. We asked the question: How much more could be accomplished in scientific discovery or beneficial usage if these agencies coordinated their activities with direction from the science and end-user communities? This paper summarizes the response from the community, garnered through workshops, surveys, and brainstorming of experts in 10 areas of research for which SAR has provided essential information, namely Ice Sheets and Glaciers, Solid Earth Science, Hazards, Forests and Biomass, Wetlands, Agriculture and Crop Monitoring, Soil Moisture, Sea Ice, Permafrost, and Oceans. After summarizing the essential value of SAR for each of these, we recommend actions that could lead to game changing advancements both near-term and with visionary next-generation coordinated missions that would form a super-constellation of Earth-observing instruments to better serve humanity than individual missions alone.

Key Points:

- Potential benefits to science and society from coordination of Earth-observing synthetic aperture radar missions are evaluated
- Actions are identified to support game-changing advancements in 10 Earth science disciplines with current and next-generation missions
- Coordinated actions and a next-generation constellation mission can benefit all disciplines despite disparate or conflicting needs

Correspondence to:

C. E. Jones and A. Rosenqvist,
cathleen.e.jones@jpl.nasa.gov;
ake.rosenqvist@soloEO.com

Citation:

Jones, C. E., Rosenqvist, A., Rommen, B., Fitrzyk, M., Rignot, E., Scheuchl, B., et al. (2026). Observation and coordination needs for current, near-future, and next generation Earth-observing SAR systems. *Earth and Space Science*, *13*, e2025EA004868. https://doi.org/10.1029/2025EA004868

Received 29 OCT 2025
Accepted 4 APR 2026

Author Contributions:

Conceptualization: Cathleen E. Jones, Ake Rosenqvist, Björn Rommen, Magdalena Fitrzyk, Eric Rignot, Bernd Scheuchl, Yujie Zheng, Andrew Hooper, Mark Simons, Tomokazu Kobayashi, Paul Siqueira, Maurizio Santoro, Takeo Tadono, Laura Hess, Heather McNairn, Laura Frulla, Malin Johansson,

1. Introduction

Since the launch of the first spaceborne Synthetic Aperture Radar (SAR) mission, Seasat, more than four decades ago (Born et al., 1979; Elachi, 1980), there have been tremendous advances in the development and use of SAR

Wolfgang Dierking, Line Rouyet, Annett Bartsch, Paco Lopez Dekker, Johnny A. Johannessen
Formal analysis: Cathleen E. Jones, Ake Rosenqvist, Björn Rommen, Magdalena Fitrzyk, Eric Rignot, Bernd Scheuchl, Yujie Zheng, Andrew Hooper, Mark Simons, Tomokazu Kobayashi, Paul Siqueira, Maurizio Santoro, Takeo Tadono, Laura Hess, Heather McNairn, Laura Frulla, Malin Johansson, Wolfgang Dierking, Line Rouyet, Annett Bartsch, Paco Lopez Dekker, Johnny A. Johannessen
Funding acquisition: Cathleen E. Jones
Investigation: Cathleen E. Jones, Ake Rosenqvist, Björn Rommen, Magdalena Fitrzyk, Eric Rignot, Bernd Scheuchl, Yujie Zheng, Andrew Hooper, Mark Simons, Tomokazu Kobayashi, Paul Siqueira, Maurizio Santoro, Takeo Tadono, Laura Hess, Heather McNairn, Laura Frulla, Malin Johansson, Wolfgang Dierking, Line Rouyet, Annett Bartsch, Paco Lopez Dekker, Johnny A. Johannessen
Methodology: Cathleen E. Jones, Ake Rosenqvist, Björn Rommen, Magdalena Fitrzyk, Eric Rignot, Bernd Scheuchl, Yujie Zheng, Andrew Hooper, Mark Simons, Tomokazu Kobayashi, Paul Siqueira, Maurizio Santoro, Takeo Tadono, Laura Hess, Heather McNairn, Laura Frulla, Malin Johansson, Wolfgang Dierking, Line Rouyet, Annett Bartsch, Paco Lopez Dekker, Johnny A. Johannessen
Project administration: Cathleen E. Jones, Ake Rosenqvist, Björn Rommen, Magdalena Fitrzyk
Resources: Cathleen E. Jones, Ake Rosenqvist, Björn Rommen, Magdalena Fitrzyk, Eric Rignot, Bernd Scheuchl, Yujie Zheng, Andrew Hooper, Mark Simons, Tomokazu Kobayashi, Paul Siqueira, Maurizio Santoro, Takeo Tadono, Laura Hess, Heather McNairn, Laura Frulla, Malin Johansson, Wolfgang Dierking, Line Rouyet, Annett Bartsch, Paco Lopez Dekker, Johnny A. Johannessen
Software: Tomokazu Kobayashi
Visualization: Cathleen E. Jones, Ake Rosenqvist, Eric Rignot, Bernd Scheuchl, Yujie Zheng, Andrew Hooper, Mark Simons, Tomokazu Kobayashi, Paul Siqueira, Maurizio Santoro, Takeo Tadono, Laura Hess, Heather McNairn, Laura Frulla, Malin Johansson, Wolfgang Dierking, Line Rouyet, Annett Bartsch, Paco Lopez Dekker, Johnny A. Johannessen
Writing – original draft: Cathleen E. Jones, Ake Rosenqvist, Björn Rommen, Magdalena Fitrzyk, Eric Rignot, Bernd Scheuchl, Yujie Zheng, Andrew Hooper, Mark Simons,

systems for Earth observation. The oft-touted capability of microwaves to penetrate clouds and haze is more than a cliché—it enables the systematic and uninterrupted collection of time series data over large areas to improve our understanding of natural and human-induced processes at different spatial and temporal scales. Notwithstanding these great advances, there remain significant data gaps and mission constraints, with the result that many key questions remain to be resolved. Some of these can be addressed by improved coordination of current and future SAR missions and other support activities undertaken by the world's space agencies.

Coordination among the space agencies has been successful in the past. An example of very successful coordination on a global scale is the International Charter on Space and Major Disasters (International Charter) (https://disasterscharter.org/web/guest/home; Bessis et al., 2004), which was started in 2000 to provide satellite data to member and partner organizations following major disasters worldwide. Since then, the International Charter has been activated over 950 times, supporting disaster response and relief in >140 countries with data from 270 Earth-observing (EO) satellites. Similar successful coordination between space agencies was carried out within the Polar Space Task Group (PSTG; see also Section 2.1), under the auspices of the World Meteorological Organization (WMO), which enabled the creation of comprehensive and coordinated polar region data sets, particularly from SAR, to support scientific research on climate change impacts. WMO recently reestablished a successor to PSTG with a broader mandate under WMO's Global Cryosphere Watch (GCW) via the WMO Commission for Observation, Infrastructure and Information Systems (INFCOM).

International coordination is ongoing through the Committee on Earth Observation Satellites (CEOS) through efforts such as the Land Surface Imaging Virtual Constellation (LSI-VC) polarimetric SAR (PolSAR) activity to advance polarimetric and multi-frequency SAR research and application development, through which time series of polarimetric SAR data from nine national space organizations' missions with different frequencies (P, L, S, C, X) are being collected over reference sites across the globe. In addition, the SARCalNet initiative was established within the CEOS Working Group on Calibration and Validation (WGCV) with the objective to publish and maintain a continuously updated database containing reliable and standardized information on SAR calibration sites and targets worldwide (https://www.sarcalnet.org). In the area of data standardization, CEOS Analysis Ready Data (CEOS-ARD) is a multi-agency effort to develop SAR and optical data product specifications intended to help broaden the EO user community and improve data interoperability through time and across different sensors (https://www.ceos.org/ard). For SAR in particular, representatives from 18 space agencies, private sector data providers, and academia developed the CEOS-ARD specifications for normalized radar backscatter, ocean radar backscatter, polarimetric radar, interferometric radar, and geocoded single-look complex data products (CEOS, 2025).

Capacity building is another area where international collaboration is of value, although now more frequently supported by individual agencies. Examples of such individually or bilaterally supported training activities include the Massive Open Online Course “Echoes in Space” offered by the European Space Agency (ESA), focusing on the basics of radar remote sensing; the Advanced Training Courses on Radar Polarimetry organized by ESA every two-three years; the U.S. National Aeronautics and Space Administration's (NASA's) Applied Remote Sensing Training Program (ARSET); and the Open PolInSAR Training Course held jointly between ESA and the Deutsches Zentrum für Luft und Raumfahrt (DLR). The CEOS Working Group on Capacity Building and Data Democracy (WGCapD) brought together CEOS agencies and non-CEOS partners to provide intensive capacity building, education, and training, with one objective, among others, being to increase the capacity of institutions in less developed countries to effectively use EO data. In more than 15 years of activity, WgCapD has offered dozens of in-person trainings around the globe, SAR summer schools, SAR data workshops, and online trainings and webinars, often in collaboration with other CEOS Working Groups. NASA has a long history of capacity building around the globe for use of remote sensing data. NASA's partnership with the U.S. Agency for International Development (USAID) on the SERVIR program supported centers for training in the use of remote sensing data in developing countries worldwide until the program's abrupt cancellation in 2025. Recognizing the immense value of SERVIR's mission, institutions, partners, and regional hubs committed to continue its work, forming the SERVIR Global Collaborative with funding coming from public and private organizations. This highlights the value of international collaborations to buffer capacity building initiatives from policy and funding changes within any single country.

Recognizing the success of multi-agency coordination in the past, we consider how it could be expanded to better enable scientific advancements in particular. Here we evaluate and recommend SAR coordination actions that can

Tomokazu Kobayashi, Paul Siqueira, Maurizio Santoro, Takeo Tadono, Laura Hess, Heather McNairn, Laura Frulla, Malin Johansson, Wolfgang Dierking, Line Rouyet, Annett Bartsch, Paco Lopez Dekker, Johnny A. Johannessen
Writing – review & editing: Cathleen E. Jones, Ake Rosenqvist, Björn Rommen, Magdalena Fitrzyk, Eric Rignot, Bernd Scheuchl, Yujie Zheng, Andrew Hooper, Mark Simons, Tomokazu Kobayashi, Paul Siqueira, Maurizio Santoro, Takeo Tadono, Laura Hess, Heather McNairn, Laura Frulla, Malin Johansson, Wolfgang Dierking, Line Rouyet, Annett Bartsch, Paco Lopez Dekker, Johnny A. Johannessen

advance science in the time from now through the 2030s, roughly the timescale for the next generation of missions to bear results. The study reported here was undertaken as part of the activities of the International Coordination Group for Spaceborne Synthetic Aperture Radar Missions (ICGS-SAR; Elachi et al., 2022; http://intl-sar-coord-group.space/), which was established in 2018 to hold community-wide discussions engaging space agencies on ways to expand and improve the international coordination of spaceborne EO SAR missions and their data providers. ICGS-SAR consists of representatives from ESA, NASA, Germany's DLR, the Japan Aerospace Exploration Agency (JAXA), Italy's Agenzia Spaziale Italiana (ASI), Argentina's Comisión Nacional de Actividades Espaciales (CONAE), the Canadian Space Agency (CSA), and the Indian Space Research Organisation (ISRO). ICGS-SAR also includes representatives from the academic community, commercial companies, and non-government organizations interested in the development and use of spaceborne SAR. Two of the ICGS-SAR Thematic Area groups focused on SAR-enabled Earth science and applications, identifying gaps and actions that could be taken to increase the benefit of the world's space missions to science and society. This paper synthesizes the findings of these two groups regarding specific coordination actions that would benefit different fields of study individually, then identifies their commonalities and conflicts to make cross-cutting recommendations.

Drawing on the expertise of the science community, we provide a high-level review of Earth observation requirements for 10 key scientific disciplines where space-based SAR sensors can contribute critical measurements: Ice Sheets and Glaciers, Solid Earth Science, Hazards, Forests and Biomass, Wetlands, Agriculture, Soil Moisture, Sea Ice, Permafrost, and Oceans. In Section 2, for each discipline, we (a) provide a brief description of the particular relevance of SAR data and the current state of the art, (b) identify key information or knowledge gaps that impede progress, and then provide recommendations on how to mitigate these gaps (c) in the 2020s through improved coordination of current and near-term SAR missions, and (d) in the 2030 decade with next-generation SAR missions. Section 3 provides the summary of an open survey undertaken with the science community as part of ICGS-SAR, and in Section 4 we condense the recommendations from all disciplines considered as a whole into a set of recommendations to the space agencies and the research community that can address the outstanding scientific needs. The recommendations for the individual disciplines and those from Section 4 together encompass identified actions that, if enacted in whole or in part, will advance science through coordination of the world's SAR assets.

Tables 1 and 2 list the key characteristics of the SAR missions discussed in this paper, which mainly include those agencies involved in ICGS-SAR. To avoid duplication of mission descriptions, the missions are referred to in the following sections only by their name and, if required for clarity, by their radar band. Commercial SAR missions, such as those operated by Capella Space, ICEYE, Synspective, iQPS and Umbra, are also relevant for certain applications, and most offer free data to selected science users or through open data collections (Umbra). These missions are characterized as constellations of single-polarization X-band sensors with small footprint but meter-/sub-meter resolution and the capacity for high temporal repeat, although most cannot be used for SAR interferometry (InSAR). Commercial SAR missions are also discussed in the sections below. Similarly, we acknowledge that China also has developed advanced EO missions, including the C-band GaoFen-3 constellation and the L-band polarimetric and interferometric LuTan-1A/B constellation missions (Z. Wang et al., 2025; Q. Zhang et al., 2025). However, as reported in a recent study (D. Chen et al., 2025), data from China's satellite fleet remain largely inaccessible to the international community due to factors such as lack of centralized and user-friendly access portals, insufficient metadata and documentation, and low interoperability with global platforms. Coordination with China's SAR missions has therefore not been considered in this study.

2. SAR-Enabled Science Disciplines

2.1. Ice Sheets and Glaciers

SAR data in interferometric mode have revolutionized the study of ice sheets and glaciers since the 1990s. These data have provided the first comprehensive coverage of ice velocity of the large ice sheets in Greenland and Antarctica and, in combination with optical data, the first comprehensive coverage of the velocity of the Earth's glaciers and ice caps (GIC). For the ice sheets, this achievement resulted from not one but multiple SAR missions not originally designed for ice mapping: ESA's Earth Remote Sensing (ERS-1/-2), Envisat ASAR, and Sentinel-1a/1b, JAXA's PALSAR-1/-2, CSA's RADARSAT-1/-2 and Radarsat Constellation Mission (RCM), ASI's COSMO-SkyMed, DLR's TerraSAR-X and TanDEM-X, and more recently the commercial venture ICEYE (Mouginot et al., 2019; Rignot et al., 2024). In addition to ice velocity, SAR data have been used to identify the

Table 1
Selected SAR Missions in Operation as of August 2025

Mission	Band	Center frequency/ wavelength	Orbit revisit	Agency	Country/Region	Launch year
Biomass	P	435 MHz/69.0 cm	N/A	ESA	Europe	2025
ALOS-4 PALSAR-3	L	1236.5 MHz/24.3 cm	14 days	JAXA	Japan	2024
ALOS-2 PALSAR-2	L	1236.5 MHz/24.3 cm	14 days	JAXA	Japan	2014
SAOCOM-1A/1B	L	1,275 MHz/23.5 cm	16 days	CONAE/ASI	Argentina/Italy	2018 & 2020
NISAR	L + S	1,257 MHz/23.9 cm 3,200 MHz/9.4 cm	12 days	NASA/ISRO	USA/India	2025
NovaSAR-1	S	3,200 MHz/9.4 cm	16~17 days (drifting orbit)	UKSA/SST	United Kingdom	2018
Sentinel-1A/B[a]/C/D	C	5,405 MHz/5.55 cm	12 days (1 sat)	ESA/EU	Europe	2014/2016/2024/ 2025
RISAT-1A (EOS-04)	C	5,350 MHz/5.61 cm	12 days	ISRO	India	2022
RCM-1/2/3	C	5,405 MHz/5.55 cm	12 days (1 sat)	CSA	Canada	2019
RADARSAT-2	C	5,405 MHz/5.55 cm	24 days	CSA/MDA	Canada	2007
TerraSAR-X/TanDEM-X	X	9,650 MHz/3.1 cm	11 days	DLR	Germany	2007/2010
COSMO-SkyMed (CSK-1/2/4)	X	9,600 MHz/3.1 cm	16 days (1 sat)	ASI	Italy	2007/2007/2010
COSMO-SkyMed 2nd Generation (CSG-1/2)	X	9,600 MHz/3.1 cm	16 days (1 sat)	ASI	Italy	2019/2022

Note. MDA = MDA Space Ltd., EU = European Union, SST = Surrey Satellite Technology Ltd., UKSA = United Kingdom Space Agency. Source: eoPortal, https: www.eoportal.org; see for information on the different modes, polarizations, and spatial resolutions. [a]Sentinel-1B failed in December 2021.

grounding line positions, where ice detaches from the glacier bed and becomes afloat in the ocean waters, with high precision, in North Greenland and the entire Antarctic periphery for the first time, thereby resolving major uncertainties in ice fluxes into the ocean and rates of ice melt in the ocean (Rignot et al., 2011). The TanDEM-X mission has provided a modern, precision reference digital elevation model (DEM) for the ice sheets, which is widely used in the science community as well as during the generation of geophysical information products like ice velocity (e.g., Figure 1) and grounding line maps.

With the exception of Sentinel-1, which has a priority commitment to cover coastal Antarctica and Greenland with interferometric data at mission repeat cycles, current science acquisitions over ice sheets happen predominantly in support of individual principal investigators' projects, as part of international collaborations, or as in-kind support by agencies. Inter-agency coordination has been working effectively for the ice sheets starting with preparations for the second International Polar Year of 2007–2008, initially thanks to the vision of program managers operating the SARs for the space agencies, and since then under the leadership of the Polar Space Task Group (PSTG). The group collected input on science requirements from the community and evaluated existing

Table 2
Selected Legacy SAR Missions

Mission	Band	Center frequency/wavelength	Orbit revisit	Agency	Country/Region	Years of operations
Seasat SAR	L	1275 MHz/23.5 cm	17 days	NASA	USA	1978–1978
JERS-1 SAR	L	1275 MHz/23.5 cm	44 days	JAXA	Japan	1992–1998
ALOS PALSAR	L	1270 MHz/23.6 cm	46 days	JAXA	Japan	2006–2011
ERS-1/2 AMI	C	5300 MHz/5.66 cm	35 days	ESA	Europe	1991–2000 1995–2011
Envisat ASAR	C	5331 MHz/5.63 cm	35 and 30 days	ESA	Europe	2002–2012
RADARSAT-1	C	5300 MHz/5.66 cm	24 days	CSA/MDA	Canada	1995–2013
RISAT-1	C	5350 MHz/5.61 cm	12 days	ISRO	India	2012–2017

Note. source: eoPortal, https:www.eoportal.org.

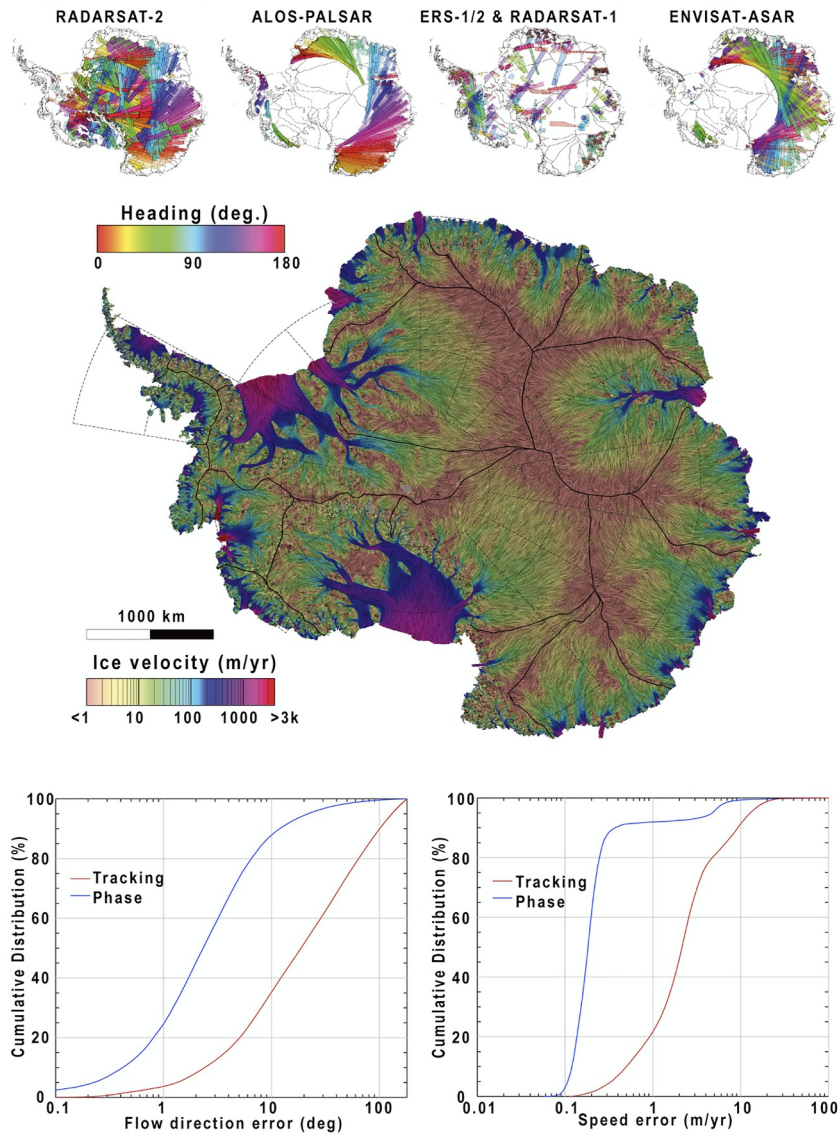

Figure 1. 2D reference velocity mapping of ice motion in Antarctica using SAR interferometric phase data collected over a period of 25 years. Upper panels show the distribution of data tracks from the contributing missions, which were coordinated through the PSTG. Central panel shows a complete map of ice motion in Antarctica combining phase data in vast sections and speckle tracking for fast-moving glaciers with speed colored on a logarithmic scale from brown (less than 1 m/yr) to red (more than 3 km/yr), and flow direction indicated by colored lines and showing the flow pattern of ice across the continent. (Bottom) Plots highlight the order of magnitude improvement of phase-based results over tracking-based results. (Adapted from Mouginot et al., 2019).

agency programs and mission capabilities to address gaps in available coverage. Acquisition plans for Envisat ASAR, ALOS PALSAR, RADARSAT-2, TerraSAR-X/TanDEM-X, and COSMO-SkyMed were coordinated through this group. Key achievements include establishing the SAR Coordination Working Group (SAR-CWG), collecting thousands of radar images for ice sheet, floating ice, permafrost, and snow studies, and acquiring crucial data for expeditions like MOSAiC (Nicolaus et al., 2022) that filled previously data-void "pole holes."

It was largely through PSTG that both full data coverage for ice sheets was enabled and regular coastal coverage was eventually implemented for Sentinel-1, augmented by more campaign-style coverages from other missions. At present, we have Sentinel-1 6-to-12-day repeat over the coastal sectors of the ice sheets and limited InSAR acquisitions and data access to ALOS-2 PALSAR-2, ALOS-4 PALSAR-3, and SAOCOM data to measure speed, grounding line position, and ice edge position. In addition, we have limited coverage over fast glaciers with focus

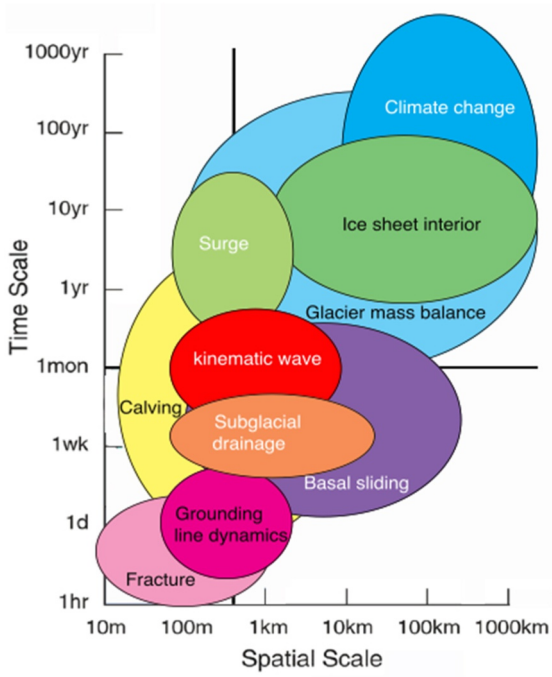

Figure 2. Stommel diagram of physical processes of importance to ice sheet evolution versus time scale and spatial scale. Past and current missions have addressed continental to glacier spatial scales and temporal scales of months to days. Key physical processes conducive to rapid change—and rapid sea level rise—operate on smaller spatial scales (10–100 m) and shorter time scales (daily to sub-daily).

on grounding line retrieval with 1-day repeat CSG-1/2 or ICEYE data, as well as 4-day repeat coverage from RCM (with wider accessibility). Yet it should be stressed that while hugely successful, most commitments are short term and/or for background or best effort acquisitions; thus ongoing coordination remains crucial in this context.

As a result of this virtual constellation, the community has obtained comprehensive information on ice flow, ice discharge, ice mass balance, and the contribution of ice sheets to sea level rise; areas of rapid change contributing to sea level due to changes in glacier speed; and insights into the role of ice dynamics in ice sheet mass balance and the role of the ocean in driving these changes, that is, information on the physical processes driving these changes, that is, most relevant to projections of sea level rise in a warming world. Ice dynamics holds the largest potential for rapid sea level rise in the future, hence the need to continue to improve our understanding and monitoring. After upgrading from multi-year comprehensive velocity maps to annual maps, the scientific community is migrating to monthly maps. Grounding line mapping previously conducted over multiple years is now conducted at the annual to monthly basis and, in select areas, even daily scales to reveal grounding line migration at tidal periods to form a grounding zone and, more importantly, provide an opportunity to measure previously unknown kilometer-scale intrusions of seawater beneath glaciers (Figure 2). These rapid interactions between ice and ocean are thought to be the cornerstone of ice sheet evolution in a warmer climate. Much remains unknown, however. To date, a number of processes that control the rapid decay of ice sheets remain poorly observed, not well understood, and not well represented in models. In turn, this lack of observations is a fundamental limitation for the reliability of projections of sea level rise from models, and in particular to assess the risks and thresholds for rapid sea level rise associated with partial collapse of the ice sheets.

While current achievements have been spectacular and will be improved upon with existing and upcoming missions, much more remains to be done. We need to extend high data quality at daily and sub-daily timescales, reduce data noise in the vast interior, and map ice velocity in three dimensions (3D) instead of two dimensions (2D) (Minchew et al., 2015, 2017; Reeh et al., 2003). Current methods assume surface parallel flow, which is acceptable in most areas except in the vast interior of the ice sheets and over rapidly melting mountain glaciers. Resolving 3D velocity vectors, however, provides additional information on ice thinning or surface mass balance or both. To do this with precision in the ice sheet interior, where speed is a few centimeters per year, it is essential to map ice velocity with the interferometric phase instead of speckle tracking, because the resulting precision is 10 times better, from 1 m/yr to 10 cm/yr (Mouginot et al., 2019). If we do so, we will resolve changes in velocity and in how far and fast upstream changes occurring at the coast propagate inland (e.g., Minchew et al., 2017). Resolving this pattern will help constrain the sliding law used in ice flow models, which remains a topic of considerable uncertainty.

In the near term, improvements can be achieved with current space assets by providing more comprehensive acquisitions and by increasing access to available data. Improvements that are already possible include: (a) regular InSAR acquisitions in coastal Antarctica with different geometries (a diversity of imaging geometry can be implemented with multiple missions); (b) occasional, but regular coverage of the ice sheet interior (i.e., 2–3 times per year), again with a diversity of imaging geometry; and (c) regular, short repeat InSAR coverage of fast flowing glaciers for grounding line retrieval. A comprehensive, multi-agency, coordinated plan together with long-term commitments by the agencies involved would likely make this possible using the currently available assets and would move the existing virtual constellation into a more sustainable and reliable data source for ice sheet science. Added to this mix will soon be the NISAR mission, a dedicated science mission with 12-day repeat InSAR L-band data collected for both ascending and descending orbits over the entire Antarctic Ice Sheet and a large portion of Greenland. NISAR also carries an S-band radar which will be useful for grounding line mapping because the shorter wavelength is more sensitive to vertical motion. NISAR, which is left-looking, is expected to

significantly strengthen the virtual constellation, but not replace it. Geometry and radar frequency diversity with existing missions will further improve our ability to precisely map speed at various spatial resolutions, look angles, and temporal revisit times. The higher revisit frequencies of RCM, COSMO-SkyMed, and ICEYE will remain a crucial component for grounding line measurements over fast-moving glaciers. Another new aspect in SAR data collection strategy will be ESA's Harmony companion satellite mission for Sentinel-1 (López-Dekker et al., 2019) to be launched in 2029, which will offer better viewing angle diversity for 3D mapping at a 12-day repeat, hence bringing to the table a cartwheel architecture of SARs (Massonnet, 2013) that enables a greater diversity in measurement strategy.

A future observation system must be capable of providing interferometric phase measurements from sub-daily to weekly time scales. Current long repeat cycles make it challenging to understand the processes of iceberg calving, ice shelf rifting, and glacier fracturing, which operate on hourly to sub-daily time scales and can be the source of rapid mass change or hazards (e.g., Bindschadler et al., 2003; Kim et al., 2024). Maintaining phase coherence over fast flow areas is essential to map grounding lines and their migration. It has also become apparent that 3D mapping with phase-only data cannot be achieved with a single SAR satellite due to the vast range of temporal and spatial requirements. For instance, data stacking and lower resolution (a few 100 m) is needed in the ice sheet interior to resolve motion of ∼1 cm/yr. In contrast, at the other end of the spectrum we have fast glaciers moving meters per hour where changes need to be captured at a spatial sampling of a few 10s of meters. Further, we will need more than one satellite, or constellation, to provide a diversity in look angles of the ice simultaneously instead of at different times in order to do a precise 3D mapping.

In terms of wavelength, prior work has demonstrated greater phase coherence at longer wavelengths, but also greater sensitivity to ionospheric effects. When phase coherence is high, shorter wavelengths yield more precise measurements. Longer wavelengths penetrate deeper into snow and firn and interact with larger scatterers, which provide better temporal stability of the interferometric phase compared to shorter wavelengths. Measurements of ice motion obtained at different wavelengths can be combined if they are weighted according to their respective noise levels (Rignot et al., 2011).

In terms of polarization, relatively little work has been conducted using polarimetric data over ice sheets. HH-polarized signals from RADARSAT tend to yield higher coherence levels than VV-polarized signals from ERS-1/2 and Envisat ASAR in Antarctica. This is generally attributed to the greater penetration of horizontally polarized signals into snow and firn (Rott et al., 2010). The value of polarization diversity is also greater at longer wavelengths (e.g., L- and P-band), because radar returns become more sensitive to ice fabric properties, such as crystal orientation.

Inter-agency coordination for SAR data acquisitions in polar regions has been shown to work well in utilizing a virtual constellation that was not planned for, but that provided more information than any single mission could. Inter-agency coordination during future mission conceptualization and formulation would provide the nucleus for an international constellation of SARs for ice sheets and glacier observations with a fast repeat, high spatial resolution, a comprehensive view of the ice sheets, with a diversity in look angles and simultaneous acquisitions, none of which is achievable by a single SAR mission.

2.2. Solid Earth Science

With centimeter-scale sensitivity, meter-scale spatial resolution, and spatial extent of 100s of kilometers, InSAR has provided essential information about the different phases of the seismic cycle (i.e., interseismic, coseismic and postseismic, as well as aseismic creep), processes associated with the migration of magma in the subsurface, seasonal and inter-annual variations in shallow aquifers pressures, and slow-moving landslides (e.g., Amelung et al., 1999, 2000; Bekaert et al., 2020; Cetin et al., 2012; Hu & Bürgmann, 2020; Hussain et al., 2016; Simons et al., 2002). InSAR observations have allowed a new generation of inferences on the distribution of subsurface slip on faults (e.g., Bletery et al., 2020; Delouis et al., 2010; Jónsson et al., 2002; Wright et al., 2004), the rheology of the crust and upper mantle (e.g., Henriquet et al., 2019; Mallick et al., 2022; Rousset et al., 2012), the location and geometry of major magma reservoirs (e.g., Fialko, Simons, & Khazan, 2001; Pritchard & Simons, 2002; T. Wang et al., 2021; Yun et al., 2006), and the impacts of natural and anthropogenic processes on aquifers (e.g., Amelung et al., 1999; Carlson et al., 2024; J. Chen et al., 2016; Riel et al., 2018). InSAR processing has now advanced to a level that with sufficiently long time series, one can quantify the translation of selected tectonic

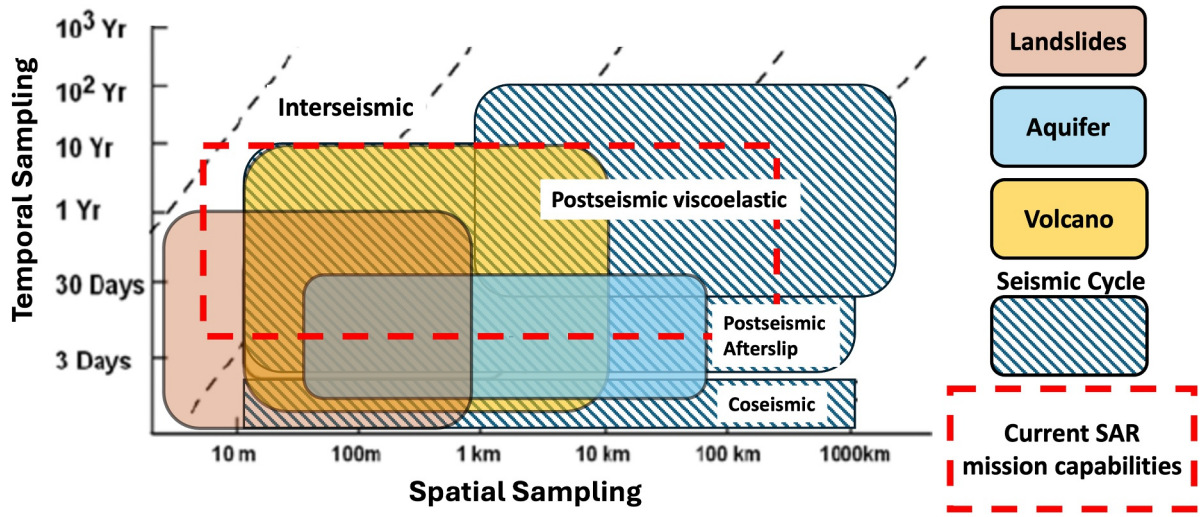

Figure 3. The temporal and spatial sampling rate required for different solid Earth science targets.

plates across the globe (Y.-K. Liu et al., 2025) and the strain rate over vast regions spanning thousands of kilometers (Elliott et al., 2026).

The expansion of the international constellation of SAR instruments has allowed an ever-expanding set of science targets, largely driven by the evolution from a few sporadic image acquisitions allowing for a few interferograms, to what is now possible with combinatorics of 100s of repeat acquisitions. A variety of imaging modes, including ScanSAR, TOPSAR, Stripmap, and Spotlight, offer a range of spatial resolutions and swath widths. Wide-swath modes, such as ScanSAR and TOPSAR, enable shorter repeat cycles and more frequent global data collection. The conventional Stripmap mode provides continuous imaging at meter-level resolution while Spotlight offers ultra-high resolution (sub-meter) measurements over small, targeted areas. Moreover, the availability of high-rate, high-resolution data sets from commercial SAR constellations has enabled unprecedented detail in monitoring some geophysical processes, such as magma movement within volcanic conduits (Wollersheim, 2022).

As we strive to separate the impacts of different geophysical processes using InSAR (e.g., co-seismic and post-seismic fault slip, the superposition of seasonal and tectonic processes, or a rapidly evolving restless caldera), having continuous and consistent data is essential. Despite the increasing volume of SAR data and the expanding range of science targets, several limitations still constrain our ability to analyze certain geophysical processes. Figure 3 shows that the major gaps given present capabilities relate to those targets requiring short temporal sampling. Not shown, but equally important, is the need for 3D imaging of deforming surfaces to improve models.

Regarding the temporal sampling, at this time the repeat interval spans nearly a week or longer for most current and near-future SAR missions, especially those with open data policies, which limits our ability to observe fast-evolving processes such as some ground movements coupled to hydrologic processes (e.g., tidal phenomena, rain-induced landslide acceleration) and rapid volcanic processes. While missions such as COSMO-SkyMed and commercial SAR satellites, such as those operated by ICEYE and Capella Space, offer daily repeat measurements over selected regions, it has become increasingly important to decrease the typical interval between global routine repeat imaging from weeks to a day or even less.

Furthermore, as we use these data to constrain geophysical models, observations of the full three-component surface displacement field also become important. Indeed, once we have sufficient observations allowing for a 3D-decomposition, it becomes possible to fold observations from the entire international constellation of InSAR-capable satellites into a single estimate of the time-dependent (east, north, up) surface displacement field. However, InSAR's inherent insensitivity to along-track motion for current missions limits our ability to achieve a full 3D decomposition. Techniques such as pixel offset tracking and Multi-Aperture SAR Interferometry (MAI) go some way in addressing this limitation but suffer from limited resolution and a precision that is orders of magnitude worse than InSAR (e.g., Fialko, Simons, & Agnew, 2001; Fielding et al., 2013; Mastro et al., 2020; C. Wang et al., 2015). Sentinel-1's TOPSAR mode provides an increased diversity in squint angles within burst

overlap areas, hence allowing burst-overlap interferometry to capture along-track motion with better resolution, although still poor precision (e.g., X. Li et al., 2021). However, this technique is restricted to burst overlap regions and cannot provide spatially continuous mapping. Satellites with a mid-inclination orbit, such as those operated by Capella Space and the upcoming ASI/ESA IRIDE constellation (Orusa et al., 2024), provide an alternative way to add sensitivity to the third component of the deformation field, although the coverage is limited to lower latitudes.

We also aim to resolve smaller and smaller surface displacement signals with InSAR. Temporal interferometric decorrelation and noise related to path delays of different origins (e.g., atmosphere, soil moisture) are the primary current limitations of our measurement ability (e.g., Agram & Simons, 2015; Ansari et al., 2020; De Zan et al., 2014; Hanssen et al., 1999; Zebker & Villasenor, 1992; Zheng et al., 2022). We can account for path delays using combinations of techniques, for example, GNSS-like split-band processing to infer ionospheric impacts or model-derived or direct inferences of troposphere delays (Bekaert et al., 2015; Jolivet et al., 2011, 2014; Liang et al., 2019). Additionally, machine learning methods have shown promise in extracting millimeter-scale signals (e.g., Rouet-Leduc et al., 2021). Short repeat intervals reduce the impact of temporal decorrelation and provide more observations for slowly evolving processes, and hence can be used to overcome the impacts of noise sources that are random in time. In addition, the use of longer wavelength radar (e.g., L- or S-band) reduces decorrelation, thereby allowing one to observe events (e.g., earthquakes and eruptions) in highly vegetated environments, as are typically found in near-equatorial regions. The NISAR mission operates with both L- and S-band left-looking radars and has near-global L-band land coverage and selected areas of multi-frequency acquisitions. Measurements from NISAR will improve data quality over densely vegetated areas compared to C-band and X-band radars.

None of the current or booked missions provide the daily repeat sampling from the same imaging geometry and SAR wavelength, line-of-sight (LOS) diversity, and path delay correction capabilities that we know are possible, albeit requiring a constellation. In the short term, coordination of acquisitions from the operational SAR missions to increase LOS diversity for limited or regional studies could be recommended through a 3D-InSAR Task Group, as was done by the PSTG. There is much that could be achieved through shared observation planning and distributed commitments among the space agencies to acquisitions over study sites. Furthermore, because InSAR requires consistent observations, moving toward a fixed observation plan is recommended, at least over tectonically active areas. Open access to L-band SAR data from SAOCOM and ALOS-2/4, even if only the archives, will help extend the time series of InSAR data for many sites of interest. Going forward, adding or maintaining InSAR capability should be encouraged for commercial SAR missions to increase their data's utility for solid Earth science. The value of multi-frequency SAR for path delay corrections should be explored with the NISAR simultaneous L-band and S-band data sets, and the results accounted for in future missions and mission coordination.

In the long term, future missions designed to address these gaps and challenges could significantly advance our ability to meet science goals in solid Earth research. One effective way to increase the temporal sampling rate of a single SAR mission is by deploying additional SAR satellites in the same orbit, as has been done for Sentinel-1 and RCM, but also considering inter-agency, international coordination of missions. A single geostationary SAR could provide daily repeat sampling, but this comes with trade-offs, such as the loss of global coverage and challenges like rotational decorrelation (C. Hu et al., 2021; Monti et al., 2025), and the data must be open source to combine with other imaging geometries. Increasing LOS diversity of observations can also be accomplished through a combination of left- and right-looking observations from ascending and descending orbits, and potentially observations from highly squinted imaging geometries. To achieve direct path delay correction and 3D deformation reconstruction, simultaneous interferometry from multiple LOS directions is necessary. Flying companion satellites in close formation with existing missions, such as the ESA's planned Harmony mission, enables new observation capabilities, which include 3D deformation reconstruction by leveraging multiple LOS directions, as well as enabling single-pass interferometry to measure high-precision changes in ground elevation.

2.3. Hazards

Hazards can be caused by either natural phenomena or human activities, and many are accompanied by surface changes detectable in the SAR amplitude or interferometric observables. The temporal development of hazardous phenomena varies greatly, from slowly developing conditions like land subsidence to catastrophic events that can

last only seconds and encompass both those that can be forewarned through observation or modeling and those for which little or no warning can be given. In all cases, a regular cadence of observations to monitor the evolution of surface conditions is needed so that the normal variation is known and possible changes forewarning disasters or at-risk areas are identified. This requirement for consistent and sustained SAR observations is shared by the other topical areas discussed in this paper. Therefore, this section addresses the needs specifically for disasters, covering the short-term period building up to an event through the response and immediate recovery phase (called herein "response").

The most common major natural disasters, measured by activations of the International Charter (https://disasterscharter.org/web/guest/home), can be generally categorized as weather-related or geological, and the most common human-related major disasters are fires and oil spills. Overall, weather-related disasters are the most common, specifically floods and hurricanes/typhoons, for which imaging without solar illumination and through clouds is paramount.

Although SAR amplitude and InSAR phase and coherence all can contain information to support disaster response, there is no one-size-fits-all solution in terms of frequency, mode, or spatial and temporal resolution for this purpose. SAR amplitude is used in operationalized measurement of ocean winds (e.g., Monaldo et al., 2013) and oil spills (e.g., KSAT Oil Detection Service, NOAA Marine Pollution Surveillance Program). Longer wavelength SAR has higher wind speed cut-offs, hence is better for measuring hurricane winds. For oil spill response the VV polarization channel is best, having the highest contrast (Espeseth et al., 2020). Coherent change detection is increasingly being used to generate damage proxy maps (Fielding & Jung, 2024; Tay et al., 2020), and monitoring volcanoes with InSAR is done in the United States by the U.S. Geological Survey (USGS) (e.g., USGS, 2023) and in Japan by the Geospatial Information Authority of Japan and the Japan Meteorological Agency (https://maps.gsi.go.jp/; https://www.jma.go.jp/jma/kishou/shingikai/ccpve/CCPVE.html). Much work has been done on flood mapping with a variety of methods (Amitrano et al., 2024) including combining SAR amplitude or optical data with weather and hydrodynamic models (e.g., Schumann et al., 2023), combining SAR amplitude and InSAR coherence (e.g., Y. Li et al., 2019), and using machine learning (ML) or artificial intelligence (AI) (Destefanis et al., 2025). Nonetheless, identifying flooding in urban areas remains a challenge (Zhao et al., 2024). Sentinel-1 is now used in the Global Flood Monitoring (GFM) service (Wagner et al., 2026) and for the Operational Products for End-Users from Remote Sensing Analysis (OPERA) surface water extent product (https://podaac.jpl.nasa.gov/dataset/OPERA_L3_DSWX-S1_V1).

Having consistent pre-to-post SAR images is crucial for most disasters since fundamentally one is observing change to identify and quantify impact. Measuring surface deformation with InSAR requires two images acquired with compatible radar characteristics (frequency, polarization) and the same imaging geometry (orbit, look direction). Observation plans that do not change, for example, those of Sentinel-1 and the NISAR L-SAR, satisfy the criterion of consistent imaging mode automatically. However, in some cases there is a competing practical desire to tailor the observations to the disaster type, that is, carry out emergency observations according to the user's requirements on observation mode, beam direction, swath, and spatial resolution given the characteristics of a particular disaster. In this case, if a set of images acquired with various observation conditions is prepared in advance of a disaster, it is possible to quickly and accurately estimate the differences pre-to-post disaster by selecting images already available, no matter what observation conditions are used for disaster response. The design and operation of a system that can continually maintain a variety of data acquired in different modes to respond flexibly to user needs, such as the ALOS-2 Basic Observation Scenario (https://www.eorc.jaxa.jp/ALOS-2/en/obs/pal2_obs_guide.htm), would satisfy this need.

Disaster response requires prompt and reliable delivery of information to responders. Reducing the time between when an event occurs and when SAR-derived information products of use to responders are available is the most critical factor influencing adoption of SAR for disaster response. One of SAR's most significant contributions to remote sensing in general, namely deriving surface displacement using InSAR, remains a capability with great but not fully realized potential for aiding response to geological disasters largely because of the latency issue. The latency needs to be reduced at each step in the process: delay in imaging an area (satellite tasking and overpass), downlinking the data, SAR processing, generating information products, and delivering products to the end users. Today's SAR products can be very large (e.g., the NISAR Hierarchical Data Format 5 (HDF5) files), so cloud computing is needed to avoid downlink. Further challenges to rapid processing of data from a diverse collection of

SAR sensors are the lack of a standard data format, no unified data storage system across sensors, different data access methods, and a lack of processing tools to go from SAR products to the information of use to non-experts.

In recent years, various systems have been built to automatically perform InSAR processing, including specifically to support disaster response, and provide crustal deformation information, such as the Advanced Rapid Imaging and Analysis (ARIA) system (https://aria.jpl.nasa.gov/), Alaska Satellite Facility (ASF) Data Search Vertex (https://search.asf.alaska.edu/#/), and the Looking Into Continents from Space with Synthetic Aperture Radar (LiCSAR) system (https://comet.nerc.ac.uk/comet-lics-portal). These efforts contribute to reduced latency for response, but more can be done to lower latency, ideally in the entire sequence of activities. As an example of a very impactful action that can be taken now, consider the fact that not all the space agencies process and deliver any SAR products with very low latency, ≤1 hr. Were these available, even within a rolling, unarchived database, a SAR mission's utility for disaster response would be greatly improved.

Nevertheless, because the frequency of observations from a single satellite is limited by the orbit repeat period, generally 12 days or more for typical swath widths, observations from multiple satellites are essential for further improvement. Multiple satellites operated by a single space agency are one of the solutions, but a virtual constellation under international cooperation would be a realistic solution to improve the frequency of observations while reducing the costs to any one agency. This could be done between two or more agencies. As an example, combining ALOS-2 and COSMO-SkyMed (CSK—Product processed under a license of the Italian Space Agency) imaging for volcano monitoring (Figure 4) reduced the time between imaging by as much as 91 hr and enabled observations with 5–6 hr separation not otherwise possible. Additionally, agencies will increasingly need to account, and possibly limit, the number of new satellites launched to avoid overuse of orbital "real estate." Shared resources will negate the need for individual agencies to have their own suite of SAR sensors, reducing the total number of satellites in orbit.

As a coordinated activity among space agencies, that is, possible within the scope of current and near-future missions, the greatest and most immediate benefit would come from a worldwide disaster response initiative through which tasking, downlink, and processing could be expedited for disaster response, expanding upon the post-disaster actions of the International Charter. This multi-agency "Smart Tasking" for Disaster Response system would automatically trigger acquisitions and processing within the suite of available instruments for a range of disaster types, for example, based on earthquake magnitude and location, and expedite activation for those without automatic triggers, for example, through API request handling from affiliated agencies. Acquisitions would not be limited to events that activate the Charter only after a major disaster, enabling pre-event acquisitions for an anticipated major disaster (typhoon, hurricane) or for smaller disasters before or without formal Charter activation. The commercial SAR companies could contribute to significantly reducing acquisition latency through their rapid tasking capability and multi-satellite constellations were they to join the initiative. Free and open access to the acquired SAR data and derived products will fully and equitably share the benefits of the initiative and encourage SAR's adoption and utilization for response.

The most significant, and challenging, advancement for both science and society will result from coordinated, increased, and targeted temporal sampling by InSAR-capable instruments that results in latency of a few hours for major disasters worldwide. Near-future missions will improve sampling simply because there will be more Earth-observing SAR instruments, but in the long-term, inter-agency coordination of orbits and observation plans for new missions, for example, focused to known areas with geological hazards, would significantly advance SAR's utility for understanding and responding to natural hazards. For general response to disasters of any type worldwide, a distributed constellation is preferred over near-simultaneous acquisitions to reduce the latency to first-imaging anywhere on the globe after a disaster occurs. A coordinated, multi-SAR, multi-mission system that supports both monitoring and imaging within hours of an event would serve both society and science by providing situational awareness information for disaster response at the same time as measuring transient and cascading processes.

2.4. Forests and Biomass

One of the longest-running applications of satellite remote sensing has been the characterization and monitoring of land cover and forest resources. With its basic sensitivity to structure, penetration through clouds, and day/night-time observing capability, SAR has long been recognized as a cornerstone in this development (Dobson et al., 1992; Le Toan et al., 1992; Pulliainen et al., 1996; Ranson et al., 1997; Ranson & Sun, 1994; Sader, 1987).

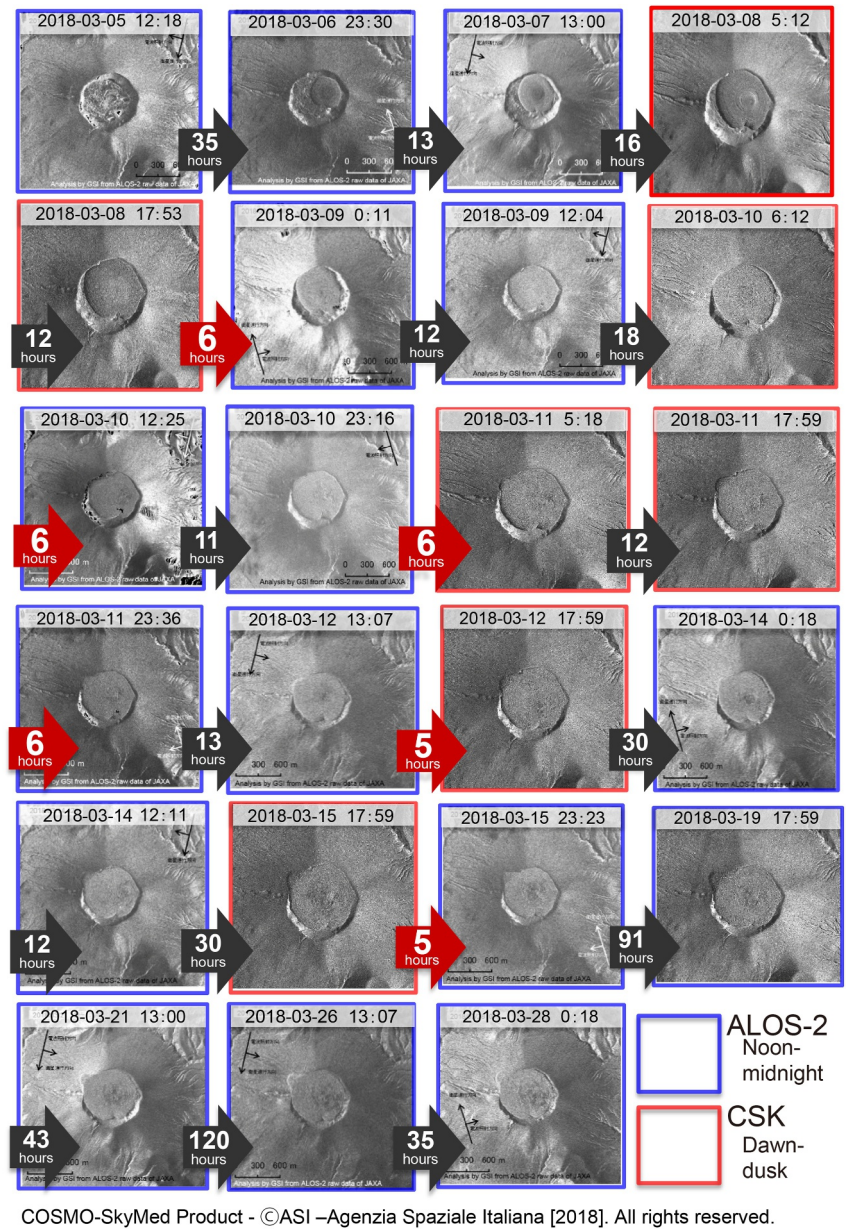

Figure 4. Time series of intensity images showing lava growth in the crater of Shinmoedake volcano in Japan. Blue and red frames represent images acquired by ALOS-2 and CSK, respectively. The number in an arrow indicates elapsed time preceding a previous observation. With the addition of CSK, latencies of 6 hr or less were achieved. The date and time are in Japan Standard Time. (CSK—Product processed under a license of the Italian Space Agency).

Because of the longer wavelengths at the lower end of the microwave regime, P- and L-band have been the most promising frequencies for forest and biomass spaceborne monitoring. C-band SAR is sensitive to forest properties, but environmental conditions (e.g., moisture and temperature) can cause substantial distortion of the signal (Pulliainen et al., 1999; Santoro et al., 2011). Forest biomass monitoring with SAR benefits from the use of multiple polarizations, particularly HH- and HV-polarized observations, due to volume scattering and the depolarizing nature of forest structure (Treuhaft & Siqueira, 2000). With fully polarimetric (horizonal transmit/horizontal receive (HH), horizonal transmit/vertical receive (HV), vertical transmit/horizontal receive (VH), and vertical transmit/vertical receive (VV); also called quad-polarimetric (QP)) data, the individual scattering mechanisms can be derived, providing more diverse information about the vegetation structure (Freeman & Durden, 1993; van Zyl et al., 1987; Yamaguchi et al., 2005).

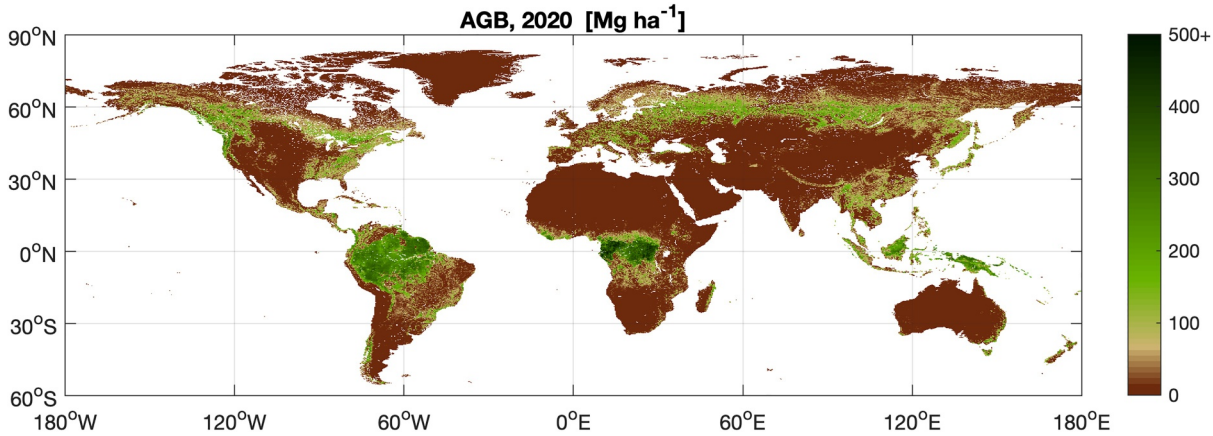

Figure 5. ESA's Climate Change Initiative (CCI) Biomass map of above-ground biomass (AGB) for 2020 with a spatial resolution of 100 m based on ALOS-2 PALSAR-2 and Sentinel-1 observations. The AGB values are clipped between 0 and 500 Mg/ha to enhance color contrast. (*Source:* Santoro et al., 2024) (https://creativecommons.org/licenses/by-nc-nd/4.0/).

The potential of SAR sensors to estimate forest above-ground biomass on a regional to global scale has been well demonstrated (e.g., Bouvet et al., 2018; Lucas et al., 2010; Rodriguez-Veiga et al., 2019; Santoro et al., 2015, 2022, 2024). In recent years, there have been several major advances in the remote sensing of forests and estimates of biomass (Figure 5). These include demonstrations of the value of (a) systematic global-scale observations of dense time series, especially when made available as free and open data; (b) increased diversity of radar frequency bands, and in particular availability of a spaceborne P-band mission; (c) the use of interferometry, sometimes polarimetric interferometry, in characterizing the vertical structure of the forest; and (d) missions with improved capacity for SAR polarimetry.

The first two of these advances began with the availability of data from ERS-1/2 and JERS-1 in the 1990s, followed by ALOS and Envisat ASAR in the 2000s, and continued in the last decade with the Sentinel-1, ALOS-2/4, SAOCOM-1, and most recently the Biomass and NISAR missions. Large-scale monitoring of forest resources at continental and global scale can now be realized, especially through the use of a dense time series as a complementary signature of equal value to polarization and frequency diversity, which has yet to be fully explored. The P-band Biomass mission (Quegan et al., 2019) can furthermore be expected to be a game-changer in the tropical zone, where the high biomass levels exceed what can be mapped with a single image acquired at shorter wavelengths (Cartus et al., 2019). In the upcoming years there will be SAR missions operating in all frequency bands and complemented by ICESat-2, Global Ecosystem Dynamics Investigation (GEDI), and Multi-sensing Observation LiDAR and Imager Demonstration (MOLI) spaceborne LiDAR observations, so major improvements in the remote sensing of forests and estimation of biomass are expected.

The third of the advances, with interferometry, has proven to be more challenging because single-pass interferometric missions like TanDEM-X and the Shuttle Radar Topography Mission (SRTM), capable of measuring the frequency-dependent topographic height in forest canopies, are more the exception than the rule and require additional spatial data sets to convert elevation to biomass (Persson et al., 2017; Schlund et al., 2015, 2020; Soja et al., 2015). Repeat pass InSAR with multiple polarizations and/or multiple baselines (Pol-InSAR and Tomo-SAR) (Garestier & Le Toan, 2009; Kugler et al., 2015; Lombardini & Pardini, 2008) to measure 3D structure has been demonstrated on the small scale (e.g., El Moussawi et al., 2019; Hajnsek et al., 2009). Repeat-pass interferometry suffers from the additional complication of temporal decorrelation, which has also been explored as a signature in its own right (Askne et al., 1997; Eriksson et al., 2003; Koskinen et al., 2001; Lei & Siqueira, 2014; Santoro et al., 2002).

The fourth advance, namely SAR polarimetry, has shown promising potential for above-ground biomass and canopy height retrieval (Omar et al., 2017; Seppi et al., 2024). However, progressing polarimetric applications from research to operations is yet to be achieved. With the SAR missions to date mainly having operated in dual-polarization mode, the scarcity of time series of fully polarimetric data over key forest ecosystems has held back the development of relevant polarimetric methods. However, the recent Biomass and ALOS-4 missions have the

capacity for operational fully polarimetric observations and could be game changers for polarimetric forest applications.

Coordination efforts to move SAR satellite technology forward for forest applications can be broken down into three basic parts: (a) an analysis of the current status of existing and soon-to-be existing sensors; (b) evaluating what can be done in the coming years (e.g., 2025–2035) with these sensors to improve the characterization and measurement of forest ecosystems; and (c) identifying what is needed in the long-term in the way of game-changing observational assets that could be used by the community. Related to the first of these, the field is in a dramatic state of flux. With the successful launches of the ALOS-4, Biomass, and NISAR missions, new multi-frequency data sets will be created that cross the spectrum of wavelengths, polarizations, and revisit times, and are expected to change the way that SAR data are used for forest and biomass applications. Several new and follow-up SAR missions are also planned to be operated in the next coming years in all frequency bands, so this type of data is expected to continue to be available. Furthermore, there is demonstrated complementarity between SAR and LiDAR and optical data, that is, addressing some of the pressing challenges of forest and biomass science (Khati et al., 2021; Lucas et al., 2006; Santoro et al., 2024; Shendryk, 2022).

Looking towards the near future, the challenges are not so much in collecting needed data, but rather in coordinating observations from these data sets, in handling the large data volumes, and in learning how to make best use of the data. Coordination with other EO sensors for near-coincident measurements would be challenging, but valuable. For example, near-coincident SAR and Sentinel-2 Multispectral Imager (MSI) collections support development of joint SAR/multispectral algorithms for above-ground biomass (AGB) estimation. To deal with the large amounts of data, forest and biomass mapping can profit from machine learning algorithms or parametric modelling frameworks. The implementation of some of these concepts and handling the necessarily large data rates and volumes will be very ambitious and therefore best realized through collaborative efforts of multiple space agencies and resource managers, a worthy goal for formulation and development in the coming decade. There also must be sufficient reference data available for training and calibrating/validating algorithms and models. Coordinated efforts to collect and provide open access data for calibration/validation (cal/val) sites is essential, as is liaising with communities that undertake field inventories to ensure that biomass estimates from SAR are unbiased.

In the long term, to realize today's futuristic concepts of Pol-InSAR/TomoSAR applications for forest and biomass monitoring, there should be a coordinated effort to establish a multi-agency SAR constellation with at least one transmit and multiple receivers that can measure more than one interferometric cross-track baseline at a time, and ideally with global coverage and open access to the data.

2.5. Wetlands

Wetlands comprise diverse land cover types, including mangroves, floodplain forests, peatlands, marshes, and bogs, that constitute important carbon pools and greenhouse gas sources and perform critical ecosystem services. Irrigated rice paddies are human-made wetlands. The significance of SAR sensors in the context of wetlands is their unique capacity to detect standing water below a closed vegetation canopy, enabled by a strong specular like-polarization (specifically HH) double-bounce backscatter, allowing characterization of both the temporal and spatial variations of flooding (e.g., Hess et al., 1995; MacDonald et al., 1980).

Signal penetration through the vegetation canopy is correlated with the radar wavelength, with L-band the most commonly used frequency in forested wetlands. JAXA's L-band SAR missions (JERS-1, ALOS, ALOS-2) have since the mid-1990s all had systematic acquisition strategies designed with wetland seasonal inundation in mind and have been used extensively for continental-scale mapping of inundation in wetlands in South America (Chapman et al., 2015; Freeman et al., 2002; Hess et al., 2015; A. Rosenqvist et al., 2000; J. Rosenqvist et al., 2020), Africa (Figure 6; Rebelo, 2010; A. Rosenqvist, 2009), southeast Asia (Hoekman et al., 2010), and Alaska (Whitcomb et al., 2009). C-band SARs such as RADARSAT and Sentinel-1 have been used for mapping inland waters and herbaceous wetlands, as well as for shorter, lower-density, and deciduous forested wetlands (Costa et al., 2002; Evans et al., 2010; Oakes et al., 2023). Short wavelengths, even X-band, have been used for mapping irrigated rice paddies and their growth stages from planting to harvest (Le Toan et al., 1989, 1997).

Despite the proven capabilities of SAR for wetlands mapping, global maps of wetlands and inundation are not available for vegetated wetlands at moderate (10–25 m) resolution, as they now are for other land cover types. The

10.1029/2025EA004868

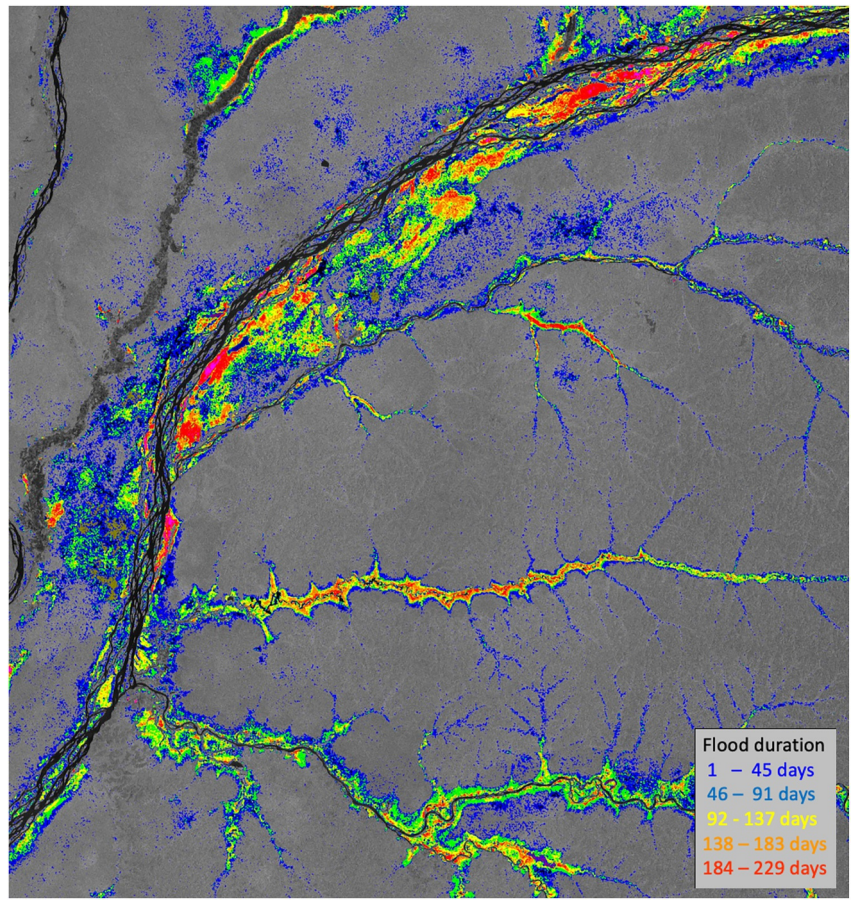

Figure 6. Flood duration derived from ALOS PALSAR L-band time series. (Central Congo river basin). (Adapted from A. Rosenqvist, 2009).

need for such maps is great, in order to (a) support member nations in meeting obligations to inventory and monitor wetlands under international agreements including the Ramsar Convention, the UNFCCC Paris Agreement, the Kunming-Montreal Global Biodiversity Framework, and the UN Sustainable Development Goals (SDG), specifically SDG Indicator 6.6.1; and (b) characterize the seasonal and interannual variability of wetland flooding and freeze/thaw state and the seasonal biomass of methane-generating aquatic macrophytes to quantify key components of global hydrologic and biogeochemical cycles.

Past obstacles to SAR-based wetlands mapping include insufficient repeat seasonal coverage, limitations on availability of free data, large data volumes, difficulty in acquiring training and validation data, a multiplicity of definitions for wetland types, and inadequate or inconsistent funding to support the generation of science products. Since 2015, an archive of now freely available Sentinel-1, ALOS, and ALOS-2 wide-swath (ScanSAR) data has been built, marking a major step in building the multi-year record needed to assess seasonal and interannual variability of flooding.

From 2025, ALOS-4 and NISAR will continue this important legacy and provide critical enhancements. NISAR is scheduled to provide significantly improved spatial (50 → 10 m) and temporal (42 → 12 days) resolution compared to that of ALOS and ALOS-2 ScanSAR, allowing in addition for InSAR-based water level measurements. ALOS-4 in turn, has the capacity to provide time series observations in full polarimetric mode, enabling PolSAR and Pol-InSAR applications to accommodate detailed characterization of wetlands vegetation structural parameters and provide a new tool for mapping boreal peatlands (Touzi et al., 2018) and irrigated rice fields. Important ancillary data sets such as the Copernicus 30 m DEM (Copernicus, 2025) and the GFPLAIN250m global floodplain data set (Nardi et al., 2019) can now be incorporated into mapping algorithms,

and very high resolution optical data are now available for validation of land cover type even during cloudy seasons, thanks to constellations of optical satellites.

With the failure of Sentinel-1B in December 2021, an unfortunate gap has been introduced into the catalogue of systematic L-band and C-band acquisitions. This can be partly compensated using historic Sentinel-1 or optical data, but inevitably the monitoring of herbaceous wetlands has been adversely impacted. To achieve the highest accuracy in flood mapping over all wetland types, both L- and C-band (or S-band) are required, ideally dual-polarization HH + HV. Combined with L-band, C-band improves discrimination between tree, shrub, and herbaceous cover, noting that C-HH is superior to C-VV for flood detection. In the absence of freely available C-HH data, L-band HH-VV phase difference, which requires dual-co-polarization or quad-polarization, may allow detection of flooding in aquatic macrophyte stands (Hess et al., 1995). Fully polarimetric data has furthermore been proven useful to monitor rice paddy phenology (Dey et al., 2021) and irrigation status (Arai et al., 2022).

For forested wetlands, NISAR and ALOS-4 are expected to address most data requirements for the remainder of the 2020s decade. The acquisition strategies of the two L-band sensors are highly complementary: NISAR will acquire dual-pol wide-swath coverage with a 12-day repeat cycle, while ALOS-4 has the capacity to acquire quad-polarization data at a lower temporal frequency. Synergy between the two sensors will thus support wetlands mapping, flood mapping, and mapping of wetland forest structure to a degree that could not be achieved with either sensor alone. The importance of continued L-HH/HV wide-swath coverage with a repeat cycle on the order of 1–2 weeks cannot be overemphasized. As Earth's hydrologic cycle is increasingly perturbed by climate change, with a higher frequency of extreme floods and droughts, consistent seasonal and interannual sampling is required to establish baselines and trends in the extent of surface waters. For forested wetlands, L-band SAR is currently the only sensor that can achieve this at 10–25 m resolution. L-band shortcomings that cannot be addressed by greater access to C- or S-band data are chiefly related to poor canopy penetration in certain very dense forest types (e.g., mangroves and some types of peat forests), where information about inundation state currently cannot be obtained. Although P-band SAR systems could be expected to resolve this, the acquisition plan for the Biomass mission is designed for tomographic observations of terrestrial forests and hence lacks the spatial resolution and temporal repeat required to capture wetland inundation dynamics.

In the near term, providing free access to RADARSAT-2 and SAOCOM-1 data and to information on coverage of RADARSAT-2 acquisitions would be useful. Given freely available SAR data sets, in the near term the challenge to delivering global wetlands products becomes one of management and funding. Users of wetland extent and type products, including governmental agencies with responsibility for wetlands inventory, Ramsar Contracting Parties, conservation groups, and land managers, employ a great variety of wetland typologies that are tailored to local conditions and needs, traditional terminology, and historical inventories. These diverse typologies cannot be adequately represented in a single global classification system. However, a global product with basic vegetation structure (tree, shrub, herb, non-vegetated) and seasonal flooding information would be immediately useful for hydrologic and biogeochemical models, and could be adapted to a desired wetland classification system through incorporation of GIS layers (e.g., estuary or urban area boundaries) or data from non-SAR sensors (e.g., optical data for water properties or floristic composition). Seasonal flooding information will also benefit other applications such as disaster assessment (by establishing average flooding patterns) and canopy height mapping (e.g., by screening GEDI data to minimize effects of flooding).

Accuracy assessment of wetland vegetation extent and type can be accomplished using very high resolution optical data, supplementary to field observations where available. Accuracy assessment of flooded/non-flooded state under vegetation canopies, however, is much more challenging, as the SAR systems themselves constitute the only means to remotely detect the presence of water below a dense forest canopy. To date, validation has mostly been based on sparse field-based point measurements coincident with the SAR observations (e.g., A. Rosenqvist et al., 2002). Innovative approaches, such as drone surveys with lightweight radar altimeters or LiDARs, are needed to carry out more robust accuracy assessments of flood mapping with SAR. Recent results showing that the Surface Water Ocean Topography (SWOT) satellite can accurately measure water surface elevation within herbaceous wetlands, and possibly some woody wetlands, are promising (Kica et al., 2025). Coordination of planning, executing, and making available the data from these campaigns among the space agencies is strongly encouraged.

Priority requirements for next-generation SAR missions include (a) continued wide-swath L-band dual-pol (HH + HV) coverage at high spatial and temporal resolution; (b) freely available dual-pol (HH + HV) C-band or S-

10.1029/2025EA004868

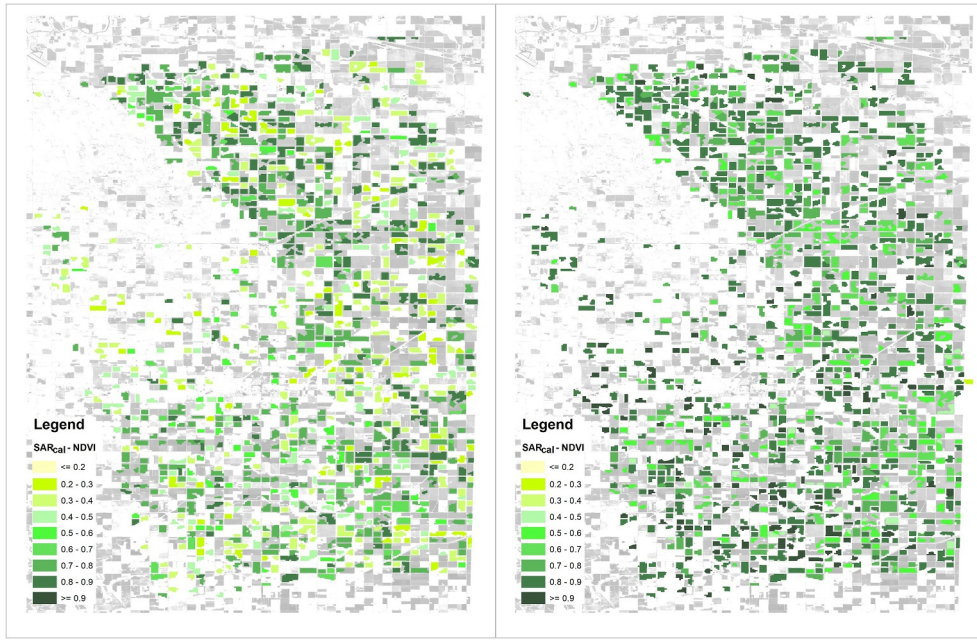

Figure 7. Tracking the development of corn, soybeans, wheat and canola using Sentinel-1 C-band SAR (Carman, Manitoba, Canada). SAR_{CAL}-NDVI represents estimates of crop productivity (from 0 to 1) for (left) June 29 and (right) 27 July 2019. NDVI = Normalized Difference Vegetation Index (Adapted from McNairn & Jiao, 2024).

band wide-swath data with temporal coverage similar to that for L-band; (c) a complete annual global L-band coverage with full or compact polarimetry (CP), coordinated with regional dry seasons to minimize the below-water component of forest height; and (d) a P-band mission with spatial and temporal resolutions accommodated for wetlands. The current spatial resolution of 10–25 m for NISAR and ALOS-4 is optimal for most applications, as higher resolutions would involve trade-offs in swath size and temporal coverage without offering significant improvements in products. Increased availability of quad-polarization data at all available SAR wavelengths should stimulate further research on estimation of water surface height in vegetated wetlands using wetland interferometry (Lu & Kwoun, 2009), monitoring water table levels in certain wetland types such as raised bogs, and the utility of HH-VV phase difference for flood detection.

2.6. Agriculture and Crop Monitoring

Agricultural applications have been subject to extensive remote sensing research and operational development since the first (optical) EO missions. The unique contributions of SAR sensors include acquisitions regardless of cloud cover and the sensitivity of microwave scattering to changes in the structure of crop canopies. These structural changes are indicative of crop type as well as the state and condition of crop canopies.

Crop type maps are base products required for monitoring changes in cropping patterns, and for modeling crop growth and productivity (Figure 7). The size, shape, and orientation of the leaves, stalks, and fruit of canopies are unique from one crop type to the next and as crops grow. Because SAR scattering (both in terms of magnitude and phase) is impacted by these structural variations, research has repeatedly demonstrated that SAR can be helpful in mapping inventories of crops (Adrian et al., 2021; Blickensdörfer et al., 2022; S. Liu et al., 2021; McNairn et al., 2009). Estimates of crop condition and productivity are also critical to the agriculture sector. Biophysical measures such as above-ground biomass, Leaf or Plant Area Index (LAI or PAI), and crop phenology (growth stage) are good proxies for crop health. Researchers have used both semi-empirical and machine learning models to estimate these crop biophysical parameters from SAR (Hosseini et al., 2021; Mandal et al., 2020a, 2020b; Mansaray et al., 2020; Passah et al., 2022; H. Wang et al., 2019). These estimates, when coupled with crop growth and yield models, can improve estimates of productivity. The agriculture sector is also interested in mapping seeding dates (to assist with yield modeling) and harvest dates (to assist with resource allocation in moving crops to market). In this case, research has demonstrated that the change in SAR coherence due to seeding activities and

removal of the crop canopy at harvest can be tracked (Amherdt et al., 2021; Dingle Robertson et al., 2023; Kavats et al., 2019; Shang et al., 2020).

As described, the needs of the agriculture sector are to monitor crop type and development, from seeding to harvest. To meet these user requirements, successful application of EO technologies requires a dense time series throughout the entire growing season: the time domain is the most important dimension. The provision of data from constellations of satellites, whether from a single provider or through virtual constellations, is thus critical in delivering accuracies needed to move research results toward operational implementation. Sentinel-1 standard coverages over land have demonstrated that if denser time series are available, the uptake of SAR in crop monitoring is improved (Dingle Robertson et al., 2020; Kraatz et al., 2021; Qadir et al., 2023; Schlund & Erasmi, 2020). However, despite the contribution of Sentinel-1 standard coverages, the temporal frequency of acquisitions, in particular at a global scale, is still not adequate. Crop canopies change rapidly, and capturing the accumulation of biomass, transitions from one growth stage to the next, and harvesting activities requires multiple observations per week at a field. This temporal repeat is not currently met for many regions of the world.

Research and operations have relied heavily on C-band SAR sensors due to the availability of data from ERS, RADARSAT, and Sentinel-1 missions. There is no single SAR frequency, that is, best suited to map crops or monitor crop development. In particular, a single frequency is not adequate for monitoring crop development. The above-ground biomass of canopies varies from crop to crop and as crops grow. Penetration into the canopy is required to capture the differences in backscatter and scattering behavior that result from variations in canopy and plant structures, yet too much penetration results in contributions from the soil, which can complicate modeling efforts. Approaches to monitor crop type and development therefore benefit tremendously when SAR data are available at multiple frequencies (X-, C-, and L-band). For mapping crop type, multi-frequency acquisitions do not necessarily have to be coincident in time. To classify crops, SAR data collected by different sensors can be acquired at different times during the season. However, when estimating biophysical parameters (biomass, LAI/PAI, and phenology), models benefit when these multi-frequency data collections are temporally coincident. Currently, dense time series of multi-frequency SAR are not available over the spatial extents needed to support operational monitoring. The near-term availability of NISAR L-band data, if coupled with Sentinel-1 C-band standard coverages, will drive innovation and uptake of SAR for operations. Missing at this moment is the availability of repeat wide area coverages from other frequencies (such as X-band).

Crop monitoring benefits most from dense time series and multi-frequency data. Nevertheless, polarization diversity also improves outcomes. Early research focused on exploiting single or multi-polarization backscatter to characterize crops. Classifications that use dual linear polarizations outperform those that use a single polarization, in particular when cross polarizations (HV or VH) are combined with the VV polarization (Mahdianpari et al., 2019; McNairn et al., 2009). Operational crop mapping has exploited VV-VH dual polarization data sets (Davidson et al., 2017). Both VV and HV/VH polarizations can also be used in monitoring crop development. These polarizations are sensitive to crop LAI (Jiao et al., 2011), biomass (Hosseini & McNairn, 2017; Mansaray et al., 2020; Wiseman et al., 2014), height (Thulasiraman et al., 2024) and phenology (Nasirzadehdizaji et al., 2019; Schlund & Erasmi, 2020; H. Wang et al., 2019). HV/VH and VV polarizations are important in classify crops and tracking crop development because cross-polarization backscatter responds to volume scattering within crop canopies while vertical polarizations couple with the vertical structure dominant for many crops.

When polarimetric data became more readily accessible, researchers discovered that as crops grow, changes in the canopy structure resulted in changes in not only backscatter intensity but also how incident waves scattered. Parameters such as volume scattering, entropy, ellipticity, and degree of polarization of the scattered wave (among others) are highly sensitive to changes in accumulated biomass, LAI/PAI, and growth stage. Although some satellites can acquire fully polarimetric data, these acquisitions are typically limited to research sites due to the narrower swaths in quad-polarization mode. Compact polarimetry (CP), although not as data-rich as fully polarimetric modes, does offer a compromise between swath coverage and information content and has proven to be sensitive to crop development (Dingle Robertson et al., 2022; Homayouni et al., 2019; Mandal et al., 2021; H. Wang et al., 2023). Several studies compared crop classification accuracies using parameters derived from multi-temporal C-band CP parameters and backscatter from dual polarizations (HH-VV, HH-HV, VV-VH). In all studies, accuracies were higher when classifications used CP data, and these results held for early, middle, and end of season classification (Brisco et al., 2013; Charbonneau et al., 2010; Dingle Robertson et al., 2022; Mahdianpari

et al., 2019). CP parameters most sensitive to crop development have included the volume component of decomposition features and the right-circular transmit and right-circular receive (RR) intensity (Mahdianpari et al., 2019) as well as the Stokes parameters and m-delta or m-chi decomposition components (Brisco et al., 2013; Dingle Robertson et al., 2022). As crops develop, the degree of polarization and circularity of scattering changes due to phenological structural changes in the canopy, which assists in separating crop types and in monitoring crop development (Dingle Robertson et al., 2022). Future missions should consider implementation of a CP mode.

The agricultural sector is heavily invested in the exploitation of optical EO data to map and monitor agricultural landscapes. Despite the impressive advances in research to monitor crops using SAR technologies, greater operational uptake by agricultural agencies will require improvements in the availability and characteristics of SAR data. Standard coverages and dense time series are needed to provide a consistent and predictable flow of data to feed operations, tracking crop development and productivity. The exact repeat interval needed is not easy to define given the variability in global cropping systems. A general rule in agricultural research has been to consider changes in the crop canopy to be relatively small within 3 days. Acquisitions 2–3 times per week, over each field, will deliver the density of data needed to monitor most changes in crop biophysical parameters.

Adding frequency and polarization diversity to this dense time series of standard coverages is also important, in particular in efforts to use SAR data to estimate the biomass, LAI/PAI, and growth stages of crops. No single frequency is preferred given the variations in canopy biomass from crop to crop, and over the growing season. Acquisitions of X-, C-, and L-band quad-polarimetric (or CP) data are therefore ideal. The value of these data is increased if more than one frequency can be acquired coincidentally.

The question of swath coverage and spatial resolution is a more difficult one to answer given the widely varying geographies and field sizes encountered across global agricultural landscapes. Nevertheless, most end users are using data from optical missions that cover swaths of 200–300 km. While the swath of the of Sentinel-1 Interferometric Wide (IW) mode satisfies this user requirement, the resolution of dual-polarization IW data (nominal resolutions of 20–30 m) can be challenging in mapping crop types and tracking crop development in regions of the world where field sizes are small.

In summary, a dense time series of standard and predictable acquisitions (2–3 times per week) is required to meet the needs of the agriculture sector. If standard coverages are provided in multiple polarizations and frequencies (e.g. coupling NISAR and Sentinel-1), the information on crop growth will increase significantly, in particular if data collections are near coincident. The richness of quad-polarimetric data has been proven in many agricultural research studies, but this mode's small swath limits its uptake in operations. Future missions should therefore consider CP as an option to increase polarimetric information to aid in crop type and crop biophysical mapping and monitoring.

2.7. Soil Moisture

Soil moisture, defined as the fractional volume of water in soil, is an Essential Climate Variable (ECV) that plays a crucial role in several Earth system processes at the soil-atmosphere interface, including agriculture, hydrology, climate, and ecology. In particular, it is a determining factor in crop growth and development, determines the distribution of precipitation in surface runoff and infiltration, and controls erosion processes, among others. Accurate and timely estimates are essential for understanding and managing these processes. For example, knowledge of soil moisture is crucial for proper water management, for identifying areas suitable for agriculture where soil moisture is a constraint, for identifying dry soils and vegetation that can increase fire risk, and for monitoring and tracking the recovery of areas affected by fire. At global and regional scales, observations of soil moisture at high spatial and temporal resolution would also provide critical input to global carbon and climate models with information about, amongst others, Arctic permafrost thaw, regional seasonal freeze/thaw dynamics, and water table variations in disturbed tropical and boreal peatlands. Soil moisture is also a critical parameter in modeling slope failures.

A key characteristic of soil moisture is its high variability in both space and time, and it is therefore difficult to obtain representative field measurements over large areas. In this sense, satellite remote sensing has proven to be a powerful tool for providing data from which soil moisture can be estimated at global and regional scales, and with an appropriate periodicity. Currently, there are several microwave-based soil moisture products available on the

global scale. Operationally produced data sets include retrievals from the ESA MetOp Advanced Scatterometer (ASCAT), JAXA's Global Change Observation Mission—Water (GCOM-W) Advanced Microwave Scanning Radiometer-2 (AMSR2), the Soil Moisture and Ocean Salinity (SMOS) mission, and the Soil Moisture Active Passive (SMAP) mission, among others. Furthermore, merged long-term soil moisture products have been produced by harmonizing and merging multiple microwave-based soil moisture products. These global soil moisture data sets provide soil moisture measurements at coarse spatial resolution, between approximately 10 and 35 km.

SAR sensors can offer soil moisture estimations at significantly higher spatial resolutions and still with adequate spatio-temporal coverage. SAR sensors are intrinsically sensitive to plant and soil moisture, which are directly correlated with crop development, stress, and diseases. Moisture content affects both backscatter intensity and polarimetric phase, and quad-polarimetric data are thus required for full inference (Dadamia et al., 2015). Soil moisture measurement with SAR is furthermore affected by the presence of dense vegetation, which can contribute to and even dominate the microwave signal. Long radar wavelengths (L-band or longer) are therefore preferred in vegetated areas to mitigate this effect. InSAR phase is also being investigated for the sensitivity of phase closure to soil and vegetation moisture (e.g., De Zan & Gomba, 2018; Rabus et al., 2010; Wig et al., 2024). Finally, soil moisture is typically measured at very low backscatter intensities, which requires well-calibrated SAR systems with a low noise floor (characterized by the noise equivalent sigma-naught (NESZ)).

Soil moisture monitoring is the mission driver for the SAOCOM-1A/1B L-band constellation, where estimations of soil moisture content are derived using time series of quad-polarimetric data acquired over the Pampas agricultural region in Argentina at every overpass with each of the two satellites. Soil moisture maps (Figure 8) are produced daily and automatically in high and low spatial resolution acquisition modes, respectively, and for both ascending and descending orbits. All soil moisture maps are validated with in situ soil moisture measurements and the corresponding errors in the estimates vary between 5% and 7% (Cáceres et al., 2016).

The SAOCOM case demonstrates the potential of L-band SAR for soil moisture monitoring over a regional scale area when an adequately dense time series of quad-polarimetric data can be acquired. To map soil moisture at the same temporal and spatial fidelity over global scales has been beyond the capacity of current (polarimetric) SAR missions. It would require substantial on-board memory for storage and broad bandwidth to download the data, especially considering that the data volume of fully polarimetric data is twice that of dual polarization. For context, the NISAR mission downlinks on average 4.4TB/day for its global L-band data set, nearly all collected in dual- or single-polarization mode. Amongst current and near future systems, the SAOCOM constellation and ALOS-4 PALSAR-3, the latter with its capacity for fine resolution quad-polarimetric observations with a wide (100 km) swath, could nonetheless be used for targeted soil moisture observations over a number of key regional hot spots. In addition, NISAR will generate a global soil moisture product from dual-polarization (HH + HV) polarimetric data with 200-m resolution (500-m in Sahara Desert), updated every 12 days.

In the near term, there are actions that should be taken to improve measurements of soil moisture. Firstly, because calibration is so critical to accurate inversions of the SAR signal for soil moisture, calibration routines and validation sites should be coordinated across missions to ensure accurate and consistent measurements. Machine learning should be explored for removal of noise, for example, from RF interference or vegetation, and generation of higher-level soil moisture products for non-experts, with or without fusion of SAR and passive microwave. The community should explore combining polarimetry and interferometry for disentangling the signals from soil moisture, vegetation moisture, and vegetation and soil type and structure using dual polarization NISAR and quad-polarization ALOS-2/4 provided over validation sites with openly available field data. Combining soil moisture information with that of relevance to other disciplines (vegetation structure, subsidence) should also be explored for improving measurement accuracy. Agencies should support the establishment of cloud-based analysis platforms for generating, processing, and visualizing SAR-derived soil moisture and increase user training and outreach to boost usage of Sentinel-1, ALOS-2/4, SAOCOM, and NISAR data in operational monitoring systems. If possible, some coordination of observations among the different missions providing polarimetric data could increase revisit frequency to daily or sub-daily for some areas to better track dynamic moisture changes.

For the soil moisture community, it is critical that we focus on the continuity of L-band missions to sustain and build on the current momentum in soil moisture monitoring. In a longer term perspective, the “holy grail” for soil moisture monitoring would be establishing an L-band quad-polarimetric SAR constellation for global monitoring

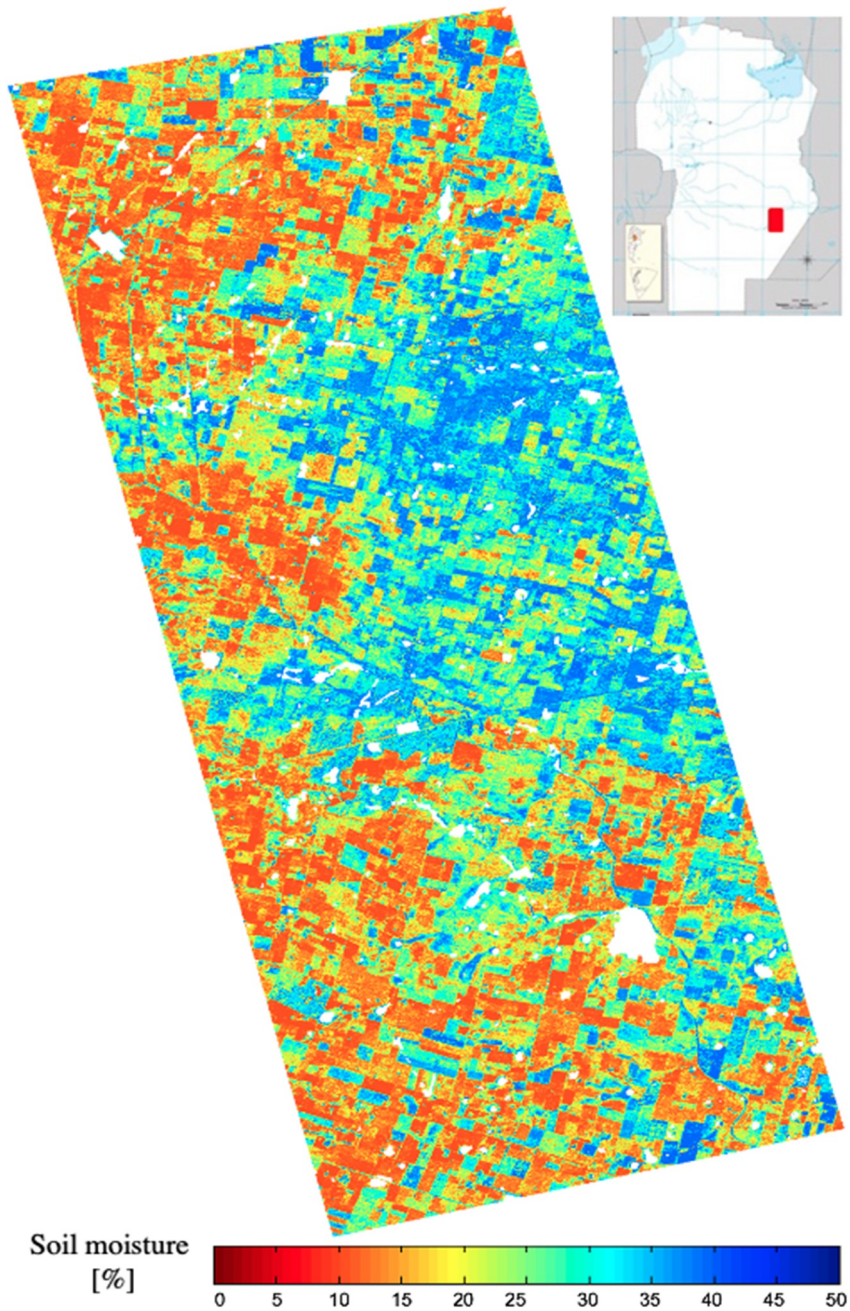

Figure 8. Soil moisture map. Bell Ville and surroundings, Córdoba Province, Argentina, 30 November 2019. Map spatial resolution: 100 m. Original image: SAOCOM-1 Stripmap Polarimetric. Red: driest. Blue: presence of water. (*Source:* https://catalog.saocom.conae.gov.ar/catalog/).

with 3–4 days revisit and 5–10-m spatial resolution. Any work to reduce mass and power needs for L-band sensors, implement on-board processing and compression, and increase onboard storage and downlink capacity will reduce the cost of building, launching, and operating the sensors. The forthcoming ROSE-L mission (Geudtner et al., 2021) has capacity for global dense time series observations, and ensuring the mission plan also accommodates systematic polarimetric observations would be highly desired. By pursuing these ambitious mission solutions, the SAR community can significantly advance the capabilities of soil and vegetation moisture monitoring, thereby contributing to a more sustainable and productive agricultural future and improved resilience through better forecasting of floods and landslides.

2.8. Sea Ice

Sea ice is classified by the Global Climate Observing System (GCOS) as an ECV. It is present in both polar regions and undergoes daily, seasonal and yearly changes. The sea ice and its changes influence the exchange of heat, gas, and momentum between the ocean and the atmosphere, affect biological productivity, and regulate the salinity of the upper ocean layers. Changes of sea ice conditions, e.g., formation of fractures, leads or ridges on local scales, and ice extent, concentration, thickness and motion on regional scales occur over time intervals between days and several months. The variations of sea ice conditions are governed by temperature, pressure, wind, and currents that cause thermodynamic sea ice growth and decay as well as mechanical growth through ridging and rafting. Monitoring of these changes requires SAR data which provide the necessary spatial resolution to resolve deformation features and changes in extent and concentration and are available also during the polar night.

The sea ice is currently transitioning from a regime dominated by old thick multi-year ice (MYI) to one dominated by younger and thinner first year ice (FYI) (Kwok, 2018). A recent study by Krumpen et al. (2025) showed that a more dynamic ocean can result in fewer pressure ridges. The monitoring of sea ice needs to capture these changes. Moreover, SAR is essential to improve our understanding of interactions between atmosphere, ice, and ocean, in particular focusing on local and regional sea ice processes, for example, sea ice kinematics at spatial resolutions on the order of 100–1000 m, and evolution of polynyas and leads. The high spatial resolution offered by SAR compared to, for example, passive microwave data, can contribute significantly to further develop and validate numerical models of sea ice dynamics. Moreover, while evidence of mesoscale eddies occurring in the interior sea ice field has been impeded by the presence of compact sea ice in the past, the recent decline in sea ice concentration and extent allow for clearer expressions of mesoscale features in the SAR-derived sea ice field as demonstrated by Cassianides et al. (2021).

Requirements for the support of maritime operations in polar regions are high spatial resolution combined with a wide areal coverage and near real-time delivery of the ice conditions, for which SAR images are essential. The support is provided through sea ice charts prepared and released by national ice services, many of which are organized in the International Ice Charting Working Group (https://nsidc.org/noaa/iicwg). Ice charts show spatial variations of ice concentration, the position of the ice edge, and the regional and local distribution of different ice types, sometimes supplemented by information such as floe sizes or occurrence of icebergs. The ice charts are usually updated daily or weekly but can also be produced on demand. Presently only C-band dual-polarized SAR systems can provide images continually and at a coverage required by the operational ice services. Until now, the ocean region around Antarctica has been less well covered by SAR satellites, although this situation is expected to improve because of the availability of SAOCOM and NISAR data.

Challenges remain in the separation between open water and sea ice areas due to, for example, similarities in radar backscatter between thick ice and open water areas roughened by strong winds, or between calm water surfaces and thin ice (Johansson et al., 2018; Zakhvatkina et al., 2017). An important challenge is the instrument noise level (NESZ), which for the cross-polarization channels often is too high for separating water and thinner ice classes (Johansson et al., 2018). The cross-polarization channels are less influenced by waves than the co-polarization channels (Chapron et al., 2005). Multi-frequency and polarimetric SAR data can help to overcome these ambiguities, for example, the use of L-band SAR imagery improves ice classification in particular during the early melt season and the separation of rough and deformed ice from smooth level ice (Figure 9; e.g., Casey et al., 2016; Karlsen et al., 2024). Uncertainties can be further reduced when SAR imagery is combined with optical or thermal data (e.g., Khachatrian et al., 2023; Wulf et al., 2024). Higher temporal resolution data over the polar regions during the melt season can address some of the ambiguities in ice type and ice-water separation (e.g., Geldsetzer & Howell, 2023; Howell et al., 2019; Spreen et al., 2017). A successful example of coordination between space agencies is the "Synergistic Use of L- and C-Band SAR Satellites for Sea Ice Monitoring" project (Dierking, 2021), through which overlapping C-band (Sentinel-1) and L-band (ALOS-2) wide-swath data were acquired over multiple years and seasons. It covers six Arctic sea ice and iceberg sites (Dierking & Davidson, 2021) and enables studies of seasonal and interannual variability (e.g., Demchev et al., 2023; Færch et al., 2024; Karlsen et al., 2024).

Sea ice drift velocities are as high as 0.23 m/s (Spreen et al., 2020; von Albedyll et al., 2024), so the parallel analysis of data from different sensors acquired with temporal gaps between tens of minutes and several hours can be difficult. The problem can be addressed by combining SAR sensors, for example, Sentinel-1 and RCM

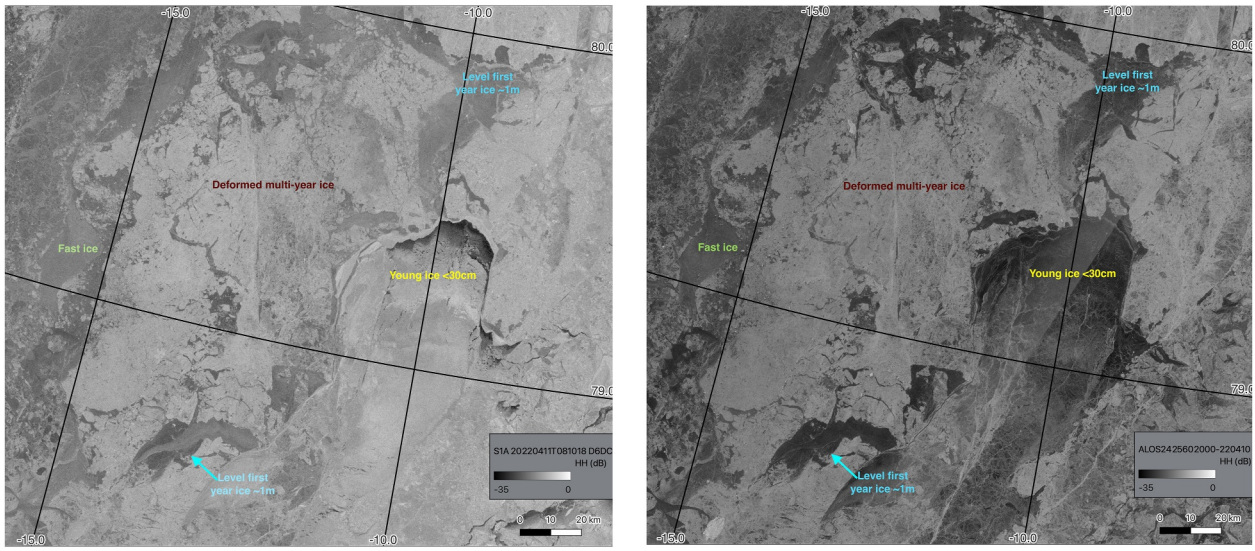

Figure 9. Sentinel-1 (left) and ALOS-2 (right) SAR images showing sea ice in Belgica Bank, northeastern Greenland in April 2022. In-situ data collected confirmed the indicated sea ice types (Dierking et al., 2022). Sentinel-1 data provided by Copernicus 2022, and ALOS-2 by JAXA (PI: PER3A2N093).

(Howell et al., 2022, 2024), or with tandem constellations consisting of L- and C- or X-band satellites, for example, Sentinel-1 paired with the planned ROSE-L mission. For sea ice motion tracking at high spatial resolution, sequences of SAR images with temporal gaps of <5 hr (<1 hr optimal) are useful. For drift retrieval, images acquired at different frequencies can also be combined (Demchev et al., 2023). As such, NISAR, launched in July 2025, will collect simultaneous S- and L-band SAR over the Beaufort Sea to further explore the usefulness of multi-frequency SAR. Using data from Envisat ASAR, Kræmer et al. (2015) demonstrated how high precision line-of-sight surface velocity derived from the Doppler shift signal can complement the SAR-based estimation of sea ice motion. Recently this method has been further developed using Sentinel-1 SAR data (Moiseev et al., 2022) showing promising capabilities for regular retrievals of line-of-sight sea ice motions.

Sea ice thickness, the knowledge of which is useful for numerical forecasts of sea ice conditions and other applications such as ice biology, cannot directly be measured by means of SAR technology. A robust method for the indirect determination does not exist presently, though temporally and spatially combined SAR and altimetry data would help to advance this field of research (e.g., Howell et al., 2024; Macdonald et al., 2024). Measuring snow thickness on ice, which is needed for the retrieval of ice thickness using altimetry data (e.g., Carret et al., 2025; Nandan et al., 2023; Willatt et al., 2023), presents a particular challenge. Snow on sea ice affects the radar signatures if wet snow causes ambiguities in the data analysis, predominantly during the melt season, in the marginal ice zone, and on flooded Antarctic sea ice (Howell et al., 2019; Melsheimer et al., 2023). Even dry snow can change radar signatures at higher radar frequencies through processes such as metamorphism, layer compaction by wind, and refreezing of wet snow (Nandan et al., 2016). SAR interferometry has also been shown to aid sea ice thickness retrieval and assessment of fast ice extent and stability, using both across- and along-track modes (e.g., Dammann et al., 2019; Huang et al., 2021; Yitayew et al., 2018). Over drifting sea ice, only single-pass interferometric data such as from Tandem-X can be used.

In the near term, coordination optimized for sea ice studies needs to be improved with focus on repeat imaging using a consistent mode of acquisition; collecting more multi-frequency data over key regions and during campaigns; more cal/val campaigns to better measure the thickness of snow on ice and involving combining acquisitions of altimeters (TerraSAR-X and ICESat-2) and SAR data; and making SAR images from the polar regions open access. For lower frequency SARs, methods must be improved to correct for the effects of the ionosphere on the interferometric phase.

In the longer term, efforts are needed to coordinate different multi-frequency satellite missions for near-simultaneous data acquisitions over sea ice; more frequent imaging with any SAR band for monitoring ice drift and deformation; and extension of the available frequency spectrum of sea ice-observing SAR missions with Ku- and Ka-band on the high-frequency side and P-band on the low-frequency side. Dual-polarimetric mode is

essential for these acquisitions, and dual-co-polarization and quad-polarization modes will further ensure that the expanding melt season evolution can be studied (Scharien et al., 2012). Thus, we expect a gain for the retrieval of snow and ice thickness and for further reducing ambiguities in ice classification in particular during the melting season, as well as a better temporal resolution for studying sea ice drift patterns and deformation and for iceberg tracking.

2.9. Permafrost

Permafrost is defined as ground remaining at or below zero-degree Celsius for at least two consecutive years. As a thermal condition, permafrost is sensitive to climate change and is therefore an ECV documented by three associated quantities: Permafrost Temperature (PT), Active Layer Thickness (ALT), and Rock Glacier Velocity (RGV) (WMO, 2022). Permafrost is a subground phenomenon separated from the surface by a layer of seasonal thawed ground (the active layer). It is therefore not directly observable from space. However, various surface parameters impact the way the heat is transferred from the atmosphere into the ground, and several proxies can indirectly document permafrost. Satellite information, including from SAR, are therefore increasingly used to map and monitor factors controlling the permafrost or indicators reflecting its state and evolution, such as land cover, soil wetness, snow cover, surface freeze and thaw cycles, coastal erosion, thermokarst lake development, and terrain change (Bartsch, Strozzi, & Nitze, 2023).

For PT and ALT, SAR products can be used to constrain the parametrization of (sub)surface conditions in permafrost models. Most current uncertainties are related to the model representations of the geocryological conditions (e.g., the ice content) and the snow acting as a buffer between the atmosphere and the ground. Land cover classification based on data fusion of reflected radiance from SAR backscatter and optical sensors, for example, combining Sentinel-1 and Sentinel-2 (Bartsch et al., 2024), can contribute to model parametrization. SAR backscatter provides valuable information related to frozen and unfrozen near-surface conditions, as well as snow properties (Bartsch, Bergstedt, et al., 2023). InSAR-derived thaw subsidence is also a useful proxy for estimating the distribution of ground ice content (Zwieback & Meyer, 2021). The value of SAR data has been demonstrated at local to regional scales, but the inconsistency of the spatial coverage and temporal resolution across the cold-climate regions currently hinders our ability to generate systematic products of comparable quality at the global scale (Bartsch, Strozzi, & Nitze, 2023).

For RGV, surface velocity can be measured from InSAR or SAR offset tracking (Y. Hu et al., 2025; Strozzi et al., 2020). With InSAR, rock glacier monitoring requires low frequency and/or short temporal baseline to retrieve coherent signals on landforms moving up to one or several m/yr. Weekly C-band acquisitions are often at the limit of the detection capability. For this application, L-band missions are highly beneficial (Zwieback et al., 2024). Using SAR offset tracking solves the issue of the detection capability over fast-moving rock glaciers, at the cost of the spatial resolution. For small landforms, the spatial resolution of most operational missions is currently too low. Higher spatial resolution should be considered for future missions.

SAR backscatter can be used to repeatedly map surface features that reflect permafrost degradation, such as thermokarst lakes (Tian et al., 2016; Trofaier et al., 2013), drained lake basins (von Baeckmann et al., 2024), and coastal erosion (Bartsch et al., 2020). Backscatter is also influenced by the thermal conditions of the ground and can therefore be used to monitor the timing of freeze and thaw onsets in case of near-daily sampling (Park et al., 2011). Simultaneous multi-frequency and multi-polarization SAR data are beneficial for such applications (Bartsch et al., 2025). Ground surface movement can be monitored by a set of techniques, depending on their velocities. Repeat-pass InSAR is well suited for monitoring thaw subsidence and frost heave in permafrost lowlands and slow mass wasting processes on slopes (Rouyet et al., 2019, 2024; Figure 10). Loss of ground ice can be documented with C- and L-band (ERS—Liu et al., 2012; ALOS PALSAR—Iwahana et al., 2016; Sentinel-1—Strozzi et al., 2018). However, for fast processes, such as thaw slumps or active layer detachment slides, alternatives must be found. Single-pass InSAR can be applied to monitor such abrupt changes using a series of DEMs (Bernhard et al., 2020), but few constellations are widely available for such purposes. Most of these applications have been demonstrated at local to regional scales only due to the lack of acquisition mode consistency and high spatial resolution required for circumpolar implementation. For SAR backscatter and InSAR applications, multiple parameters (e.g., temperature, soil moisture) can ambiguously impact the radar amplitude and phase, leading to a potential misinterpretation of the measured properties. In general, there is a lack of SAR cal/val supersites and campaigns targeting permafrost monitoring (Zwieback et al., 2024).

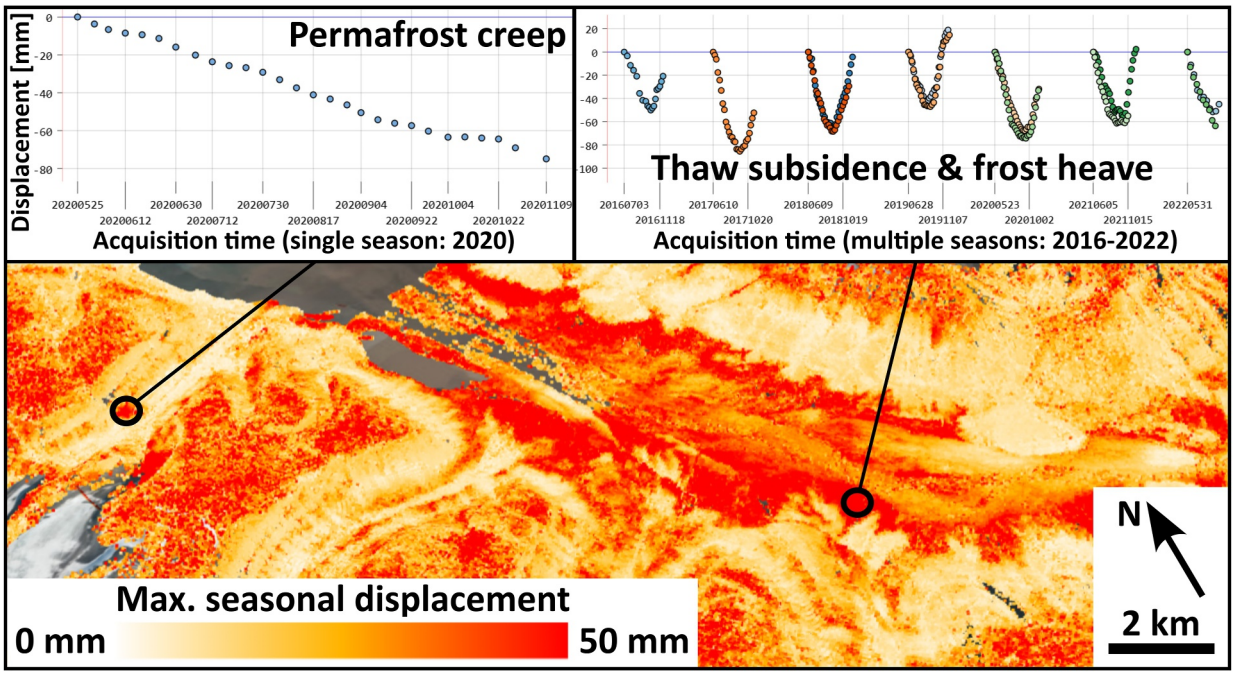

Figure 10. Example of InSAR pilot product around Longyearbyen and Adventdalen (Spitsbergen) under development for the InSAR Svalbard Ground Motion Service (GMS) (Modified from Rouyet et al., 2024). See similar example in the Copernicus Polar Roadmap for Service Evolution (Duchossois et al., 2024).

A major knowledge gap in climate change projection is the impact of permafrost thaw on carbon fluxes. Quantification of the amount of carbon stored in frozen soils and representations of the heterogeneity of tundra landscapes and soil saturation conditions (wetland distribution) are needed. Land surface descriptions incorporating SAR have been shown to be a suitable proxy for soil organic carbon (C-band HH, Bartsch et al., 2016) and soil wetness (C-band VV fused with multispectral data, Bartsch et al., 2024) in tundra. InSAR has also been found to represent wetness gradients (J. Chen et al., 2020; Widhalm et al., 2025). Knowledge of the dynamics of wetlands specifically is required, but SAR acquisitions with sufficient spatial resolution at sub-weekly sampling are currently lacking for Arctic regions.

In summary, permafrost monitoring from space requires the combined use of a large set of parameters. The integration of multiple proxies and advanced data fusion strategies for assimilation into models are necessary. Although applicable SAR data are accessible (e.g., Sentinel-1), the utility of these missions for global assessment remains limited due to acquisition strategies that generally disadvantage high-latitude permafrost regions. In addition, for several applications, C-band with a 12-day repeat-pass is not sufficient to fill the gap in knowledge. Indeed, due to the diversity of the parameters studied by the permafrost community, there is no single SAR system that can address all the needs. Permafrost monitoring requires a combination of frequencies, polarizations, acquisition strategies, and modes. For lowland permafrost applications, the priority is to have consistent acquisition and data delivery strategies over the whole circumpolar regions, including Siberia. For mountain permafrost applications, consistent low frequency missions are best suited and high spatio-temporal resolution is necessary. To ensure high-quality products tailored for permafrost monitoring, there is also a need for SAR cal/val supersites and campaigns targeting permafrost in particular.

Coordination between agencies should focus in the near term on consistent, InSAR-enabling coverage of all the permafrost regions using the combination of assets, preferably with <12-day repeat if possible; support for cal/val activities; and collection of multi-frequency data over key sites. In the long term, future missions with shorter repeat-pass intervals and lower SAR frequencies will be highly beneficial. Efforts to coordinate the simultaneous acquisitions of complementary SAR missions providing different frequencies and polarizations is mandatory for game-changing advancements.

10.1029/2025EA004868

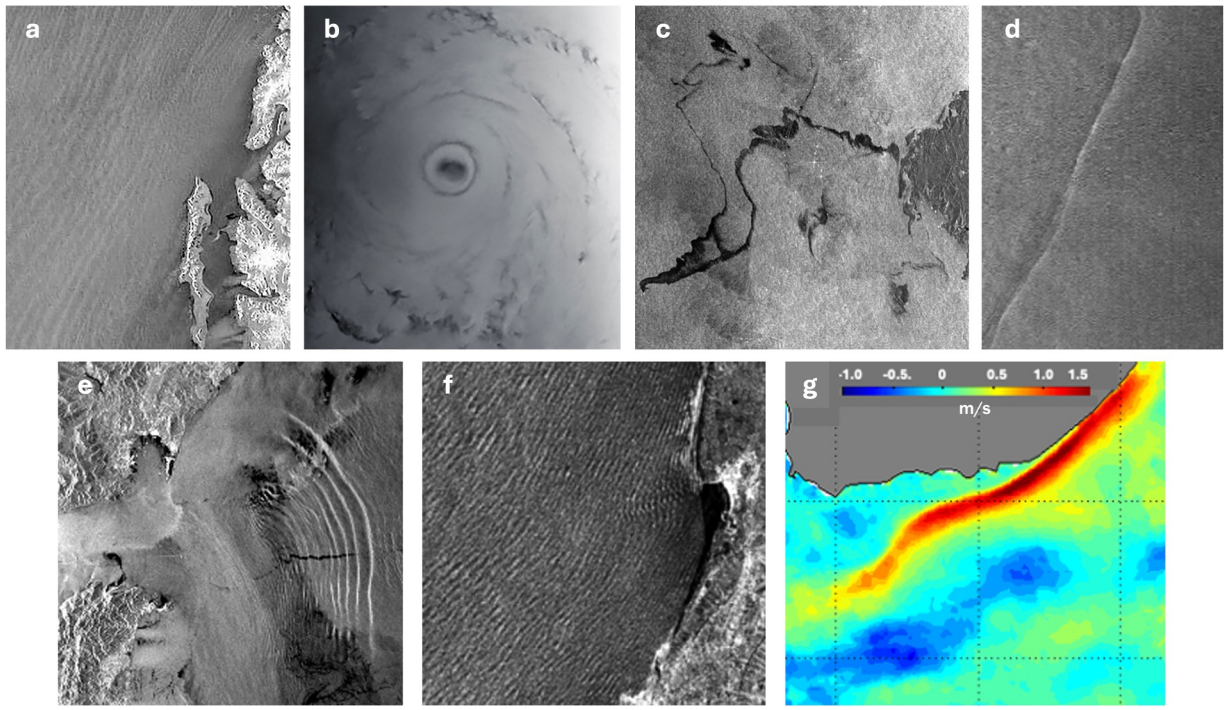

Figure 11. SAR image expressions of atmospheric boundary layer and upper ocean structures. (a) Wind streaks off the west coast of Svalbard; (b) Hurricane Katrina in the Gulf of Mexico; (c) Oil spill from Prestige off the northwest coast of Spain; (d) Oceanic front in the western Pacific; (e) Internal waves in the Alborian Sea; (f) Ocean surface waves in the northeast Atlantic; (g) Mean Doppler-based surface current in the greater Agulhas Current region. Panels (a–c) were acquired by Envisat C-band ASAR, (d) by ALOS L-band PALSAR, (e) by ERS-1 C-band SAR, (f) by Sentinel-1A C-band SAR, and (g) from 500 Envisat ASAR acquisitions.

2.10. Oceans

Starting with Seasat, SAR instruments have revolutionized oceanographic studies, providing information on ocean currents, mesoscale structures, wave spectra, internal waves, surface slicks, near surface wind fields, and marine atmosphere boundary layer (MABL) processes and extremes as evidenced in Figure 11.

SAR intensity images reveal kilometer-scale (O(500–1,000 m)) variability of the ocean-surface roughness that can be correlated to specific conditions for parameterization of the MABL (e.g., O'Driscoll et al., 2023). While air-sea interactions and ocean surface roughness patterns and their relationships to SAR NRCS measurements are still imperfectly understood, numerous satellite radar measurements at C-band now routinely provide unique 2D surface expressions of extreme atmospheric phenomena (Combot et al., 2020), mesoscale upper ocean dynamics and frontal boundaries (Kudryavtsev et al., 2012), and internal waves (Santos-Ferreira et al., 2025). Furthermore, observations acquired with the Sentinel-1's Wave Mode, which collects 20 km × 20 km imagettes separated by 100 km in the along-track direction, provide global insight of ocean swell dynamics including propagation and dissipation, as well as the structure and intensity of the wave generating areas. Analysis of the long-range propagation of ocean swell systems also enables mapping of wave-current refractions, and thus a means to study upper ocean surface currents. In addition to the imaging SARs, the Surface Water and Ocean Topography (SWOT) mission launched in 2022 (Fu et al., 2024) operates a single pass SAR interferometer (KaRiN instrument) that provides ∼1 km resolution measurements of sea surface height (Chelton, 2024) enabling detection of mesoscale and sub-mesoscale eddies (Z. Zhang et al., 2024), estimation of ocean surface currents (Fablet et al., 2024), near surface wind speed (Stiles et al., 2024), and measurements of wave height, wavelength, and direction across ocean basins (Ardhuin et al., 2024).

SAR imaging radars measure near surface winds at much finer spatial scale than microwave scatterometers, functioning as high-resolution, single antenna, wind scatterometers for capturing kilometer-scale O(1 km)) MABL phenomena, including coastal winds (Pulvirenti et al., 2018). Cross-polarized C-band radar is highly sensitive to wind speeds (van Zadelhoff et al., 2014) with very low sensitivity to wind direction and radar incidence angle, opening new and robust high-resolution mapping of severe storms (e.g., Mouche et al., 2017).

Today, the ever-increasing sampling capability of satellite active and passive microwave observations, including high-resolution imaging radar instruments, opens new and needed opportunities to derive improved surface forcing properties under extreme conditions (e.g., tropical cyclones (TC), extra-tropical cyclones, polar lows) as demonstrated in the ESA-funded MAXSS project (https://www.maxss.org), and characterize storm inner core structures, such as the eyewall, radius of maximum wind (RMW) speed, and rain bands (e.g., Horstmann et al., 2013). Regarding ocean wind measurements, currently available and most planned future imaging SAR missions are restricted to a single line-of-sight direction, so cannot unambiguously resolve the wind direction or directly measure the non-axisymmetric aspects of the wind field, which play a major role in the formation and intensification of the storms. Ancillary information from Numerical Weather Prediction (NWP) models is used to aid the inversion, but deficiencies remain in the spatial and temporal characteristics of the modeled surface wind vectors (Belmonte Rivas & Stoffelen, 2019; Trindade et al., 2019).

The nonlinear inversion mapping of SAR normalized radar cross section (NRCS) to ocean wave spectra is understood and its associated forward transform well-described (e.g., Engen & Johnsen, 1995; Tripathi et al., 2024; Wu & Li, 2024). However SAR-based wave spectral retrieval algorithms are far from fully satisfactory as there are fundamental challenges imposed by the use in SAR processing of the Doppler shift to achieve fine spatial resolution in the along-track (azimuth) direction. This azimuth focusing step works very well for a stationary target or for a target (e.g., ship) moving at a constant velocity, but the variable or random motion of the ocean surface leads to smearing of the along-track resolution, which in turn limits the SAR ocean imaging capabilities. The velocity variance, σ_v, caused by surface wave motion results in a minimum wavelength below which the ocean spectrum cannot be resolved. This is called the azimuth cut-off, $\lambda_c \approx R \cdot \sigma_v / v_{orb}$, where R is the slant range to the surface and v_{orb} is the orbital velocity of the satellite. Therefore, the effective resolution of a SAR intensity product is 50–400 m, depending on the sea-state, scales at which modulations due to swell and long wind-waves are captured, while the shorter scale waves associated with the local wind sea are missed. Combining near-collocated directional diversity with the use of both co- and cross-polarized intensity and Doppler shift signals can provide improved local wind sea information to better constrain the nonlinear SAR-wave mapping inversion.

One of the long-standing promises of SAR observations of the ocean is the exploitation of the measurable Doppler spectrum imbedded in the SAR imagery to estimate surface currents based on the Doppler centroid anomaly (shift from expected value for a stationary surface) as suggested by Chapron et al. (2005) and shown to be mostly caused by NRCS-weighted wave motion contributions. Improving the estimation of this shift is one of the major challenges to produce reliable SAR-based surface current products. Although the quality of the measured Doppler spectrum is severely limited by systematic errors, most notably associated with satellite attitude knowledge and antenna pointing uncertainties, there is growing evidence of the capability to retrieve estimates of line-of-sight surface velocity from SAR image mode data (e.g., Johannessen et al., 2008; Moiseev et al., 2022).

The azimuth cut-off is frequency-independent and changing this limit cannot be addressed with any commonly used single SAR antenna system. An important implication is that SAR architectures using multiple azimuth phase centers within a single antenna, in order to achieve High Resolution Wide Swath (HRWS) imaging, are not beneficial for ocean imaging applications. In contrast, these instruments should therefore be operated in a narrow azimuth-beam mode over the ocean, maximizing the antenna gain, and exploiting the available resources either to increase the range resolution, to minimize the NESZ (in particular for cross-polarized channels), or to provide widely separated azimuth looks to add directional diversity, for example, by toggling between forward and backward squinted beams to increase the temporal lag between the looks and better estimate wave-motion parameters.

Many of the limitations mentioned above are solved by the implementation of along-track interferometric (ATI) modes, either in dedicated systems that require instruments on multiple platforms (e.g., Harmony) or by multi-squinted operation with a narrow azimuth transmit pattern (Chapron et al., 2005; Gommenginger et al., 2019; Röhrs et al., 2023; Romeiser et al., 2013). The Harmony mission, planned to launch in 2029, will fly two companion satellites in receive-only mode accompanying Sentinel-1D, one ∼350 km in front and one ∼350 km behind the Sentinel-1 transmitter. The mission objectives include improving the understanding of the upper ocean dynamics and the interactions between the lower atmosphere and the ocean surface by providing, for the first time, large-scale simultaneous measurements of wind, waves, surface currents, sea surface temperature, and cloud motion vectors. This combination of simultaneous measurements will provide new information on small-scale processes, upper ocean dynamics, and the MABL.

In addition to the short-term contributions already in the works from Harmony, there are several other near-term coordination activities to greatly benefit oceanography, specifically related to calibration/validation and handling large data volumes from the SAR Wave Mode data sets. Validation of SAR-derived ocean products is notoriously challenging due to the fine scale of the features, O(100 m–1 km), combined with the snapshot nature of SAR, which contrasts with point-like measurements of typical in situ devices that would require a large network of well-distributed in situ sensors to allow spatiotemporal data comparison. A more robust cal/val approach for SAR-derived ocean products will require experimental campaigns and ocean super-sites, maximizing the synergies with related international efforts. In addition, coordination of SAR observations from as many imaging sensors as possible for the campaigns and supersites would be of great benefit without adding extensive data volumes to any single mission's acquisition plan.

Images of the oceans are anecdotal in that features have lifetimes O(minutes), which is several orders of magnitude below the repeat visit of any spaceborne mission. Most of the value from SAR observations is linked to the statistics (including high-order ones) within a scene and over large collections of imagery. Given the associated data volumes, this severely hinders the use of SAR data over oceans by most potential users. However, today the WAVE-TAC multi-mission SAR (Sentinel-1) data processing system operated by CLS Group (France) delivers near-real time global wave products to operational oceanography and climate forecasting centers (https://data.marine.copernicus.eu/product/WAVE_GLO_PHY_SPC_L4_NRT_014_004/description). Nonetheless, there remains a growing need to develop algorithms to efficiently handle large volumes of acquisitions, likely supported by Generative AI approaches and implemented in the cloud, to compress and extract the relevant geophysical information. Promising examples of this are demonstrated by Wang et al. (2020) and Santos-Ferreira et al. (2025).

In the longer term, in addition to adding or continuing support for global Wave Mode observations from Sentinel-1 and other missions, incorporation of ATI configurations through multi-national collaboration on SAR missions is encouraged with sufficient acquisition, storage, downlink, processing, and archive capability to support ocean observations. Future missions should also collect cross-polarization data over the ocean, particularly with low NESZ. Also, given the stringent instrument calibration for ocean studies associated with an accurate surface stress equivalent wind estimation, these should be considered in the design of the architecture and/or operating modes, with fixed antenna patterns typically offering better repeatability than scanning beams.

3. Survey

In 2021 CEOS space agencies and the ICGS-SAR conducted a survey to identify gaps and needs across the various Earth science communities regarding current and future SAR observations and data availability, as well as to shape recommendations for near-term and long-term spaceborne SAR activities. More than 80 representatives from space agencies, academia, and private companies participated in the survey. This section synthesizes the key findings from the survey, focusing on measurement significance, application requirements, and emerging needs and challenges. The survey respondents were primarily professionals in the scientific and engineering sectors focused on a variety of applications, including all those addressed in this paper.

In terms of key SAR measurements, polarization-dependent backscatter intensity showed the highest relevance across all applications, particularly for agriculture, soil moisture, forest, anthropogenic and weather-related hazards, sea ice, and ocean applications, although it was generally important for all disciplines. Interferometry is essential for geological hazards, solid Earth science, permafrost, and glacier and ice cap studies, and is a new area of study for soil moisture measurements. Both polarimetric and interferometric phases showed significant relevance in applications related to land cover assessment, particularly forest applications, whereas their significance was notably lower in agricultural applications, indicating variability in data requirements across disciplines.

For frequency requirements, the C- or L-band emerged as the most commonly requested if only one frequency is used, possibly because of historically greater availability of data in these bands. However, most respondents expressed a preference for multi-frequency combinations, especially C+L, C+L+X, or P+L, reflecting the diversity of SAR frequencies for many different applications. It is worth noting that most of the respondents emphasized the importance of regular, short-revisit acquisitions at any frequency.

Regarding the polarization requirement, relatively few respondents required only a single polarization, mainly those using it for geological hazards and solid Earth studies for which horizontal transmit polarization is

preferred. Most applications require dual or even quad-polarization, with fully polarized data of particular value for forest applications.

The survey also solicited input on the needed spatial and temporal resolution, revealing that for most applications a spatial resolution of 10 m and weekly revisit frequency are optimal. However, certain applications observing dynamic conditions and processes benefit from daily observations, particularly for monitoring growing season agriculture and for hazard monitoring (but not response), for example, oil spills, floods, or active volcanoes. Sub-daily data collection was indicated for disaster response and applications observing highly active tectonic features, glaciers, sea ice, and some ice sheets. Regular global or regional coverage was favoured, with many respondents stressing the need for selected areas to be monitored with more frequent, multi-frequency SAR observations than currently available.

The respondents identified main obstacles inhibiting wider adoption and usage of SAR and shared recommendations for filling gaps both in an incremental approach and with "game-changing" actions. These fell into three general categories: SAR data and derived products, observation strategies for current missions, and future mission concepts. The overwhelming request was for open access to SAR data from missions other than those of ESA and NASA, which have open data policies, because sharing data openly drives research, innovation, and commercial enterprise. Data accessibility is also an issue, specifically that there is no standardized data format across the different SAR data sets; no single service to search all missions' data; and no open access operational environment for data processing. Recommendations from the survey respondents included additional coordination between missions and data providers to address the availability issues and incorporation of AI for advanced processing algorithms and higher-level product generation (even onboard in future missions).

The needs for more multi-frequency and quad-polarization data, and more frequent imaging were highlighted by many respondents. For example, the lack of regular data acquisitions with global coverage in L-and P-band to support forest and wetland studies was identified, and, that is, now being addressed in part with the Biomass, ALOS-2/4, and NISAR missions. Generally, it was thought that joint coordination of the existing missions' observation plans could provide consistent, standard satellite coverage of calibration and validation sites, at least, and possibly other discipline-specific areas. The need for consistent and continued funding of current missions was also identified as important to maintaining the time series of SAR data.

Most of the recommendations from the survey related to coordinated investments in future missions: multi-agency cooperation to launch SAR constellations enabling frequent revisit (hazards, glaciers/ice sheets, sea ice, agriculture); multi-frequency tandem satellites (forests); global coverage with quad-polarimetry (ecosystems sciences); and possibly specialized missions targeting specific areas of interest, optimized for particular measurements (e.g., wetlands, ice sheets) with a consistent monitoring plan, optimal frequency selection, and product generation for non-specialists. An interesting request that recurred was to coordinate SAR missions' observation plans with those carrying other sensor types to have systematic and effective monitoring frameworks that include multiple sensor types (optical, IR, SAR, LiDAR).

4. Summary and Recommendations

Previous sections have identified coordination activities and future missions that benefit a specific discipline, largely isolated from the needs of other disciplines and independent of whether the recommendations support or detract from the others' science gains and societal benefits. As no one single SAR system or agency has the capacity to address the full suite of requirements identified here for all the science disciplines, a constellation of missions and their coordinated activities is consequently required, thus calling for a confederated approach. Here we provide findings on the synergies and differences between the needs of the different disciplines, then consider SAR science and applications as a whole to identify suggested coordination actions among the space agencies and the science communities that can benefit many or all. By considering the capabilities and SAR assets of the ICGS-SAR space agency members in combination, we hope to help advance toward greater overall scientific discovery and societal benefit both effectively and efficiently, without undue burden on any one agency and taking advantage of the priorities and unique contributions of each. Recommendations include (a) incremental actions, implementable starting now to make progress in the near-term (next 5–10 years) with operational SAR assets plus those in the pipeline, for example, the Copernicus/ESA ROSE-L (Geudtner et al., 2021), and (b) next-generation missions (2030s timeframe).

Table 3
Game-Changing Requirements by Discipline

		InSAR		Fast repeat interval			
Discipline	CP/QP?	InSAR?	3D velocity	≤1 week	2–3 obs/week	≤1 day	Simultaneous multifrequency?[a]
Ice sheets/glaciers		X	X			X	
Solid Earth science		X	X			X	
Hazards		X				X	
Forest/biomass	X	X[b]					X
Wetlands	X			X			X
Agriculture	X				X		X
Soil moisture	X					X	
Permafrost		X			X		X
Sea ice	X					X	X
Ocean		X[c]				X	

[a]Not indicated is the fact that most disciplines regularly use data from more than one frequency, but it is not required to be simultaneously acquired or very nearly coincident. [b]Requires non-zero cross-track baseline for increased height sensitivity and tomography. [c]Requires non-zero along-track baseline for Along-Track Interferometry (ATI).

In looking for overlaps and conflicts between the disciplines assessed, we consider the "must have" needs for game-changing advancement of each discipline given what we know now from prior research (Section 2). The intent is to identify mission requirements that are currently expected to enable or preclude significant overall advancement of the field. Table 3 summarizes the general breakdown based on high priority needs for polarimetry, interferometry, angle diversity, temporal repeat, and multi-frequency SAR for near-coincident or coincident imaging. As in Section 2.3, hazard requirements pertain to the period encompassing a disaster, since needs for other phases of the disaster management cycle are covered by the other disciplines. The table is not meant to be interpreted strictly or for all situations, and obviously there are exceptions for specific topics within any discipline, for example, wetlands mapping during floods might require daily imaging, but, that is, covered in hazards; InSAR is being shown useful for soil moisture, but it is not the driving game-changer; multi-frequency data can be used in solid earth or other InSAR-enabled studies for phase unwrapping but is not essential.

The disciplines first break down into two basic classes: those that require polarimetry, specifically QP or in its absence CP, and those that require repeat-pass InSAR, with Forest/Biomass studies the exceptions in requiring both and Hazards so diverse as to fall in one or the other category depending on the type of hazard. Among those requiring InSAR, zero baselines are required for all except Forest/Biomass, which requires non-zero baselines for increased height sensitivity as well as to allow for tomography, and for those Ocean applications using along-track interferometry. We note that altimetry from LiDAR or single-pass InSAR is used by many disciplines but is not the exclusive driver of advancement in any considered here. Imaging geometry diversity to derive 3D velocity fields is critical to Ice Sheets/Glaciers and Solid Earth Science. Quad-polarimetry is expected to be game-changing for the ecosystem disciplines and sea ice studies. More frequent observations (<1 week) are needed for all disciplines except Forest/Biomass. Fortunately, those requiring daily or more frequent repeats need limited coverage (e.g., Oceans need supersites) if less frequent global data for background monitoring is available. There is strong overlap between the disciplines needing QP data and those needing multi-frequency data. Table 4 gives the bands preferred for multi-frequency data, showing that L-band is the most useful overall, split equally between those combining with shorter or longer wavelengths (S-band is not included for lack of sufficiently high-temporal resolution and availability prior to NISAR). It is likely that P-band will be increasingly used once the Biomass mission provides data for studies. This distribution highlights the importance of continued coverage with L-band using NISAR, ALOS-2/4, and later ROSE-L. Frankly, too few multi-frequency data sets are available to assess its full potential so this table is just a starting point for what we will learn in the near future. Likewise, the full potential of polarimetry across all disciplines is unexplored due to the general lack of systematic polarimetric observations. The exception is soil moisture where the SAOCOM mission demonstrates the potential.

Table 4
Preferred Multi-Frequency Bands by Discipline Based on Our Current Scientific Understanding

Topic	X-band	C-band	L-band	P-band
Forest/biomass			X	X
Wetlands		X	X	X
Agriculture	X	X	X	
Soil moisture			X	X
Permafrost		X	X	X
Sea ice		X	X	

Note. This could change with more open data from, for example, P-band, S-band, and X-band sensors.

We make several concrete recommendations for actions to take in the near-term involving data access and coordination of observations that, if implemented in whole or in part, will go a long way toward advancing SAR science and applications. Firstly, long or dense time series and open access to data are of value for all disciplines, and in that regard specific recommendations to the space agencies for the near-term are:

- Provide open access to more data, even if only contained in archives or acquired for selected areas. For L-band, consider making SAOCOM-1A/B, ALOS, and ALOS-2 global archives open for scientific use.
- Prioritize consistent observation modes over changing modes for systematic monitoring to enable shorter temporal baseline InSAR over longer time scales and more dense time series for change detection in general.

The next recommendation relates to near-term coordination of observations to provide more frequent imaging, incidence angle diversity, multi-frequency observations, and consistent coverage of high priority areas. Inter-agency coordination for SAR data acquisitions in polar regions through the PSTG has clearly demonstrated the potential of the combined SAR missions operating as a virtual constellation to enable advancements not achievable with any single mission. However, equally important is that through the PSTG the community first assessed its needs, prioritizing and limiting them, then approached the space agencies with specific requests justified by the science. The PSTG was formally organized through WMO, with members selected to represent cryosphere science. A similar effort is underway through the CEOS LSI-VC. We recommend that other working groups organize around common needs, like the 3D-InSAR Task Group mentioned in Section 2.2, forming a cohesive community with well-defined goals. These groups can also organize field campaigns and supersites for international collaboration with extensive imaging. The space agencies, perhaps within a group like the ICGS-SAR, can consider requests from all the working groups and share the tasking based on agency programs, mission capabilities, and scientific justification. As the PSTG has proven, seemingly minor contributions from many agencies can contribute to major advancements. Examples of coordinated observations of value are:

- Coordinate observations for the Arctic, Antarctic, Greenland, and Siberia regions to provide spatially comprehensive coverage with sustained observations at the orbit repeat period.
- Acquire ALOS-4 and SAOCOM-1 wide-swath full-polarimetric observations of global vegetated areas with dual seasonal (summer/winter & dry/wet season) or four-season coverages. (This complements NISAR's dual polarization12-day repeat)
- Acquire systematically time series data over selected discipline-specific study sites with a wide diversity of frequency bands (P, L, S, C, X) and with as many polarization channels as possible for each instrument. Study sites are needed for vegetation (forests and agriculture areas), soil moisture estimation, and sea ice, land ice, snow and permafrost studies.
- Coordinate with LiDAR and optical missions for campaigns and supersites.

The last recommendation for near-term action pertains to SAR's value for disaster response, namely that the space agencies work toward implementing a global system for “Smart Tasking” for disaster response. This could take the form of updating the International Charter to better match modern capabilities, i.e., automatic activation for major tectonic disasters based on input from existing sensor networks, activation prior to forewarned events (e.g., hurricanes), and activation without requests in some cases. Most major disasters now elicit international support, so these changes would enable lower latency information delivery and more rapid and effective response. Additionally, all providers should endeavor to deliver low latency data products (ideally <1 hr).

We mainly have considered the non-commercial, non-military space agencies, particularly those that have participated in the ICSG-SAR activity. However, commercial Very High Resolution X-band SAR missions have a potential complementary role to play through their capacity for targeted backscatter and interferometric observations at high spatial and temporal resolution. However, as these missions typically acquire data on demand only, consistent global- or regional scale data archives are not available and even lacking at the local scale for many scientifically important sites. Dedicated observation scheduling is therefore imperative to make the data useful, so agencies considering governmental data purchases for science are recommended to consider tasking rights a requirement for procurement. We also recommend that the commercial companies make their data open

access when it is no longer of economic value or restricted by the original purchaser. We also note that the value of commercial SAR for science and disaster response is greatly improved if the systems have repeat pass InSAR or multi-polarization capability.

In the longer perspective, that is, through the 2030s, and considering missions still to be defined, there is significant potential for the joint development of an ambitious multi-agency, multi-mission, mega-constellation of constellations that would fully address the outstanding scientific requirements for temporal revisit, LOS and baseline diversity, polarimetry and multi-frequency observations. The addition of cooperative receive-only systems to typical backbone SAR missions (Sentinel-1, NISAR, ROSE-L) designed as zero-baseline missions will enable LOS and baseline diversity, single pass interferometry, or tomography. These companion missions must be able to operate without interfering with backbone missions, requiring standards for interfaces, synchronization links, and operational coordination. ESA's current approach is to keep backbone missions unchanged, but with "companion friendliness levels" added to enable companion contributions (e.g., for Sentinel-1 Next Generation, ROSE-L, or future flagship missions). Passive companions could address missing capabilities in programs like Copernicus, such as across-track single-pass acquisitions for forestry. Inter-agency cooperation will be vital for the success of bistatic and multistatic SAR. Shared infrastructures, common standards, and coordinated mission design will be necessary to enable next-generation SAR systems and to fully exploit the opportunities of multi-static SAR architectures. In general, future SAR missions that are currently in formulation would benefit even more if inter-agency coordination would start at the mission conceptualization stage, adding representatives from other agencies to their science definition teams to continue and improve long-term coordination beyond the near-term actions recommended here.

The ICGS-SAR was proposed by Charles Elachi, who had a vision of the world's SAR-operating space agencies working together to achieve more than their individual goals by reducing duplication, thereby making better use of funding, capabilities, and assets—in his words achieving the equivalent of one plus one equals four. Since its first workshop in 2018, the ICGS-SAR has brought together mission managers, engineers, and scientists to brainstorm ways that this can be achieved, considering all aspects of coordination in missions, data, and operations. This paper summarized the work done specifically for advancing SAR-enabled science toward game-changing discoveries and realizing the many benefits offered by SAR for addressing the world's problems. The advantages of coordination for science, applications, and disaster response are clear: optimum utilization of space assets based on their strength and availability, and higher probability of an agency's buy-in if its respective requirements can be relaxed given other agencies' shared contributions.

Conflict of Interest

The authors declare no conflicts of interest relevant to this study.

Availability Statement

This paper synthesizes research from the existing literature, referenced herein. No specific data or software were used or generated in its preparation.

Acronyms

AGB	Above-ground biomass
AI	Artificial Intelligence
ALT	Active Layer Thickness
AMSR2	Advanced Microwave Scanning Radiometer-2
ARD	Analysis Ready Data
ARIA	Advanced Rapid Imaging and Analysis
ARSET	Applied Remote Sensing Training Program
ASCAT	Advanced Scatterometer

ASF	Alaska Satellite Facility
ASI	Agenzia Spaziale Italiana
ATI	Along-track interferometry/Along-track interferometric
CCI	Climate Change Initiative
CEOS	Committee on Earth Observation Satellites
CONAE	Comisión Nacional de Actividades Espaciales
CP	Compact polarization/Compact polarimetry
CSA	Canadian Space Agency
CSG	COSMO-SkyMed Generation
CSK	COSMO-SkyMed
DEM	Digital elevation model
DLR	Deutsches Zentrum für Luft und Raumfahrt
ECV	Essential Climate Variable
EO	Earth-observing
ERS	Earth Remote Sensing
ESA	European Space Agency
EU	European Union
FYI	First-year ice
GCOM-W	Global Change Observation Mission - Water
GCOS	Global Climate Observing System
GCW	Global Cryosphere Watch
GEDI	Global Ecosystem Dynamics Investigation
GFM	Global Flood Monitoring
GIC	Glaciers and Ice Caps
GMS	Ground Motion Service
HDF5	Hierarchical Data Format 5
HH	Horizontal transmit/Horizonal receive
HRWS	High Resolution Wide Swath
HV	Horizontal transmit/Vertical receive
ICGS-SAR	International Coordination Group for Spaceborne Synthetic Aperture Radar Missions
INFCOM	Commission for Observation, Infrastructure and Information Systems
InSAR	Interferometric SAR
ISRO	Indian Space Research Organisation
IW	Interferometric Wide
JAXA	Japan Aerospace Exploration Agency
KSAT	Kongsberg Satellite Services

LAI	Leaf Area Index
LiCSAR	Looking Into Continents from Space with Synthetic Aperture Radar
LOS	Line-of-sight
LSI-VC	Land Surface Imaging Virtual Constellation
MABL	Marine atmosphere boundary layer
MDA	MDA Space Ltd.
MIA	Multi-Aperture SAR Interferometry
ML	Machine learning
MOLI	Multi-sensing Observation LiDAR and Imager Demonstration
MSI	Multispectral Imager
MYI	Multi-year ice
NASA	National Aeronautics and Space Administration
NDVI	Normalized Difference Vegetation Index
NESZ	Noise equivalent sigma-naught
NISAR	NASA-ISRO Synthetic Aperture Radar
NOAA	National Oceanic and Atmospheric Administration
NRCS	Normalized radar cross section
NWP	Numerical Weather Prediction
OPERA	Operational Products for End-Users from Remote Sensing Analysis
PAI	Plant Area Index
Pol-InSAR	Polarimetric interferometric SAR
PolSAR	Polarimetric SAR
PSTG	Polar Space Task Group
PT	Permafrost Temperature
QP	Quad-polarimetry/Quad-polarimetric
RCM	Radarsat Constellation Mission
RGV	Rock Glacier Velocity
RMW	Radius of maximum wind
RR	Right circular transmit, right circular receive
SAR	Synthetic Aperture Radar
SAR-CWG	SAR Coordination Working Group
SDG	Sustainable Development Goals
SMAP	Soil Moisture Active Passive
SMOS	Soil Moisture and Ocean Salinity
SRTM	Shuttle Radar Topography Mission
SST	Surrey Satellite Technology Ltd.

SWOT	Surface Water Ocean Topography
TC	Tropical cyclone
TomoSAR	Tomographic SAR
UKSA	United Kingdom Space Agency
USA	United States of America
USAID	U.S. Agency for International Development
USGS	U.S. Geological Survey
VH	Vertical transmit/Horizonal receive
VV	Vertical transmit/Vertical receive
WgCapD	Working Group on Capacity Building and Data Democracy
WGCV	Working Group on Calibration and Validation
WMO	World Meteorological Organization

Acknowledgments
This research was carried out in part at the Jet Propulsion Laboratory, California Institute of Technology, under contract with the National Aeronautics and Space Administration under contract 80NM0018F0591/209249.04.01.01.71, the European Space Agency, contract 4000123681/18/I-NB–Permafrost_CCI+ and through the Japan Aerospace Exploration Agency, Earth Observation Research Center, contact 25RT000247. Support for this work was also received from ESA under the Purchase Order N. 5001037041. CEJ, AR, BR, and MF led the preparation of the manuscript overall; individual discipline sections were led by ER and BS (Ice Sheets and Glaciers); YZ, AH, and MS (Solid Earth); CEJ and TK (Hazards); PS and MS (Forests and Biomass); LH, TT, and AR (Wetlands); HM (Agriculture); LF (Soil Moisture), MJ and WD (Sea Ice); LR and AB (Permafrost); PLD and JAJ (Oceans).

References

Adrian, J., Sagan, V., & Maimaitijiang, M. (2021). Sentinel SAR-optical fusion for crop type mapping using deep learning and Google Earth Engine. *ISPRS Journal of Photogrammetry and Remote Sensing*, *175*, 215–235. https://doi.org/10.1016/j.isprsjprs.2021.02.018

Agram, P. S., & Simons, M. (2015). A noise model for InSAR time series. *Journal of Geophysical Research: Solid Earth*, *120*(4), 2752–2771. https://doi.org/10.1002/2014JB011271

Amelung, F., Galloway, D. L., Bell, J. W., Zebker, H. A., & Laczniak, R. J. (1999). Sensing the ups and downs of Las Vegas: InSAR reveals structural control of land subsidence and aquifer-system deformation. *Geology*, *27*(6), 483–486. https://doi.org/10.1130/0091-7613(1999)027<0483:STUADO>2.3.CO;2

Amelung, F., Jónsson, S., Zebker, H., & Segall, P. (2000). Widespread uplift and 'trapdoor' faulting on Galapagos volcanoes observed with radar interferometry. *Nature*, *407*(6807), 993–996. https://doi.org/10.1038/35039604

Amherdt, S., Di Leo, N. C., Balbarani, S., Pereira, A., Cornero, C., & Pacino, M. C. (2021). Exploiting Sentinel-1 data time series for crop classification and harvest date detection. *International Journal of Remote Sensing*, *42*(19), 7313–7331. https://doi.org/10.1080/01431161.2021.1957176

Amitrano, D., Di Martino, G., Di Simone, A., & Imperatore, P. (2024). Flood detection with SAR: A review of techniques and datasets. *Remote Sensing*, *16*(4), 656. https://doi.org/10.3390/rs16040656

Ansari, H., De Zan, F., & Parizzi, A. (2020). Study of systematic bias in measuring surface deformation with SAR interferometry. *IEEE Transactions on Geoscience and Remote Sensing*, *59*(2), 1285–1301. https://doi.org/10.1109/TGRS.2020.3003421

Arai, H., Le Toan, T., Takeuchi, W., Oyoshi, K., Fumoto, T., & Inubushi, K. (2022). Evaluating irrigation status in the Mekong Delta through polarimetric L-band SAR data assimilation. *Remote Sensing of Environment*, *279*, 113139. https://doi.org/10.1016/j.rse.2022.113139

Ardhuin, F., Molero, B., Bohé, A., Nouguier, F., Collard, F., Houghton, I., et al. (2024). Phase-resolved swells across ocean basins in SWOT altimetry data: Revealing centimeter-scale wave heights including coastal reflection. *Geophysical Research Letters*, *51*(16), e2024GL109658. https://doi.org/10.1029/2024GL109658

Askne, J., Dammert, P., Ulander, L., & Smith, G. (1997). C-band repeat-pass interferometric SAR observations of the forest. *IEEE Transactions on Geoscience and Remote Sensing*, *35*(1), 25–35. https://doi.org/10.1109/36.551931

Bartsch, A., Bergstedt, H., Pointner, G., Muri, X., Rautiainen, K., Leppänen, L., et al. (2023). Towards long-term records of rain-on-snow events across the Arctic from satellite data. *The Cryosphere*, *17*(2), 889–915. https://doi.org/10.5194/tc-17-889-2023

Bartsch, A., Efimova, A., Widhalm, B., Muri, X., von Baeckmann, C., Bergstedt, H., et al. (2024). Circumarctic land cover diversity considering wetness gradients. *Hydrology and Earth System Sciences*, *28*(11), 2421–2481. https://doi.org/10.5194/hess-28-2421-2024

Bartsch, A., Ley, S., Nitze, I., Pointner, G., & Vieira, G. (2020). Feasibility study for the application of synthetic aperture radar for coastal erosion rate quantification across the arctic. *Frontiers in Environmental Science*, *8*, 143. https://doi.org/10.3389/fenvs.2020.00143

Bartsch, A., Muri, X., Hetzenecker, M., Rautiainen, K., Bergstedt, H., Wuite, J., et al. (2025). Benchmarking passive-microwave-satellite-derived freeze–thaw datasets. *The Cryosphere*, *19*(1), 459–483. https://doi.org/10.5194/egusphere-2024-2518

Bartsch, A., Strozzi, T., & Nitze, I. (2023). Permafrost monitoring from space. *Surveys in Geophysics*, *44*(5), 1579–1613. https://doi.org/10.1007/s10712-023-09770-3

Bartsch, A., Widhalm, B., Kuhry, P., Hugelius, G., Palmtag, J., & Siewert, M. (2016). Can C-band SAR be used to estimate soil organic carbon storage in tundra? *Biogeosciences*, *13*(19), 5453–5470. https://doi.org/10.5194/bg-13-5453-2016

Bekaert, D., Walters, R., Wright, T., Hooper, A., & Parker, D. (2015). Statistical comparison of InSAR tropospheric correction techniques. *Remote Sensing of Environment*, *170*, 40–47. https://doi.org/10.1016/j.rse.2015.08.035

Bekaert, D. P., Handwerger, A. L., Agram, P., & Kirschbaum, D. B. (2020). InSAR-based detection method for mapping and monitoring slow-moving landslides in remote regions with steep and mountainous terrain: An application to Nepal. *Remote Sensing of Environment*, *249*, 111983. https://doi.org/10.1016/j.rse.2020.111983

Belmonte Rivas, M., & Stoffelen, A. (2019). Characterizing ERA-Interim and ERA5 surface wind biases using ASCAT. *Ocean Science*, *15*(3), 831–852. https://doi.org/10.5194/os-15-831-2019

Bernhard, P., Zwieback, S., Leinss, S., & Hajnsek, I. (2020). Mapping retrogressive thaw slumps using single-pass TanDEM-X observations. *IEEE Journal of Selected Topics in Applied Earth Observations and Remote Sensing*, *13*, 3263–3280. https://doi.org/10.1109/JSTARS.2020.3000648

Bessis, J. L., Bequignon, J., & Mahmood, A. (2004). The international charter "space and major disasters" initiative. *Acta Astronautica*, *54*(3), 183–190. https://doi.org/10.1016/S0094-5765(02)00297-7

Bindschadler, R., King, M. A., Alley, R., Anandakrishnan, S., & Padman, L. (2003). Tidally controlled stick-slip discharge of a West Antarctic ice stream. *Science*, *301*, 1087–1090. https://doi.org/10.1126/science.1087231

Bletery, Q., Cavalié, O., Nocquet, M., & Ragon, T. (2020). Distribution of interseismic coupling along the North and East Anatolian Faults inferred from InSAR and GPS data. *Geophysical Research Letters*, *47*(16), e2020GL087775. https://doi.org/10.1029/2020GL087775

Blickensdörfer, L., Schwieder, M., Pflugmacher, D., Nendel, C., Erasmi, S., & Hostert, P. (2022). Mapping of crop types and crop sequences with combined time series of Sentinel-1, Sentinel-2 and Landsat 8 data for Germany. *Remote Sensing of Environment*, *269*, 112831. https://doi.org/10.1016/j.rse.2021.112831

Born, G. H., Dunne, J. A., & Lame, D. B. (1979). Seasat mission overview. *Science*, *204*(4400), 1405–1406. https://doi.org/10.1126/science.204.4400.1405

Bouvet, A., Mermoz, S., Le Toan, T., Villard, L., Mathieu, R., Naidoo, L., & Asner, G. P. (2018). An above-ground biomass map of African savannahs and woodlands at 25 m resolution derived from ALOS PALSAR. *Remote Sensing of Environment*, *206*, 156–173. https://doi.org/10.1016/j.rse.2017.12.030

Brisco, B., Kun, L., Tedford, B., Charbonneau, F., Yun, S., & Murnaghan, K. (2013). Compact polarimetry assessment for rice and wetland mapping. *International Journal of Remote Sensing*, *34*(6), 1949–1964. https://doi.org/10.1080/01431161.2012.730156

Cáceres, M., Dadamia, D., Thibeault, M., Müller, S., Righetti, S., & Skabar, Y. (2016). Estimación del error de mapas de humedad de suelo satelitales. In *8° Congreso Argentino de AgroInformática*. Retrieved from https://core.ac.uk/download/pdf/301073395.pdf

Carlson, G., Werth, S., & Shirzaei, M. (2024). A novel hybrid GNSS, GRACE, and InSAR joint inversion approach to constrain water loss during a record-setting drought in California. *Remote Sensing of Environment*, *311*, 114303. https://doi.org/10.1016/j.rse.2024.114303

Carret, A., Fleury, S., Di Bella, A., Landy, J., Lawrence, I., Kurtz, N., et al. (2025). A multi-frequency altimetry snow depth product over Arctic sea ice. *Scientific Data*, *12*(1), 104. https://doi.org/10.1038/s41597-024-04343-4

Cartus, O., Santoro, M., Wegmüller, U., & Rommen, B. (2019). Benchmarking the retrieval of biomass in boreal forests using P-band SAR backscatter with multi-temporal C- and L-band observations. *Remote Sensing*, *11*(14), 1695. https://doi.org/10.3390/rs11141695

Casey, J. A., Howell, S. E. L., Tivy, A., & Haas, C. (2016). Separability of sea ice types from wide swath C- and L-band synthetic aperture radar imagery acquired during the melt season. *Remote Sensing of Environment*, *174*, 314–328. https://doi.org/10.1016/j.rse.2015.12.021

Cassianides, A., Lique, C., & Korosov, A. (2021). Ocean eddy signature on sar-derived sea ice drift and vorticity. *Geophysical Research Letters*, *48*(6), e2020GL092066. https://doi.org/10.1029/2020GL092066

CEOS. (2025). CEOS analysis ready data, product family specification synthetic aperture radar, v1.2. *Committee on Earth Observation Satellites*. Retrieved from https://ceos.org/ard/files/PFS/SAR/v1.1/CEOS-ARD_PFS_Synthetic_Aperture_Radar_v1.1.pdf

Cetin, E., Meghraoui, M., Cakir, Z., Akoglu, A. M., Mimouni, O., & Chebbah, M. (2012). Seven years of postseismic deformation following the 2003 Mw = 6.8 Zemmouri earthquake (Algeria) from InSAR time series. *Geophysical Research Letters*, *39*(10), L10307. https://doi.org/10.1029/2012GL051344

Chapman, B., McDonald, K., Shimada, M., Rosenqvist, A., Schroeder, R., & Hess, L. (2015). Mapping regional inundation with spaceborne L-Band SAR. *Remote Sensing*, *7*(5), 5440–5470. https://doi.org/10.3390/rs70505440

Chapron, B., Collard, F., & Ardhuin, F. (2005). Direct measurements of ocean surface velocity from space: Interpretation and validation. *Journal of Geophysical Research*, *110*(C7), C07008. https://doi.org/10.1029/2004JC002809

Charbonneau, F. J., Brisco, B., Raney, R. K., McNairn, H., Liu, C., Vachon, P. W., et al. (2010). Compact polarimetry overview and applications assessment. *Canadian Journal of Remote Sensing*, *36*(Suppl. 2), S298–S315. https://doi.org/10.5589/m10-062

Chelton, D. B. (2024). A postlaunch update on the effects of instrumental measurement errors on SWOT estimates of sea surface height, velocity, and vorticity. *Journal of Atmospheric and Oceanic Technology*, *41*(9), 865–888. https://doi.org/10.1175/JTECH-D-24-0035.1

Chen, D., Roy, D. P., Zhu, Z., McVicar, T. R., Sheffield, J., Atkinson, P. M., et al. (2025). A call for integrated and coordinated global sharing of China's Earth observation data. *Nature Geoscience*. Retrieved from https://www.nature.com/articles/s41561-025-01833-x

Chen, J., Knight, R., Zebker, H. A., & Schreüder, W. A. (2016). Confined aquifer head measurements and storage properties in the San Luis Valley, Colorado, from spaceborne InSAR observations. *Water Resources Research*, *52*(5), 3623–3636. https://doi.org/10.1002/2015WR018466

Chen, J., Wu, Y., O'Connor, M., Cardenas, M. B., Schaefer, K., Michaelides, R., & Kling, G. (2020). Active layer freeze-thaw and water storage dynamics in permafrost environments inferred from InSAR. *Remote Sensing of Environment*, *248*, 112007. https://doi.org/10.1016/j.rse.2020.112007

Combot, C., Mouche, A., Knaff, J., Zhao, Y., Zhao, Y., Vinour, L., et al. (2020). Extensive high-resolution synthetic aperture radar (SAR) data analysis of tropical cyclones: Comparisons with SFMR flights and best track. *Monthly Weather Review*, *148*(11), 4545–4563. https://doi.org/10.1175/MWR-D-20-0005.1

Copernicus. (2025). Copernicus DEM—Global and European digital elevation model. *Copernicus Data Space*. https://doi.org/10.5270/ESA-c5d3d65

Costa, M. P. F., Niemann, O., Novo, E., & Ahern, F. (2002). Biophysical properties and mapping of aquatic vegetation during the hydrological cycle of the Amazon floodplain using JERS-1 and Radarsat. *International Journal of Remote Sensing*, *23*(7), 1401–1426. https://doi.org/10.1080/01431160110092957

Dadamia, D., Acuna, M., Luca, E., Oviedo, A., Palomeque, M., Thibeault, M., et al. (2015). Generating a synthetic data base of polarimetric signatures to exploit SAOCOM observations over Pampas. 267-270. In *2015 IEEE International Geoscience and Remote Sensing Symposium (IGARSS)*. https://doi.org/10.1109/IGARSS.2015.7325751

Dammann, D. O., Eriksson, L. E. B., Mahoney, A. R., Eicken, H., & Meyer, F. J. (2019). Mapping pan-Arctic landfast sea ice stability using Sentinel-1 interferometry. *The Cryosphere*, *13*(2), 57–577. https://doi.org/10.5194/tc-13-557-2019

Davidson, A. M., Fisette, T., McNairn, H., & Daneshfar, B. (2017). Detailed crop mapping using remote sensing data (Crop Data Layers). In *Handbook on remote sensing for agricultural statistics* (pp. 91–117). Food and Agriculture Organization of the United Nations.

Delouis, B., Nocquet, M., & Vallée, M. (2010). Slip distribution of the February 27, 2010 Mw = 8.8 Maule Earthquake, central Chile, from static and high-rate GPS, InSAR, and broadband teleseismic data. *Geophysical Research Letters*, *37*(17), L17305. https://doi.org/10.1029/2010GL043899

Demchev, D., Eriksson, L. E., Hildeman, A., & Dierking, W. (2023). Alignment of multifrequency sAR images acquired over sea ice using drift compensation. *IEEE Journal of Selected Topics in Applied Earth Observations and Remote Sensing*, *16*, 7393–7402. https://doi.org/10.1109/JSTARS.2023.3302576

Destefanis, T., Guliyeva, S., Boccardo, P., & Fissore, V. (2025). Advancing flood detection and mapping: A review of Earth observation services, 3D data integration, and AI-Based techniques. *Remote Sensing*, *17*(17), 2943. https://doi.org/10.3390/rs17172943

Dey, S., Bhogapurapu, N., Bhattacharya, A., Mandal, D., Lopez-Sanchez, J., McNairn, H., & Frery, A. (2021). Rice phenology mapping using novel target characterization parameters from polarimetric SAR data. *International Journal of Remote Sensing*, *42*(14), 5519–5543. https://doi.org/10.1080/01431161.2021.1921876

De Zan, F., & Gomba, G. (2018). Vegetation and soil moisture inversion from SAR closure phases: First experiments and results. *Remote Sensing of Environment*, *217*, 562–572. https://doi.org/10.1016/j.rse.2018.08.034

De Zan, F., Parizzi, A., Prats-Iraola, P., & Lopez-Dekker, P. (2014). A SAR interferometric model for soil moisture. *IEEE Transactions on Geoscience and Remote Sensing*, *52*(1), 418–425. https://doi.org/10.1109/TGRS.2013.2241069

Dierking, W. (2021). Synergistic use of L-and C-band SAR satellites for sea ice monitoring. In *2021 IEEE International Geoscience and Remote Sensing Symposium IGARSS* (pp. 877–880). IEEE.

Dierking, W., & Davidson, M. (2021). Use of L- and C-band SAR satellites for sea ice and iceberg monitoring (LC-ICE). In *EGU general assembly*. https://doi.org/10.5194/egusphere-egu21-3916.EGU21-3916

Dierking, W., Schneider, A., Eltoft, W., & Gerland, S. (2022). *CIRFA Cruise 2022*. Cruise report. Zenodo. https://doi.org/10.5281/zenodo.7314066

Dingle Robertson, L., Davidson, A. M., McNairn, H., Hosseini, M., Mitchell, S., de Abelleyra, D., et al. (2020). C-band synthetic aperture radar (SAR) imagery for the classification of diverse cropping systems. *International Journal of Remote Sensing*, *41*, 9628–9649. https://doi.org/10.1080/01431161.2020.1805136

Dingle Robertson, L., McNairn, H., Jiao, X., McNairn, C., & Ihuoma, S. O. (2022). Monitoring crops using compact polarimetry and the RADARSAT Constellation Mission. *Canadian Journal of Remote Sensing*, *48*(6), 793–813. https://doi.org/10.1080/07038992.2022.2121271

Dingle Robertson, L., McNairn, H., van der Kooij, M., Jiao, X., Ihuoma, S., & Joosse, P. (2023). Monitoring autumn agriculture activities using Synthetic Aperture Radar (SAR) and coherence change detection. *Heliyon*, *9*(6), e17322. https://doi.org/10.1016/j.heliyon.2023.e17322

Dobson, C., Ulaby, F., LeToan, T., Beaudoin, A., Kasischke, E., & Christensen, N. (1992). Dependence of radar backscatter on coniferous forest biomass. *IEEE Transactions on Geoscience and Remote Sensing*, *30*(2), 412–415. https://doi.org/10.1109/36.134090

Duchossois, G., Berdahl, M., Diehl, T., Garric, G., Humbert, A., Itkin, P., et al. (2024). *Copernicus polar roadmap for service evolution – Copernicus polar task force*. Publications Office of the European Union. https://doi.org/10.2889/644108

Elachi, C. (1980). Spaceborne imaging radar: Geologic and oceanographic applications. *Science*, *209*(4461), 1073–1082. https://doi.org/10.1126/science.209.4461.1073

Elachi, C., Borgeaud, M., Rosenqvist, A., Bawden, G., Jones, C., & Rosen, P. (2022). Coordination of international spaceborne SAR missions. In *IGARSS 2022-2022 IEEE international geoscience and remote sensing symposium* (pp. 7398–7400).

Elliott, J. R., Fang, J., Lazecky, M., Maghsoudi, Y., Ou, Q., Payne, J., et al. (2026). Deformation, strains and velocities for the Alpine Himalayan Belt from trans-continental Sentinel-1 InSAR & GNSS. *Remote Sensing of Environment*, *338*, 115320. https://doi.org/10.1016/j.rse.2026.115320

El Moussawi, I., Ho Tong Minh, D., Baghdadi, N., Abdallah, C., Jomaah, J., Strauss, O., et al. (2019). Monitoring tropical forest structure using SAR tomography at L-and P-band. *Remote Sensing*, *11*(16), 1934. https://doi.org/10.3390/rs11161934

Engen, G., & Johnsen, H. (1995). SAR-ocean wave inversion using image cross spectra. *IEEE Transactions on Geoscience and Remote Sensing*, *33*(4), 1047–1056. https://doi.org/10.1109/36.406690

Eriksson, L. E. B., Santoro, M., Wiesmann, A., & Schmullius, C. C. (2003). Multitemporal JERS repeat-pass coherence for growing-stock volume estimation of Siberian forest. *IEEE Transactions on Geoscience and Remote Sensing*, *41*(7 PART I), 1561–1570. https://doi.org/10.1109/TGRS.2003.814131

Espeseth, M. M., Brekke, C., Jones, C. E., Holt, B., & Freeman, A. (2020). The impact of system noise in polarimetric SAR imagery on oil spill observations. *IEEE Transactions on Geoscience and Remote Sensing*, *58*(6), 4194–4214. https://doi.org/10.1109/TGRS.2019.2961684

Evans, T. L., Costa, M., Telmer, K., & Silva, T. S. F. (2010). Using ALOS/PALSAR and RADARSAT-2 to map land cover and seasonal inundation in the Brazilian Pantanal. *Ieee Journal of Selected Topics in Applied Earth Observations and Remote Sensing*, *3*(4), 560–575. https://doi.org/10.1109/JSTARS.2010.2089042

Fablet, R., Chapron, B., Le Sommer, J., & Sévellec, F. (2024). Inversion of sea surface currents from satellite-derived SST-SSH synergies with 4DVarNets. *Journal of Advances in Modeling Earth Systems*, *16*(6), e2023MS003609. https://doi.org/10.1029/2023MS003609

Færch, L., Dierking, W., Hughes, N., & Doulgeris, A. P. (2024). Mapping icebergs in sea ice: An analysis of seasonal SAR backscatter at C- and L-band. *Remote Sensing of Environment*, *304*, 114074. https://doi.org/10.1016/j.rse.2024.114074

Fialko, Y., Simons, M., & Agnew, D. (2001). The complete (3-D) surface displacement field in the epicentral area of the 1999 Mw7. 1 Hector Mine earthquake, California, from space geodetic observations. *Geophysical Research Letters*, *28*(16), 3063–3066. https://doi.org/10.1029/2001GL013174

Fialko, Y., Simons, M., & Khazan, Y. (2001). Finite source modelling of magmatic unrest in Socorro, New Mexico, and Long Valley, California. *Geophysical Journal International*, *146*(1), 191–200. https://doi.org/10.1046/j.1365-246X.2001.00453.x

Fielding, E. J., & Jung, J. (2024). Damage Proxy Mapping with SAR interferometric coherence change. *Procedia Computer Science*, *239*, 2322–2328. https://doi.org/10.1016/j.procs.2024.06.425

Fielding, E. J., Lundgren, P. R., Taymaz, T., Yolsal-Çevikbilen, S., & Owen, S. E. (2013). Fault-slip source models for the 2011 M 7.1 Van earthquake in Turkey from SAR interferometry, pixel offset tracking, GPS, and seismic waveform analysis. *Seismological Research Letters*, *84*(4), 579–593. https://doi.org/10.1785/0220120164

Freeman, A., Chapman, B., & Siqueira, P. (2002). The JERS-1 Amazon Multi-season Mapping Study (JAMMS): Science objectives and implications for future missions. *International Journal of Remote Sensing*, *23*(7), 1447–1460. https://doi.org/10.1080/01431160110092975

Freeman, A., & Durden, S. L. (1993). Three-component scattering model to describe polarimetric SAR data. In *Radar polarimetry* (Vol. 1748, pp. 213–224). SPIE. https://doi.org/10.1117/12.140618

Fu, L. L., Pavelsky, T., Cretaux, J. F., Morrow, R., Farrar, J. T., Vaze, P., et al. (2024). The Surface Water and Ocean Topography mission: A breakthrough in radar remote sensing of the ocean and land surface water. *Geophysical Research Letters*, *51*(4), e2023GL107652. https://doi.org/10.1029/2023GL107652

Garestier, F., & Le Toan, T. (2009). Forest modeling for height inversion using single-baseline InSAR/Pol-InSAR data. *IEEE Transactions on Geoscience and Remote Sensing*, *48*(3), 1528–1539. https://doi.org/10.1109/TGRS.2009.2032538

Geldsetzer, T., & Howell, S. E. L. (2023). Incidence angle dependencies for C-band backscatter from sea ice during both the winter and melt season. *IEEE Transactions on Geoscience and Remote Sensing*, *61*, 1–15. https://doi.org/10.1109/TGRS.2023.3315056

Geudtner, D., Gebert, N., Tossaint, M., Davidson, M., Heliere, F., Traver, I. N., et al. (2021). Copernicus and ESA SAR missions. In *2021 IEEE radar conference (RadarConf21)* (pp. 1–6). IEEE. https://doi.org/10.1109/RadarConf2147009.2021.9455262

Gommenginger, C., Chapron, B., Hogg, A., Buckingham, C., Fox-Kemper, B., Eriksson, L., et al. (2019). SEASTAR: A mission to study ocean submesoscale dynamics and small-scale atmosphere-ocean processes in coastal, shelf and polar seas. *Frontiers in Marine Science*, *6*, 457. https://doi.org/10.3389/fmars.2019.00457

Hajnsek, I., Kugler, F., Lee, S. K., & Papathanassiou, K. P. (2009). Tropical-forest-parameter estimation by means of Pol-InSAR: The INDREX-II campaign. *IEEE Transactions on Geoscience and Remote Sensing*, *47*(2), 481–493. https://doi.org/10.1109/TGRS.2008.2009437

Hanssen, R. F., Weckwerth, T. M., Zebker, H. A., & Klees, R. (1999). High-resolution water vapor mapping from interferometric radar measurements. *Science*, *283*(5406), 1297–1299. https://doi.org/10.1126/science.283.5406.1297

Henriquet, M., Avouac, J. P., & Bills, B. G. (2019). Crustal rheology of southern Tibet constrained from lake-induced viscoelastic deformation. *Earth and Planetary Science Letters*, *506*, 308–322. https://doi.org/10.1016/j.epsl.2018.11.014

Hess, L. L., Melack, J. M., Affonso, A. G., Barbosa, C., Gastil-Buhl, M., & Novo, E. M. L. M. (2015). Wetlands of the lowland Amazon Basin: Extent, vegetative cover, and dual-season inundated area as mapped with JERS-1 synthetic aperture radar. *Wetlands*, *35*(4), 745–756. https://doi.org/10.1007/s13157-015-0666-y

Hess, L. L., Melack, J. M., Filoso, J. M., & Wang, Y. (1995). Delineation of inundated area and vegetation along the Amazon floodplain with the SIR-C synthetic aperture radar. *IEEE Transactions on Geoscience and Remote Sensing*, *33*(4), 896–904. https://doi.org/10.1109/36.406675

Hoekman, D., Vissers, M., & Wielaard, N. (2010). PALSAR wide-area mapping of Borneo: Methodology and map validation. *IEEE Journal of Selected Topics in Applied Earth Observations and Remote Sensing*, *3*(4), 605–617. https://doi.org/10.1109/JSTARS.2010.2070059

Homayouni, S., McNairn, H., Hosseini, M., Jiao, X., & Powers, J. (2019). Quad and compact multitemporal C-band PolSAR observations for crop characterization and monitoring. *International Journal of Applied Earth Observation and Geoinformation*, *74*, 78–87. https://doi.org/10.1016/j.jag.2018.09.009

Horstmann, J., Wackerman, C., Falchetti, S., & Maresca, S. (2013). Tropical cyclone winds retrieved from synthetic aperture radar. *Oceanography*, *26*(2), 46–57. https://doi.org/10.5670/oceanog.2013.30

Hosseini, M., & McNairn, H. (2017). Using multi-polarization C- and L-band radar to estimate biomass and soil moisture for wheat fields. *International Journal of Applied Earth Observation and Geoinformation*, *58*, 50–64. https://doi.org/10.1016/j.jag.2017.01.006

Hosseini, M., McNairn, H., Mitchell, S., Dingle Robertson, L., Davidson, D., Ahmadian, N., et al. (2021). A comparison between support vector machine and water cloud model for estimating crop leaf area index. *Remote Sensing*, *13*(7), 1348. https://doi.org/10.3390/rs13071348

Howell, S. E. L., Babb, D. G., Landy, J. C., Moore, G. W. K., Ballinger, T. J., McNeil, K., et al. (2024). Baffin Bay ice export and production from Sentinel-1, the RADARSAT Constellation Mission, and CryoSat-2: 2016–2022. *Geophysical Research Letters*, *51*(22), e2024GL111364. https://doi.org/10.1029/2024GL111364

Howell, S. E. L., Brady, M., & Komarov, A. S. (2022). Generating large-scale sea ice motion from Sentinel-1 and the RADARSAT constellation mission using the environment and climate change Canada automated sea ice tracking system. *The Cryosphere*, *16*(3), 1125–1139. https://doi.org/10.5194/tc-16-1125-2022

Howell, S. E. L., Small, D., Rohner, C., Mahmud, M. S., Yackel, J. J., & Brady, M. (2019). Estimating melt onset over Arctic sea ice from time series multi-sensor Sentinel-1 and RADARSAT-2 backscatter. *Remote Sensing of Environment*, *229*, 48–59. https://doi.org/10.1016/j.rse.2019.04.031

Hu, C., Chen, Z., Li, Y., Dong, X., & Hobbs, S. (2021). Research progress on geosynchronous synthetic aperture radar. *Fundamental Research*, *1*(3), 346–363. https://doi.org/10.1016/j.fmre.2021.04.008

Hu, X., & Bürgmann, R. (2020). Aquifer deformation and active faulting in Salt Lake Valley, Utah, USA. *Earth and Planetary Science Letters*, *547*, 116471. https://doi.org/10.1016/j.epsl.2020.116471

Hu, Y., Arenson, L. U., Barboux, C., Bodin, X., Cicoira, A., Delaloye, R., et al. (2025). Rock glacier velocity: An Essential Climate Variable quantity for permafrost. *Reviews of Geophysics*, *63*(1), e2024RG000847. https://doi.org/10.1029/2024RG000847

Huang, L., Fischer, G., & Hajnsek, I. (2021). Antarctic snow-covered sea ice topography derivation from TanDEM-X using polarimetric SAR interferometry. *The Cryosphere*, *15*(12), 5323–5344. https://doi.org/10.5194/tc-15-5323-2021

Hussain, E., Hooper, A., Wright, T. J., Walters, R. J., & Bekaert, D. P. (2016). Interseismic strain accumulation across the central North Anatolian Fault from iteratively unwrapped InSAR measurements. *Journal of Geophysical Research: Solid Earth*, *121*(12), 9000–9019. https://doi.org/10.1002/2016JB013108

Iwahana, G., Uchida, M., Liu, L., Gong, W., Meyer, F. J., Guritz, R., et al. (2016). InSAR detection and field evidence for thermokarst after a tundra wildfire, using ALOS-PALSAR. *Remote Sensing*, *8*(3), 218. https://doi.org/10.3390/rs8030218

Jiao, X., McNairn, H., Shang, J., Pattey, E., Liu, J., & Champagne, C. (2011). The sensitivity of RADARSAT-2 polarimetric SAR data to corn and soybean Leaf Area Index. *Canadian Journal of Remote Sensing*, *37*(1), 69–81. https://doi.org/10.5589/m11-023

Johannessen, J. A., Chapron, B., Collard, F., Kudryavtsev, V., Mouche, A., Akimov, D., & Dagestad, K.-F. (2008). Direct ocean surface velocity measurements from Space: Improved quantitative interpretation of Envisat ASAR observations. *Geophysical Research Letters*, *35*(22). https://doi.org/10.1029/2008GL035709

Johansson, A. M., Brekke, C., Spreen, G., & King, J. A. (2018). X-C-and L-band SAR signatures of newly formed sea ice in Arctic leads during winter and spring. *Remote Sensing of Environment*, *204*, 162–180. https://doi.org/10.1016/j.rse.2017.10.032

Jolivet, R., Agram, P. S., Lin, N. Y., Simons, M., Doin, M.-P., Peltzer, G., & Li, Z. (2014). Improving InSAR geodesy using global atmospheric models. *Journal of Geophysical Research: Solid Earth*, *119*(3), 2324–2341. https://doi.org/10.1002/2013JB010588

Jolivet, R., Grandin, R., Lasserre, C., Doin, M.-P., & Peltzer, G. (2011). Systematic InSAR tropospheric phase delay corrections from global meteorological reanalysis data. *Geophysical Research Letters*, *38*(17). https://doi.org/10.1029/2011GL048757

Jónsson, S., Zebker, H., Segall, P., & Amelung, F. (2002). Fault slip distribution of the 1999 Mw 7.1 Hector Mine, California, earthquake, estimated from satellite radar and GPS measurements. *Bulletin of the Seismological Society of America*, *92*(4), 1377–1389. https://doi.org/10.1785/0120000922

Karlsen, T., Johansson, M., Lohse, J., & Doulgeris, A. P. (2024). Incidence angle dependency and seasonal evolution of L and C-band SAR backscatter over landfast sea ice. *Annals of Glaciology*, *65*, e29. https://doi.org/10.1017/aog.2024.30

Kavats, O., Khramov, D., Sergieieva, K., & Vasyliev, V. (2019). Monitoring harvesting by time series of Sentinel-1 SAR data. *Remote Sensing*, *11*(21), 2496. https://doi.org/10.3390/rs11212496

Khachatrian, E., Dierking, W., Chlaily, S., Eltoft, T., Dinessen, F., Hughes, N., & Marinoni, A. (2023). SAR and passive microwave fusion scheme: A test case on Sentinel-1/AMSR-2 for sea ice classification. *Geophysical Research Letters*, *50*(4), e2022GL102083. https://doi.org/10.1029/2022GL102083

Khati, U., Lavalle, M., & Singh, G. (2021). The role of time series L-Band SAR and GEDI in mapping sub-tropical above-ground biomass. *Frontiers in Earth Science*, *9*, 752254. https://doi.org/10.3389/feart.2021.752254

Kica, S., Pavelsky, T., Fayne, J., & Williams, B. (2025). SWOT Water surface elevation in herbaceous wetlands of Florida's everglades. *Geophysical Research Letters*, *52*(9), e2025GL114956. https://doi.org/10.1029/2025GL114956

Kim, J. H., Rignot, E., Holland, D., & Holland, D. (2024). Seawater intrusion at the grounding line of Jakobshavn Isbrae, Greenland, from terrestrial radar interferometry. *Geophysical Research Letters*, *51*(6), e2023GL106181. https://doi.org/10.1029/2023GL106181

Koskinen, J. T., Pulliainen, J. T., Hyyppä, J. M., Engdahl, M. E., & Hallikainen, M. T. (2001). The seasonal behavior of interferometric coherence in boreal forest. *IEEE Transactions on Geoscience and Remote Sensing*, *39*(4), 820–829. https://doi.org/10.1109/36.917903

Kraatz, S., Torbick, N., Jiao, X., Huang, X., Dingle Robertson, L., Davidson, A., et al. (2021). Comparison between dense L-band and C-band Synthetic Aperture Radar (SAR) time series for crop area mapping over a NISAR calibration-validation site. *Agronomy*, *11*(2), 273. https://doi.org/10.3390/agronomy11020273

Kræmer, T., Johnsen, H., & Brekke, C. (2015). Emulating Sentinel-1 Doppler radial ice drift measurements using Envisat ASAR data. *IEEE Transactions on Geoscience and Remote Sensing*, *53*(12), 6407–6418. https://doi.org/10.1109/TGRS.2015.2439044

Krumpen, T., von Albedyll, L., Bünger, H. J., Castellani, G., Hartmann, J., Helm, V., et al. (2025). Smoother sea ice with fewer pressure ridges in a more dynamic Arctic. *Nature Climate Change*, *15*(1), 66–72. https://doi.org/10.1038/s41558-024-02199-5

Kudryavtsev, V., Myasoedov, A., Chapron, B., Johannessen, J. A., & Collard, F. (2012). Imaging mesoscale upper ocean dynamics using synthetic aperture radar and optical data. *Journal of Geophysical Research*, *117*(C4). https://doi.org/10.1029/2011JC007492

Kugler, F., Lee, S. K., Hajnsek, I., & Papathanassiou, K. P. (2015). Forest height estimation by means of Pol-InSAR data inversion: The role of the vertical wavenumber. *IEEE Transactions on Geoscience and Remote Sensing*, *53*(10), 5294–5311. https://doi.org/10.1109/TGRS.2015.2420996

Kwok, R. (2018). Arctic sea ice thickness, volume, and multiyear ice coverage: Losses and coupled variability (1958–2018). *Environmental Research Letters*, *13*(10), 105005. https://doi.org/10.1088/1748-9326/aae3ec

Lei, Y., & Siqueira, P. (2014). Estimation of forest height using spaceborne repeat-pass L-band InSAR correlation magnitude over the US state of Maine. *Remote Sensing*, *6*(11), 10252–10285. https://doi.org/10.3390/rs61110252

Le Toan, T., Beaudoin, A., Riom, J., & Guyon, D. (1992). Relating forest biomass to SAR data. *IEEE Transactions on Geoscience and Remote Sensing*, *30*(2), 403–411. https://doi.org/10.1109/36.134089

Le Toan, T., Laur, H., Mougin, E., & Lopez, A. (1989). Multitemporal and dual-polarization observations of agricultural vegetation covers by X-Band SAR images. *IEEE Transactions on Geoscience and Remote Sensing*, *27*(6), 709–718. https://doi.org/10.1109/TGRS.1989.1398243

Le Toan, T., Ribbes, F., Wang, L.-F., Floury, N., Ding, K.-H., Kong, J. A., et al. (1997). Rice crop mapping and monitoring using ERS-1 data based on experiment and modeling results. *IEEE Transactions on Geoscience and Remote Sensing*, *35*, 41–56. https://doi.org/10.1109/36.551933

Li, X., Jónsson, S., & Cao, Y. (2021). Interseismic deformation from Sentinel-1 burst-oOverlap interferometry: Application to the Southern Dead Sea Fault. *Geophysical Research Letters*, *48*(16), e2021GL093481. https://doi.org/10.1029/2021GL093481

Li, Y., Martinis, S., Wieland, M., Schlaffer, S., & Natsuaki, R. (2019). Urban flood mapping using SAR intensity and interferometric coherence via Bayesian network fusion. *Remote Sensing*, *11*(19), 2231. https://doi.org/10.3390/rs11192231

Liang, C., Agram, P., Simons, M., & Fielding, E. J. (2019). Ionospheric correction of InSAR time series analysis of C-band Sentinel-1 TOPS data. *IEEE Transactions on Geoscience and Remote Sensing*, *57*(9), 6755–6773. https://doi.org/10.1109/TGRS.2019.2908494

Liu, L., Schaefer, K., Zhang, T., & Wahr, J. (2012). Estimating 1992–2000 average active layer thickness on the Alaskan North Slope from remotely sensed surface subsidence. *Journal of Geophysical Research*, *117*(F1). https://doi.org/10.1029/2011JF002041

Liu, S., Zhou, Z., Ding, H., Zhong, Y., & Shi, Q. (2021). Crop mapping using Sentinel full-year dual-polarized SAR data and a CPU-optimized convolutional neural network with two sampling strategies. *Ieee Journal of Selected Topics in Applied Earth Observations and Remote Sensing*, *14*, 7017–7031. https://doi.org/10.1109/JSTARS.2021.3094973

Liu, Y.-K., Yunjun, Z., & Simons, M. (2025). Inferring tectonic plate rotations from InSAR time series. *Geophysical Research Letters*, *52*(12), e2025GL115137. https://doi.org/10.1029/2025GL115137

Lombardini, F., & Pardini, M. (2008). 3-D SAR tomography: The multibaseline sector interpolation approach. *IEEE Geoscience and Remote Sensing Letters*, *5*(4), 630–634. https://doi.org/10.1109/LGRS.2008.2001283

López-Dekker, P., Rott, H., Prats-Iraola, P., Chapron, B., Scipal, K., & De Witte, E. (2019). Harmony: An Earth explorer 10 mission candidate to observe land, ice, and ocean surface dynamics. In *IGARSS 2019-2019 IEEE international geoscience and remote sensing symposium* (pp. 8381–8384). IEEE. https://doi.org/10.1109/IGARSS.2019.8897983

Lu, Z., & Kwoun, O. I. (2009). Interferometric synthetic aperture radar (INSAR) study of coastal wetlands over Southeastern Louisiana. In *Remote sensing of coastal environments, U.S. Geological Survey* (pp. 25–60). https://doi.org/10.1201/9781420094428-c2

Lucas, R., Armston, J., Fairfax, R., Fensham, R., Accad, A., Carreiras, J., et al. (2010). An evaluation of the ALOS PALSAR L-band backscatter—Above ground biomass relationship Queensland, Australia: Impacts of surface moisture condition and vegetation structure. *Ieee Journal of Selected Topics in Applied Earth Observations and Remote Sensing*, *3*(4), 576–593. https://doi.org/10.1109/JSTARS.2010.2086436

Lucas, R. M., Cronin, N., Lee, A., Moghaddam, M., Witte, C., & Tickle, P. (2006). Empirical relationships between AIRSAR backscatter and LiDAR-derived forest biomass, Queensland, Australia. *Remote Sensing of Environment*, *100*(3), 407–425. https://doi.org/10.1016/j.rse.2005.10.019

Macdonald, G. J., Scharien, R. K., Duncan, K., Farrell, S. L., Rezania, P., & Tavri, A. (2024). Arctic sea ice topography information from RADARSAT Constellation Mission (RCM) synthetic aperture radar (SAR) backscatter. *Geophysical Research Letters*, *51*(4), e2023GL107261. https://doi.org/10.1029/2023GL107261

MacDonald, H. C., Waite, W. P., & Demarcke, J. S. (1980). Use of Seasat satellite radar imagery for the detection of standing water beneath forest vegetation. In *Proceedings of the American Society of Photogrammetry annual technical meeting RS-3(B)* (pp. 1–13). Retrieved from https://ntrs.nasa.gov/citations/19810059339

Mahdianpari, M., Mohammadimanesh, F., McNairn, H., Davidson, A., Rezaee, M., Salehi, B., & Homayouni, S. (2019). Mid-season crop classification using dual-compact-and full-polarization in preparation for the RADARSAT Constellation Mission (RCM). *Remote Sensing*, *11*(13), 1582. https://doi.org/10.3390/rs11131582

Mallick, R., Lambert, V., & Meade, B. (2022). On the choice and implications of rheologies that maintain kinematic and dynamic consistency over the entire earthquake cycle. *Journal of Geophysical Research: Solid Earth*, *127*(9), e2022JB024683. https://doi.org/10.1029/2022JB024683

Mandal, D., Kumar, V., Bhattacharya, A., McNairn, H., & Rao, Y. S. (2021). A multi-year cross-validation experiment for estimating rice plant area index (PAI) over the JECAM-India test site from simulated RADARSAT Constellation Mission (RCM) compact polarimetric SAR data. *International Journal of Remote Sensing*, *42*(24), 9490–9522. https://doi.org/10.1080/01431161.2021.1999528

Mandal, D., Kumar, V., Lopez-Sanchez, J., Bhattacharya, A., McNairn, H., & Rao, S. (2020). Crop biophysical parameter retrieval from Sentinel-1 SAR data with a multi-target inversion of Water Cloud Model. *International Journal of Remote Sensing*, *41*(14), 5503–5524. https://doi.org/10.1080/01431161.2020.1734261

Mandal, D., Ratha, D., Bhattacharya, A., Kumar, V., McNairn, H., Rao, Y. S., & Frery, A. (2020). A radar vegetation index for crop monitoring using compact polarimetric SAR data. *IEEE Transactions on Geoscience and Remote Sensing*, *58*(9), 6321–6335. https://doi.org/10.1109/TGRS.2020.2976661

Mansaray, L. R., Zhang, K., & Kanu, A. S. (2020). Dry biomass estimation of paddy rice with Sentinel-1A satellite data using machine learning regression algorithms. *Computers and Electronics in Agriculture*, *176*, 105674. https://doi.org/10.1016/j.compag.2020.105674

Massonnet, D. (2013). Cartwheel. In M. D'Errico (Ed.), *Distributed space missions for Earth system monitoring*, *Space technology library* (Vol. 31, pp. 437–446). Springer. https://doi.org/10.1007/978-1-4614-4541-8_14

Mastro, P., Serio, C., Masiello, G., & Pepe, A. (2020). The multiple aperture SAR interferometry (MAI) technique for the detection of large ground displacement dynamics: An overview. *Remote Sensing*, *12*(7), 1189. https://doi.org/10.3390/rs12071189

McNairn, H., Champagne, C., Shang, J., Holmstrom, D. A., & Reichert, G. (2009). Integration of optical and Synthetic Aperture Radar (SAR) imagery for delivering operational annual crop inventories. *ISPRS Journal of Photogrammetry and Remote Sensing*, *64*(5), 434–449. https://doi.org/10.1016/j.isprsjprs.2008.07.006

McNairn, H., & Jiao, X. (2024). Monitoring crop condition at field scales and at a daily time step using Synthetic Aperture Radar (SAR). *Canadian Journal of Remote Sensing*, *50*(1), 2407163. https://doi.org/10.1080/07038992.2024.2407163

Melsheimer, C., Spreen, G., Ye, Y., & Shokr, M. (2023). First results of Antarctic sea ice type retrieval from active and passive microwave remote sensing data. *The Cryosphere*, *17*(1), 105–126. https://doi.org/10.5194/tc-17-105-2023

Minchew, B., Simons, M., Hensley, S., Björnsson, H., & Pálsson, F. (2015). Early melt season velocity fields of Langjökull and Hofsjökull, central Iceland. *Journal of Glaciology*, *61*(226), 253–266. https://doi.org/10.3189/2015JoG14J023

Minchew, B., Simons, M., Riel, B., & Milillo, P. (2017). Tidally induced variations in vertical and horizontal motion on Rutford Ice Stream, West Antarctica, inferred from remotely sensed observations. *Journal of Geophysical Research: Earth Surface*, *122*(1), 167–190. https://doi.org/10.1002/2016JF003971

Moiseev, A., Johannessen, J. A., & Johnsen, H. (2022). Towards retrieving reliable ocean surface currents in the coastal zone from the Sentinel-1 Doppler shift observations. *Journal of Geophysical Research: Oceans*, *127*(5), e2021JC018201. https://doi.org/10.1029/2021JC018201

Monaldo, F. M., Jackson, C. R., & Pichel, W. G. (2013). Seasat to Radarsat-2: Research to operations. *Oceanography*, *26*(2), 34–45. https://doi.org/10.5670/oceanog.2013.29

Monti, M., Guarnieri, A. M., Pelliccia, F., & Renga, A. (2025). Geostationary interferometric SAR: Orbit design and control implementation. *IEEE Transactions on Geoscience and Remote Sensing*, *63*, 1–17. https://doi.org/10.1109/TGRS.2025.3565889

Mouche, A. A., Chapron, B., Zhang, B., & Husson, R. (2017). Combined co-and cross-polarized SAR measurements under extreme wind conditions. *IEEE Transactions on Geoscience and Remote Sensing*, *55*(12), 6746–6755. https://doi.org/10.1109/TGRS.2017.2732508

Mouginot, J., Rignot, E., & Scheuchl, B. (2019). Continent-wide, interferometric SAR phase, mapping of Antarctic ice velocity. *Geophysical Research Letters*, *46*(16), 9710–9718. https://doi.org/10.1029/2019GL083826

Nandan, V., Geldsetzer, T., Islam, T., Yackel, J. J., Gill, J. P. S., Fuller, M. C., et al. (2016). Ku-X- and C-band measured and modeled microwave backscatter from a highly saline snow cover on first-year sea ice. *Remote Sensing of Environment*, *187*, 62–75. https://doi.org/10.1016/j.rse.2016.10.004

Nandan, V., Willatt, R., Mallett, R., Stroeve, J., Geldsetzer, T., Scharien, R., et al. (2023). Wind redistribution of snow impacts the Ka- and Ku-band radar signatures of Arctic sea ice. *The Cryosphere*, *17*(6), 2211–2229. https://doi.org/10.5194/tc-17-2211-2023

Nardi, F., Annis, A., Di Baldassarre, G., Vivoni, E. R., & Grimaldi, S. (2019). GFPLAIN250m, a global high-resolution dataset of Earth's floodplains. *Scientific Data*, *6*(1), 180309. https://doi.org/10.1038/sdata.2018.309

Nasirzadehdizaji, R., Balik Sanli, F., Abdikan, S., Cakir, Z., Sekertekin, A., & Ustuner, M. (2019). Sensitivity analysis of multi-temporal Sentinel-1 SAR parameters to crop height and canopy coverage. *Applied Sciences*, *9*(4), 655. https://doi.org/10.3390/app9040655

Nicolaus, M., Perovich, D. K., Spreen, G., Granskog, M. A., von Albedyll, L., Angelopoulos, M., et al. (2022). Overview of the MOSAiC expedition: Snow and sea ice. *Elementa-Science of the Anthropocene*, *10*(1), 000046. https://doi.org/10.1525/elementa.2021.000046

Oakes, G., Hardy, A., & Bunting, P. (2023). RadWet: An improved and transferable mapping of open water and inundated vegetation using Sentinel-1. *Remote Sensing*, *15*(6), 1705. https://doi.org/10.3390/rs15061705

O'Driscoll, O., Mouche, A., Chapron, B., Kleinherenbrink, M., & López-Dekker, P. (2023). Obukhov length estimation from spaceborne radars. *Geophysical Research Letters*, *50*(15), e2023GL104228. https://doi.org/10.1029/2023GL104228

Omar, H., Misman, M., & Kassim, A. (2017). Synergetic of PALSAR-2 and Sentinel-1A SAR polarimetry for retrieving aboveground biomass in Dipterocarp Forest of Malaysia. *Applied Sciences*, *7*(7), 675. https://doi.org/10.3390/app7070675

Orusa, T., Viani, A., & Borgogno-Mondino, E. (2024). IRIDE, the Euro-Italian Earth observation program: Overview, current progress, global expectations, and recommendations. *Environmental Sciences Proceedings*, *29*(1), 74. https://doi.org/10.3390/ECRS2023-16839

Park, S. E., Bartsch, A., Sabel, D., Wagner, W., Naeimi, V., & Yamaguchi, Y. (2011). Monitoring freeze/thaw cycles using ENVISAT ASAR Global Mode. *Remote Sensing of Environment*, *115*(12), 3457–3467. https://doi.org/10.1016/j.rse.2011.08.009

Passah, A., Sur, S. N., Paul, B., & Kandar, D. (2022). SAR image classification: A comprehensive study and analysis. *IEEE Access*, *10*, 20385–20399. https://doi.org/10.1109/ACCESS.2022.3151089

Persson, H. J., Olsson, H., Soja, M. J., Ulander, L. M. H., & Fransson, J. E. S. (2017). Experiences from large-scale forest mapping of Sweden using TanDEM-X data. *Remote Sensing*, *9*(12), 1253. https://doi.org/10.3390/rs9121253

Pritchard, M. E., & Simons, M. (2002). A satellite geodetic survey of large-scale deformation of volcanic centres in the central Andes. *Nature*, *418*(6894), 167–171. https://doi.org/10.1038/nature00872

Pulliainen, J. T., Kurvonen, L., & Hallikainen, M. T. (1999). Multitemporal behavior of L- and C-band SAR observations of boreal forests. *IEEE Transactions on Geoscience and Remote Sensing*, *37*(2), 927–937. https://doi.org/10.1109/36.752211

Pulliainen, J. T., Mikkelä, P. J., Hallikainen, M. T., & Ikonen, J.-P. (1996). Seasonal dynamics of C-band backscatter of boreal forests with applications to biomass and soil moisture estimation. *IEEE Transactions on Geoscience and Remote Sensing*, *34*(3), 758–770. https://doi.org/10.1109/36.499781

Pulvirenti, L., Parodi, A., Lagasio, M., Pierdicca, N., Venuti, G., Realini, E., et al. (2018). Incorporating Sentinel-derived products into numerical weather models: The ESA STEAM project. In *Proc. SPIE 10788, active and passive microwave remote sensing for environmental monitoring II*. https://doi.org/10.1117/12.2325710.107880F

Qadir, A., Skakun, S., Eun, J., Prashnani, M., & Shumilo, L. (2023). Sentinel-1 time series data for sunflower (Helianthus annuus) phenology monitoring. *Remote Sensing of Environment*, *295*, 113689. https://doi.org/10.1016/j.rse.2023.113689

Quegan, S., Le Toan, T., Chave, J., Dall, J., Exbrayat, J.-F., Minh, D. H. T., et al. (2019). The European Space Agency BIOMASS mission: Measuring forest above-ground biomass from space. *Remote Sensing of Environment*, *227*, 44–60. https://doi.org/10.1016/j.rse.2019.03.032

Rabus, B., Wehn, H., & Nolan, M. (2010). The importance of soil moisture and soil structure for InSAR phase and backscatter, as determined by FDTD modeling. *IEEE Transactions on Geoscience and Remote Sensing*, *48*(5), 2421–2429. https://doi.org/10.1109/TGRS.2009.2039353

Ranson, K. J., & Sun, G. (1994). Mapping biomass of a northern forest using multifrequency SAR data. *IEEE Transactions on Geoscience and Remote Sensing*, *32*(2), 388–396. https://doi.org/10.1109/36.295053

Ranson, K. J., Sun, G., Lang, R. H., Chauhan, N. S., Cacciola, R. J., & Kilic, O. (1997). Mapping of boreal forest biomass from spaceborne synthetic aperture radar. *Journal of Geophysical Research*, *102*(D24), 29599–29610. https://doi.org/10.1029/96JD03708

Rebelo, L.-M. (2010). Eco-hydrological characterization of inland wetlands in Africa using L-band SAR. *Ieee Journal of Selected Topics in Applied Earth Observations and Remote Sensing*, *3*(4), 554–559. https://doi.org/10.1109/JSTARS.2010.2070060

Reeh, N., Mohr, J. J., Madsen, S., Oerter, H., & Gundestrup, N. (2003). Three-dimensional surface velocities of Storstrømmen glacier, Greenland, derived from radar interferometry and ice-sounding radar measurements. *Journal of Glaciology*, *49*(165), 201–209. https://doi.org/10.3189/172756503781830818

Riel, B., Simons, M., Ponti, D., Agram, P., & Jolivet, R. (2018). Quantifying ground deformation in the Los Angeles and Santa Ana coastal basins due to groundwater withdrawal. *Water Resources Research*, *54*(5), 3557–3582. https://doi.org/10.1029/2017WR021978

Rignot, E., Ciracì, E., Scheuchl, B., Tolpekin, V., Wollersheim, M., & Dow, C. (2024). Widespread seawater intrusions beneath the grounded ice of Thwaites Glacier, West Antarctica. *Proceedings of the National Academy of Sciences*, *121*(22), e2404766121. https://doi.org/10.1073/pnas.2404766121

Rignot, E., Mouginot, J., & Scheuchl, B. (2011). Ice flow of the Antarctic ice sheet. *Science*, *333*(6048), 1427–1430. https://doi.org/10.1126/science.1208336

Rodríguez-Veiga, P., Quegan, S., Carreiras, J., Persson, H. J., Fransson, J. E. S., Hoscilo, A., et al. (2019). Forest biomass retrieval approaches from Earth Observation in different biomes. *International Journal of Applied Earth Observation and Geoinformation*, *77*, 53–68. https://doi.org/10.1016/j.jag.2018.12.008

Röhrs, J., Sutherland, G., Jeans, G., Bedington, M., Sperrevik, A. K., Dagestad, K.-F., et al. (2023). Surface currents in operational oceanography: Key applications, mechanisms, and methods. *Journal of Operational Oceanography*, *16*(1), 60–88. https://doi.org/10.1080/1755876X.2021.1903221

Romeiser, R., Runge, H., Suchandt, S., Kahle, R., Rossi, C., & Bell, P. S. (2013). Quality assessment of surface current fields from TerraSAR-X and TanDEM-X along-track interferometry and Doppler centroid analysis. *IEEE Transactions on Geoscience and Remote Sensing*, *52*(5), 2759–2772. https://doi.org/10.1109/TGRS.2013.2265659

Rosenqvist, A. (2009). Mapping of seasonal inundation in the Congo River basin—Prototype study using ALOS PALSAR. In *33rd int. Symp. of remote sensing of environment (ISRSE 33)*.

Rosenqvist, A., Forsberg, B., Pimentel, T., Rauste, Y., & Richey, J. (2002). The use of spaceborne radar data to model inundation patterns and trace gas emissions in the central Amazon floodplain. *International Journal of Remote Sensing*, *23*(7), 1303–1328. https://doi.org/10.1080/01431160110092911

Rosenqvist, A., Shimada, M., Chapman, B., Freeman, A., De Grandi, G., Saatchi, S., & Rauste, Y. (2000). The Global Rain Forest Mapping project—A review. *International Journal of Remote Sensing*, *21*(6&7), 1375–1387. https://doi.org/10.1080/014311600210227

Rosenqvist, J., Rosenqvist, A., Jensen, K., & McDonald, K. (2020). Mapping of maximum and minimum inundation extents in the Amazon basin 2014–2017 with ALOS-2 PALSAR-2 ScanSAR time series data. *Remote Sensing*, *12*(8), 1326. https://doi.org/10.3390/rs12081326

Rott, H., Yueh, S. H., Cline, D. W., Duguay, C., Essery, R., Haas, C., et al. (2010). Cold regions hydrology high-resolution observatory for snow and cold land processes. *Proceedings of the IEEE*, *98*(5), 752–765. https://doi.org/10.1109/JPROC.2009.2038947

Rouet-Leduc, B., Jolivet, R., Dalaison, M., Johnson, P. A., & Hulbert, C. (2021). Autonomous extraction of millimeter-scale deformation in InSAR time series using deep learning. *Nature Communications*, *12*(1), 6480. https://doi.org/10.1038/s41467-021-26254-3

Rousset, B., Barbot, S., Avouac, P., & Hsu, J. (2012). Postseismic deformation following the 1999 Chi-Chi earthquake, Taiwan: Implication for lower-crust rheology. *Journal of Geophysical Research*, *117*(B12), B12405. https://doi.org/10.1029/2012JB009571

Rouyet, L., Bredal, M. B., Lauknes, T. R., Dehls, J. F., Larsen, Y., van Oostveen, J. G., et al. (2024). InSAR Svalbard – User requirements, technical considerations, and product development plan. Retrieved from https://hdl.handle.net/11250/3125660

Rouyet, L., Lauknes, T. R., Christiansen, H. H., Strand, S. M., & Larsen, Y. (2019). Seasonal dynamics of a permafrost landscape, Adventdalen, Svalbard, investigated by InSAR. *Remote Sensing of Environment*, *231*, 111236. https://doi.org/10.1029/2024RG000847

Sader, S. A. (1987). Forest biomass, canopy structure, and species composition relationships with multipolarization L-band synthetic aperture radar data. *Photogrammetric Engineering & Remote Sensing*, *53*(2), 193–202.

Santoro, M., Askne, J., Smith, G., & Fransson, J. E. S. (2002). Stem volume retrieval in boreal forests from ERS-1/2 interferometry. *Remote Sensing of Environment*, *81*(1), 19–35. https://doi.org/10.1016/S0034-4257(01)00329-7

Santoro, M., Beaudoin, A., Beer, C., Cartus, O., Fransson, J. E. S., Hall, R. J., et al. (2015). Forest growing stock volume of the northern hemisphere: Spatially explicit estimates for 2010 derived from Envisat ASAR. *Remote Sensing of Environment*, *168*, 316–334. https://doi.org/10.1016/j.rse.2015.07.005

Santoro, M., Beer, C., Cartus, O., Schmullius, C., Shvidenko, A., McCallum, I., et al. (2011). Retrieval of growing stock volume in boreal forest using hyper-temporal series of Envisat ASAR ScanSAR backscatter measurements. *Remote Sensing of Environment*, *115*(2), 490–507. https://doi.org/10.1016/j.rse.2010.09.018

Santoro, M., Cartus, O., & Fransson, J. E. S. (2022). Dynamics of the Swedish forest carbon pool between 2010 and 2015 estimated from satellite L-band SAR observations. *Remote Sensing of Environment*, *270*, 112846. https://doi.org/10.1016/j.rse.2021.112846

Santoro, M., Cartus, O., Quegan, S., Kay, H., Lucas, R. M., Araza, A., et al. (2024). Design and performance of the Climate Change Initiative Biomass global retrieval algorithm. *Science of Remote Sensing*, *10*, 100169. https://doi.org/10.1016/j.srs.2024.100169

Santos-Ferreira, A. M., Pinelo, J., da Silva, J. C., Johannessen, J. A., Chapron, B., Gommenginger, C., et al. (2025). The Internal Waves Service Workshop: Observing internal waves globally with deep learning and synthetic aperture radar. *Bulletin of the American Meteorological Society*, *106*(7), E1462–E1470. https://doi.org/10.1175/BAMS-D-25-0133.1

Scharien, R. K., Yackel, J. J., Barber, D. G., Asplin, M., Gupta, M., & Isleifson, D. (2012). Geophysical controls on C band polarimetric backscatter from melt pond covered Arctic first-year sea ice: Assessment using high-resolution scatterometry. *Journal of Geophysical Research*, *117*(C9), C00G18. https://doi.org/10.1029/2011JC007353

Schlund, M., & Erasmi, S. (2020). Sentinel-1 time series data for monitoring the phenology of winter wheat. *Remote Sensing of Environment*, *246*, 111814. https://doi.org/10.1016/j.rse.2020.111814

Schlund, M., Erasmi, S., & Scipal, K. (2020). Comparison of aboveground biomass estimation from InSAR and LiDAR canopy height models in tropical forests. *IEEE Geoscience and Remote Sensing Letters*, *17*(3), 367–371. https://doi.org/10.1109/LGRS.2019.2925901

Schlund, M., von Poncet, F., Kuntz, S., Schmullius, C., & Hoekman, D. H. (2015). TanDEM-X data for aboveground biomass retrieval in a tropical peat swamp forest. *Remote Sensing of Environment*, *158*, 255–266. https://doi.org/10.1016/j.rse.2014.11.016

Schumann, G., Giustarini, L., Tarpanelli, A., Jarihani, B., & Martinis, S. (2023). Flood modeling and prediction using Earth Observation data. *Surveys in Geophysics*, *44*(5), 1553–1578. https://doi.org/10.1007/s10712-022-09751-y

Seppi, S., López-Martinez, C., & Joseau, M. J. (2024). An assessment of SAOCOM L-Band PolInSAR capabilities for canopy height estimation: A case study over managed forests in Argentina. *Ieee Journal of Selected Topics in Applied Earth Observations and Remote Sensing*, *17*, 5001–5014. https://doi.org/10.1109/JSTARS.2024.3363435

Shang, J., Liu, J., Poncos, V., Geng, X., Qian, B., Chen, Q., et al. (2020). Detection of crop seeding and harvest through analysis of time series Sentinel-1 interferometric SAR data. *Remote Sensing*, *12*(10), 1551. https://doi.org/10.3390/rs12101551

Shendryk, Y. (2022). Fusing GEDI with Earth observation data for large area aboveground biomass mapping. *International Journal of Applied Earth Observation and Geoinformation*, *115*, 103108. https://doi.org/10.1016/j.jag.2022.103108

Simons, M., Fialko, Y., & Rivera, L. (2002). Coseismic deformation from the 1999 Mw 7.1 Hector Mine, California, Earthquake as inferred from InSAR and GPS observations. *Bulletin of the Seismological Society of America*, *92*(4), 1390–1402. https://doi.org/10.1785/0120000933

Soja, M. J., Persson, H. J., & Ulander, L. M. H. (2015). Estimation of forest biomass from two-level model inversion of single-pass InSAR data. *IEEE Transactions on Geoscience and Remote Sensing*, *53*(9), 5083–5099. https://doi.org/10.1109/TGRS.2015.2417205

Spreen, G., de Steur, L., Divine, D., Gerland, S., Hansen, E., & Kwok, R. (2020). Arctic sea ice volume export through Fram Strait from 1992 to 2014. *Journal of Geophysical Research: Oceans*, *125*(6), e2019JC01603. https://doi.org/10.1029/2019JC016039

Spreen, G., Kwok, R., Menemenlis, D., & Nguyen, A. T. (2017). Sea-ice deformation in a coupled ocean–sea-ice model and in satellite remote sensing data. *The Cryosphere*, *11*(4), 1553–1573. https://doi.org/10.5194/tc-11-1553-2017

Stiles, B. W., Fore, A. G., Bohe, A., Chen, A. C., Chen, C. W., Molero, B., & Dubois, P. (2024). Ocean surface wind speed retrieval for SWOT Ka-band radar interferometer. In *IGARSS 2024-2024 IEEE international geoscience and remote sensing symposium* (pp. 1422–1425). IEEE. https://doi.org/10.1109/IGARSS53475.2024.10640472

Strozzi, T., Antonova, S., Günther, F., Mätzler, E., Vieira, G., Wegmüller, U., et al. (2018). Sentinel-1 SAR interferometry for surface deformation monitoring in low-land permafrost areas. *Remote Sensing*, *10*(9), 1360. https://doi.org/10.3390/rs10091360

Strozzi, T., Caduff, R., Jones, N., Barboux, C., Delaloye, R., Bodin, X., et al. (2020). Monitoring rock glacier kinematics with satellite synthetic aperture radar. *Remote Sensing*, *12*(3), 559. https://doi.org/10.3390/rs12030559

Tay, C. W., Yun, S. H., Chin, S. T., Bhardwaj, A., Jung, J., & Hill, E. M. (2020). Rapid flood and damage mapping using synthetic aperture radar in response to Typhoon Hagibis, Japan. *Scientific Data*, *7*(1), 100. https://doi.org/10.1038/s41597-020-0443-5

Thulasiraman, D., Haldar, D., Kumar, S., Ramathilagam, A. B., & Patel, N. R. (2024). Pearl millet crop biophysical parameter retrieval from space borne polarimetric SAR data using machine learning. *Earth and Space Science*, *11*(1), e2022EA00279. https://doi.org/10.1029/2022EA002799

Tian, B., Li, Z., Tang, P., Zou, P., Zhang, M., & Niu, F. (2016). Use of intensity and coherence of X-band SAR data to map thermokarst lakes on the Northern Tibetan Plateau. *IEEE Journal of Selected Topics in Applied Earth Observations and Remote Sensing*, *9*(7), 3164–3176. https://doi.org/10.1109/JSTARS.2016.2549740

Touzi, R., Omari, K., Sleep, B., & Jiao, X. (2018). Scattered and received wave polarization optimization for enhanced peatland classification and fire damage assessment using polarimetric PALSAR. *Ieee Journal of Selected Topics in Applied Earth Observations and Remote Sensing*, *11*(11), 4452–4477. https://doi.org/10.1109/JSTARS.2018.2873740

Treuhaft, R., & Siqueira, P. (2000). Vertical structure of vegetated land surfaces from interferometric and polarimetric radar. *Radio Science*, *35*(1), 145–177. https://doi.org/10.1029/1999RS900108

Trindade, A., Portabella, M., Stoffelen, A., Lin, W., & Verhoef, A. (2019). ERAstar: A high-resolution ocean forcing product. *IEEE Transactions on Geoscience and Remote Sensing*, *58*(2), 1337–1347. https://doi.org/10.1109/TGRS.2019.2946019

Tripathi, S. P., Chapron, B., Collard, F., Guitton, G., Lopez-Radcenco, M., Mouche, A., & Fablet, R. (2024). Deep learning inversion of Ocean wave spectrum from SAR satellite observations. In *ICASSP 2024-2024 IEEE international conference on acoustics, speech and signal processing (ICASSP)* (pp. 8711–8715). IEEE. https://doi.org/10.1109/ICASSP48485.2024.10446834

Trofaier, A. M., Bartsch, A., Rees, W. G., & Leibman, M. O. (2013). Assessment of spring floods and surface water extent over the Yamalo-Nenets Autonomous District. *Environmental Research Letters*, *8*(4), 045026. https://doi.org/10.1088/1748-9326/8/4/045026

United States Geological Survey (USGS). (2023). Volcano monitoring from space: InSAR time series success in Alaska, Volcano Watch series. Retrieved from https://www.usgs.gov/observatories/hvo/news/volcano-watch-volcano-monitoring-space-insar-timeseries-success-alaska

van Zadelhoff, G. J., Stoffelen, A., Vachon, P. W., Wolfe, J., Horstmann, J., & Belmonte Rivas, M. (2014). Retrieving hurricane wind speeds using cross-polarization C-band measurements. *Atmospheric Measurement Techniques*, *7*(2), 437–449. https://doi.org/10.5194/amt-7-437-2014

van Zyl, J., Zebker, H., & Elachi, C. (1987). Imaging radar polarization signatures: Theory and observation. *Radio Science*, *22*(4), 529–543. https://doi.org/10.1029/RS022i004p00529

von Albedyll, L., Hendricks, S., Hutter, N., Murashkin, D., Kaleschke, L., Willmes, S., et al. (2024). Lead fractions from SAR-derived sea ice divergence during MOSAiC. *The Cryosphere*, *18*(3), 1259–1285. https://doi.org/10.5194/tc-18-1259-2024

von Baeckmann, C., Bartsch, A., Bergstedt, H., Efimova, A., Widhalm, B., Ehrich, D., et al. (2024). Land cover succession for recently drained lakes in permafrost on the Yamal Peninsula, Western Siberia. *The Cryosphere*, *18*(10), 4703–4722. https://doi.org/10.5194/tc-18-4703-2024

Wagner, W., Bauer-Marschallinger, B., Roth, F., Raiger-Stachl, T., Reimer, C., McCormick, N., et al. (2026). The fully-automatic Sentinel-1 Global Flood Monitoring service: Scientific challenges and future directions. *Remote Sensing of Environment*, *333*, 115108. https://doi.org/10.1016/j.rse.2025.115108

Wang, C., Ding, X., Li, Q., Shan, X., Zhu, W., Guo, B., & Liu, P. (2015). Coseismic and postseismic slip models of the 2011 Van earthquake, Turkey, from InSAR, offset-tracking, MAI, and GPS observations. *Journal of Geodynamics*, *91*, 39–50. https://doi.org/10.1016/j.jog.2015.08.006

Wang, C., Vandemark, D., Mouche, A., Chapron, B., Li, H., & Foster, R. C. (2020). An assessment of marine atmospheric boundary layer roll detection using Sentinel-1 SAR data. *Remote Sensing of Environment*, *250*, 112031. https://doi.org/10.1016/j.rse.2020.112031

Wang, H., Magagi, R., Goïta, K., Duguay, Y., Trudel, M., & Muhuri, A. (2023). Retrieval performances of different crop growth descriptors from full- and compact-polarimetric SAR decompositions. *Remote Sensing of Environment*, *285*, 13381. https://doi.org/10.1016/j.rse.2022.113381

Wang, H., Magagi, R., Goita, K., Trudel, M., McNairn, H., & Powers, J. (2019). Crop phenology retrieval via polarimetric decomposition and random forest algorithm. *Remote Sensing of Environment*, *231*, 111234. https://doi.org/10.1016/j.rse.2019.111234

Wang, T., Zheng, Y., Pulvirenti, F., & Segall, P. (2021). Post-2018 caldera collapse re-inflation uniquely constrains Kīlauea's magmatic system. *Journal of Geophysical Research: Solid Earth*, *126*(6), e2021JB021803. https://doi.org/10.1029/2021JB021803

Wang, Z., Qin, Y., Zhang, Q., Li, Y., Liu, J., Yuan, X., et al. (2025). China's GaoFen-3 Mission: A review. *IEEE Geoscience and Remote Sensing Magazine*, *13*(2), 79–115. https://doi.org/10.1109/MGRS.2024.3523924

Whitcomb, J., Moghaddam, M., McDonald, K., Kellndorfer, J., & Podest, E. (2009). Mapping vegetated wetlands of Alaska using L-band radar satellite imagery. *Canadian Journal of Remote Sensing*, *35*(1), 54–72. https://doi.org/10.5589/m08-080

Widhalm, B., Bartsch, A., Strozzi, T., Jones, N., Khomutov, A., Babkina, E., et al. (2025). InSAR-derived seasonal subsidence reflects spatial soil moisture patterns in Arctic lowland permafrost regions. *The Cryosphere*, *19*(3), 1103–1133. https://doi.org/10.5194/tc-19-1103-2025

Wig, E., Michaelides, R., & Zebker, H. (2024). Fine-resolution measurement of soil moisture from cumulative InSAR closure phase. *IEEE Transactions on Geoscience and Remote Sensing*, *62*, 5212315-15. https://doi.org/10.1109/TGRS.2024.3399069

Willatt, R., Stroeve, J. C., Nandan, V., Newman, T., Mallett, R., Hendricks, S., et al. (2023). Retrieval of snow depth on Arctic sea ice from surface-based, polarimetric, dual-frequency radar altimetry. *Geophysical Research Letters*, *50*(20), e2023GL104461. https://doi.org/10.1029/2023GL104461

Wiseman, G., McNairn, H., Homayouni, S., & Shang, J. (2014). RADARSAT-2 polarimetric SAR response to crop biomass for agricultural production monitoring. *IEEE Journal of Selected Topics in Applied Earth Observations and Remote Sensing*, *7*(11), 4461–4471. https://doi.org/10.1109/JSTARS.2014.2322311

Wollersheim, M. (2022). Pioneering the tracking of rapid changes on Earth. Retrieved from https://www.iceye.com/blog/iceye-x-esa-pioneering-the-tracking-of-rapid-changes-on-earth

World Meteorological Organization (WMO). (2022). 2022 GCOS implementation plan (p. 98). https://doi.org/10.1038/sdata.2016.18

Wright, T. J., Parsons, B., England, P. C., & Fielding, E. J. (2004). InSAR observations of low slip rates on the major faults of western Tibet. *Science*, *305*(5681), 236–239. https://doi.org/10.1126/science.1096388

Wu, K., & Li, X.-M. (2024). Deep learning for retrieving omni-directional ocean wave spectra from spaceborne synthetic aperture radar. *Remote Sensing of Environment*, *314*, 114386. https://doi.org/10.1016/j.rse.2024.114386

Wulf, T., Buus-Hinkler, J., Singha, S., Shi, H., & Kreiner, M. B. (2024). Pan-Arctic sea ice concentration from SAR and passive microwave. *The Cryosphere*, *18*(11), 5277–5300. https://doi.org/10.5194/tc-18-5277-2024

Yamaguchi, Y., Moriyama, T., Ishido, M., & Yamada, H. (2005). Four-component scattering model for polarimetric SAR image decomposition. *IEEE Transactions on Geoscience and Remote Sensing*, *43*(8), 1699–1706. https://doi.org/10.1109/TGRS.2005.852084

Yitayew, T. G., Dierking, W., Divine, D. V., Eltoft, T., Ferro-Famil, L., Rösel, A., & Negrel, J. (2018). Validation of sea-ice topographic heights derived from TanDEM-X interferometric SAR data with results from laser profiler and photogrammetry. *IEEE Transactions on Geoscience and Remote Sensing*, *56*(11), 6504–6520. https://doi.org/10.1109/TGRS.2018.2839590

Yun, S., Segall, P., & Zebker, H. (2006). Constraints on magma chamber geometry at Sierra Negra Volcano, Galápagos Islands, based on InSAR observations. *Journal of Volcanology and Geothermal Research*, *150*(1–3), 232–243. https://doi.org/10.1016/j.jvolgeores.2005.07.009

Zakhvatkina, N., Korosov, A., Muckenhuber, S., Sandven, S., & Babiker, M. (2017). Operational algorithm for ice–water classification on dual-polarized RADARSAT-2 images. *The Cryosphere*, *11*(1), 33–46. https://doi.org/10.5194/tc-11-33-2017

Zebker, H. A., & Villasenor, J. (1992). Decorrelation in interferometric radar echoes. *IEEE Transactions on Geoscience and Remote Sensing*, *30*(5), 950–959. https://doi.org/10.1109/36.175330

Zhang, Q., Fan, H., Qin, Y., & Zhou, Y. (2025). Advances in interferometric synthetic aperture radar technology and systems and recent advances in Chinese SAR missions. *Sensors*, *25*(15), 4616. https://doi.org/10.3390/s25154616

Zhang, Z., Miao, M., Qiu, B., Tian, J., Jing, Z., Chen, G., et al. (2024). Submesoscale eddies detected by SWOT and moored observations in the Northwestern Pacific. *Geophysical Research Letters*, *51*(15), e2024GL110000. https://doi.org/10.1029/2024GL110000

Zhao, J., Li, M., Li, Y., Matgen, P., & Chini, M. (2024). Urban flood mapping using satellite synthetic aperture radar data: A review of characteristics, approaches, and datasets. *IEEE Geoscience and Remote Sensing Magazine*, *13*(1), 237–268. https://doi.org/10.1109/MGRS.2024.3496075

Zheng, Y., Fattahi, H., Agram, P., Simons, M., & Rosen, P. (2022). On closure phase and systematic bias in multilooked SAR interferometry. *IEEE Transactions on Geoscience and Remote Sensing*, *60*, 5226611-11. https://doi.org/10.1109/TGRS.2022.3167648

Zwieback, S., Liu, L., Rouyet, L., Short, N., & Strozzi, T. (2024). Advances in InSAR analysis of permafrost terrain. *Permafrost and Periglacial Processes*, *35*(4), 544–556. https://doi.org/10.1002/ppp.2248

Zwieback, S., & Meyer, F. J. (2021). Top-of-permafrost ground ice indicated by remotely sensed late-season subsidence. *The Cryosphere*, *15*(4), 2041–2055. https://doi.org/10.5194/tc-15-2041-2021